مجلة المختار للعلوم

AL-Mukhtar Journal of Sciences

Volume: Issue:

30 years

ذكرى التأسيس

1992

ISSN:26-17-2178 (Print)

SSN:26-17-2186 (Online)

دار الكتب الوطنية - رقم الإيداع القانوني 280-2013

مجلة المختار للعلوم

جامعة عمر المختار

البيضاء، ليبيا

مجلة علمية محكّمة، المجلد السابع والثلاثون، العدد الثاني، 2022

تصدر عن جامعة عمر المختار، البيضاء، ليبيا.

مجلة المختار للعلوم

رقم الايداع في المكتبة الوطنية 2013/280/بنغازي

جامعة عمر المختار – البيضاء – ليبيا

مجلة محكّمة تصدر عن جامعة عمر المختار، البيضاء، ليبيا

مجلة علمية محكّمة، المجلد السابع والثلاثون، العدد الثاني، 2022

بريد إلكتروني: omu.j.sci@omu.edu.ly

ص.ب. 919 البيضاء – ليبيا، فاكس: 7053 463 69 218+

EDITORS & STAFF

مجلة المختار للعلوم 37:(2)، 2022

Al-Mukhtar Journal of Sciences 37: (2), 2022

Al-Mukhtar Journal of Sciences 37 (2): 105-112, 2022
ISSN: online 2617-2186 print 2617-2178
Journal Homepage https://omu.edu.ly/journals/index.php/mjsc/index

Synthesis and Study of the Crystal Structure of 2-[(Dipyrrolidin-1-yl) methylene] malononitrile

Wedad M. Al-Adiwish*, Wedad M. Barag and Mariam S. Saleh

Department of Chemistry, Faculty of Science, Zawia University, Libya

Received: 16 December 2020./ Accepted: 03 January 2022
Doi: https://doi.org/10.54172/mjsc.v37i2.383

Abstract: This study aims to synthesis 2-[(dipyrrolidin-1-yl)methylene] malononitrile 2 and identify its crystal structure by X-ray diffraction analysis. 2-[(dipyrrolidin-1-yl)methylene] malononitrile was prepared by a direct displacement of the methylthio group (SMe) in the 2-[bis(methylthio)methylene] malononitrile 1 with pyrrolidine as cyclic secondary amine by conjugating addition-elimination reaction under reflux conditions for two hours. The compound was obtained in high yield (80%). The structure of compound 2-[(dipyrrolidin-1-yl)methylene] malononitrile 2 was identified by performing X-ray diffraction analysis. Suitable crystals of compound 2 were grown by slow evaporation of methanol solution of the compound. The compound 2 crystallized in an orthorhombic crystal system with a space group of *Pbcn*. In the title compound, the two cyanide groups and the two pyrrolidine rings adopted *trans* configurations across the C2=C3 bond. The bond lengths and angles of the two pyrrolidinyl rings in the compound are within the normal range. The maximum deviation of N5/C2/C3/C4/N5^a/C4^a is 0.002(1) around C4, and no deviation has been recorded for the fragment N1/N1^a/C2/C3 (0.000 (1)°). The dihedral angle between the pyrrolidine ring and N1/N1^a/C2/C3 is 33.06(8)°, and the dihedral angle between the pyrrolidine ring and N5/C2/C3/C4/N5^a/C4^a is 50.57(7)°. The crystal packing is stabilized by two intermolecular and one intramolecular C---H…N hydrogen bonds, which form a one-dimensional polymeric chain along the axis.

Keywords: single-crystal X-ray study; crystal structure; orthorhombic crystal system; direct displacement; R factor = 0.040, wR = 0.110.

INTRODUCTION

Ketene-*N,S*- and -*N,N*-acetals, which are a group of compounds derived from enamines and belong to the acetal chitin family, are very reactive and electronically rich. Ketene acetals are of interest not only because of their unique electronic properties but also for their importance as versatile building blocks in organic synthesis. According to the number and types of compounds, keten N,S-acetal is the biggest family in the world of ketene acetals (Zhang et al., 2016). Having the structural feature of ketene S,S-cetals and enaminones make ketene N,S-acetals versatile and easy to use, particularly in multicomponent and cyclization reactions for the synthesis of various heterocyclic systems and related natural products (Al-Adiwish et al., 2019; Al-Adiwish et al., 2013; Gouda et al., 2010; Khalil et al., 2009; Misra et al., 2007; Zhang et al., 2016). In addition, they; are used as intermediates in dye and are often used in pharmaceutical industries (Al-Adiwish et al.,

***Corresponding author**: Wedad M. Al-Adiwish w.aladiwish@zu.edu.ly Department of Chemistry, Faculty of Science, Zawia University, Zawia, Libya.

2019; Al-Adiwish et al., 2013; Al-Afaleq, 2001; El-Saghier et al., 2008; Elgemeie et al., 2007; Gouda et al., 2010; Khalil et al., 2009; Misra et al., 2007). Due to the push-pull alkene skeleton, they are useful reactants and synthetic building blocks for other highly functionalized molecules (Zhang et al., 2016). In spite of the characteristics of ketene acetals and the increasing wealth of information about their synthesis and synthetic applications, there are limited routes to their formation as isolable products (Paris, Schwartz, Sundall, et al., 2021; Paris, Schwartz, & Willand-Charnley, 2021; Zhang et al., 2016). The α-Cyanoketene-*N,N*-acetals are generally prepared by the direct amination reaction of *α*-cyanoketene-*S,S*- and *N,S*-acetals with appropriate amine (Elgemeie, Ali, et al., 2003; Elgemeie, Elghandour, et al., 2003; Elgemeie et al., 2004; Elgemeie et al., 2007; Ma et al., 2009; Sommen et al., 2003; Suryawanshi et al., 2007).

Therefore, we report here an easy and efficient method to prepare 2-[(dipyrrolidin-1-yl) methylene] malononitrile 2 by direct displacement of the methylthio group (SMe) in the 2-[bis (methylthio) methylene] malononitrile 1 with pyrrolidine by conjugating addition-elimination reaction.

MATERIALS AND METHODS

All chemicals were of reagent grade. In this study, X-ray diffraction was used. CRYSTAL, SIR92, CAMERON, and ORTEP2 software were used for molecular drawing and preparing the crystallographic data. The following symbols are used; 2-[bis (methylthio) methylene] malononitrile is compound 1; 2-[(dipyrrolidin-1-yl) methylene] malononitrile is compound 2.

Synthesis of 2-[dipyrrolidin-1-ylmethylene] malononitrile 2: Reflux of 2-[bis (methylthio) methylene] malononitrile 1 (1.93 g, 0.01 mol) with pyrrolidine (1.50 ml, 0.02 mol) in (20 ml) of ethanol for 2 hours (Al-Adiwish et al., 2013). The solvent was evaporated in a vacuum to obtain a solid crude yellow, which was collected and purified using methanol, and the percentage yield was 80%. Suitable crystals of compound 2 were grown by slow evaporation of the methanolic solution of the compound. The melting point of compound 2 was determined using a hot stage Gallenkamp melting point apparatus, which was 166-168 ^{0}C.

Crystal structure determination: The data were collected at room temperature with the Bruker SMART APEX CCD spectrometer. The crystal of compound 2 was placed in the cold stream of an Oxford Cryosystems open-flow nitrogen cryostat with a nominal stability of 0.1K. TLC analysis was carried out on silica gel of Merck No. 5545 to monitor the completion of reactions, in which ethyl acetate-methanol (4:1) was used as eluent. The software used for the direct method, least-squares F^2 analysis, molecular drawing, and preparing the crystallographic materials are CRYSTAL, SIR92, CAMERON, and ORTEP2. For further information, see references (Allen et al., 1987; Altomare et al., 1994; Betteridge et al., 2003; Pro, 2010; Watkin et al., 1996).

RESULT AND DISCUSSION

Synthesis: The α-Cyanoketene-*N,N*-acetals are generally prepared by the direct amination reaction of *α*-cyanoketene-*S,S*- and *N,S*-acetals with appropriate amine. The crystal structure of 2-[(dipyrrolidin-1-yl)methylene] malononitrile 2, is reported here, which was synthesized by direct displacement of the methylthio group (SMe) in the 2-[bis (methylthio) methylene] malononitrile 1 with cyclic secondary aliphatic amine as pyrrolidine by conjugating addition-elimination reaction in refluxing ethanol for 2 h. The solvent was evaporated in a vacuum to produce an oily viscous crude product that was purified by performing column chromatography with an ethyl acetate and hexane (1:1) eluent. The solvent was concentrated in vacuum to obtain a solid crude product, which was collected

and purified using methanol. The percentage yield was 80%, and this high yield indicates the efficiency of the method used to prepare the target compound 2. Equation 1 illustrates the synthesis method of the target compound 2.

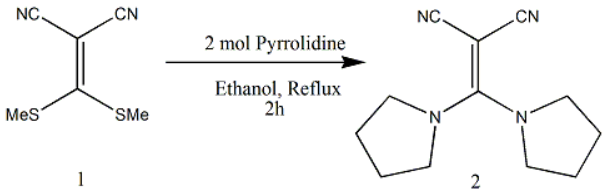

Equation (1). Synthesis of 2-[dipyrrolidin-1-ylmethylene] malononitrile 2.

The formation of 2-[(dipyrrolidin-1-yl) methylene] malononitrile can be explained by the proposed mechanism shown in Equation 2 (Elgemeie et al., 1997). The 2-[(dipyrrolidin-1-yl)methylene] malononitrile 2 was produced *via* a nucleophilic attack of the NH group of the pyrrolidine on the β-carbon of the ethylenic bond in compound 1, followed by the elimination of methanethiol. Intermolecular attack by another pyrrolidine with the loss of another methanethiol yielded the corresponding 2-[(dipyrrolidin-1-yl) methylene] malononitrile 2.

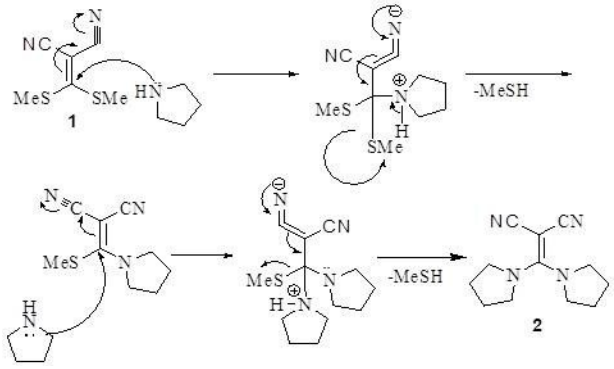

Equation (2). Mechanism formation of 2-[(dipyrrolidin-1-yl)methylene]malononitrile 2

X-ray crystallography: The structure of 2-[(dipyrrolidin-1-yl) methylene] malononitrile 2 was identified by x-ray diffraction analysis. Suitable crystals of the compound were grown by slow evaporation of the methanol solution of the compound. Table 1 has a summary of the crystal data and x-ray data collection, data reduction, and structure refinement results for compound 2.

Table (1). Crystal data and structure refinement for 2-[(dipyrrolidin-1-yl)methylene]malononitrile 2.

Crystal data (1)	
Chemical formula	$C_6H_8N_2$
M_r	108.14
Crystal system, space group	Orthorhombic, *Pbcn*
Temperature (K)	150
a, *b*, *c* (Å)	16.7024 (5), 8.2383 (3), 8.5041 (3)
V (Å^3)	1170.15 (7)
Z	8
Radiation type	Cu $K\alpha$
μ (mm^{-1})	0.61
Crystal size (mm)	0.13 × 0.10 × 0.06
Data collection (2)	
Diffractometer	Area
No. of measured, independent and observed [$I > 2.0\sigma(I)$] reflections	12227, 1137, 977
R_{int}	0.027
$(\sin \theta/\lambda)_{max}$ (Å^{-1})	0.614
Refinement (3)	
$R[F^2 > 2\sigma(F^2)]$, $wR(F^2)$, S	0.040, 0.110, 0.94
No. of reflections	1134
No. of parameters	74
$\Delta\rho_{max}$, $\Delta\rho_{min}$ (e Å^{-3})	0.19, −0.18

The *ORTEP* plot of 2 with the numbering equation is presented in Figure 1. The compound crystallized in orthorhombic crystal system with space group of *Pbcn*

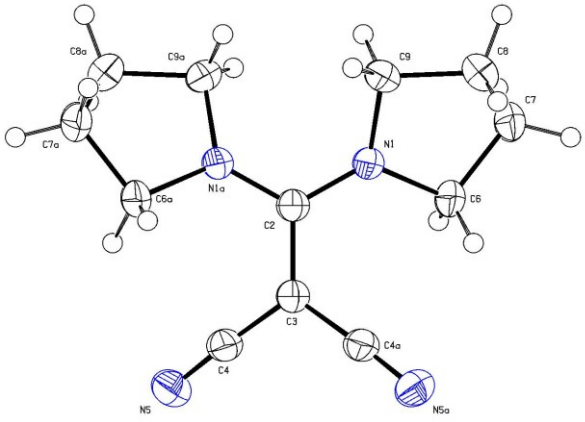

Figure (1). The structure of 2-[(dipyrrolidin-1- yl) methylene]malononitrile 2 showing the atom numbering equation with ellipsoids drawn at the 50% probability level.

In the title compound, the two cyanide groups and the two pyrrolidine rings adopting *trans* configurations across the C2=C3 bond, as shown in Figure 2.

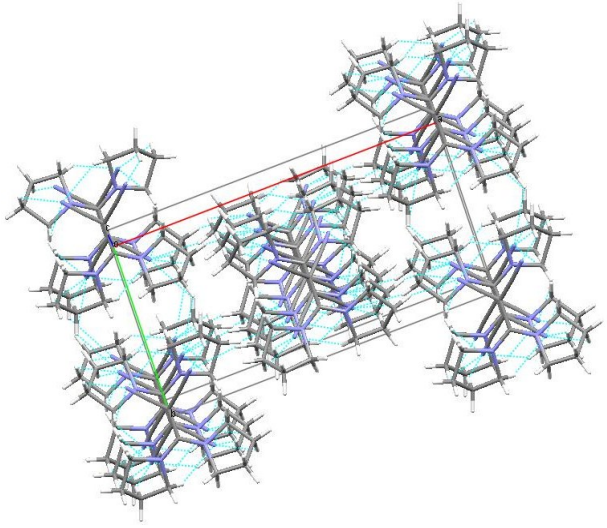

Figure (2). Crystal packing of 2-[(dipyrrolidin-1-yl) methylene] malononitrile 2 viewed down the c axis

The bond lengths and angles of the two pyrrolidinyl rings in the compound 2 are within the normal range (Allen et al., 1987). Selected bond distances, angles and torsion angles, are presented in Table 2. The bond length of C2=C3 [1.429(2) Å] is longer than the average [C=C (1.34Å)] and indicates the single C–C bond character (1.455Å).

In addition, the bond length of C2–N1 [1.3400(13)Å] and the bond length of C3–C4 [1.4148(16)Å] are shorter than the normal [C–N (1.47Å)] and the average [C–C (1.455Å)], respectively. This is probably due to the strong π-delocalization between the C2 and nitrogen atoms which is give rise to a decrease in the bond length of the C–N and an increase in the bond length of the C=C and became highly polarized.

The mean planes data for compound 2 and the dihedral angles between the planes, are listed in Table 3. The fragments N1/N1^a/C2/C3 and N5/C2/C3/C4/N5a/C4a are both planar. The maximum deviation of N5/C2/C3/C4/N5a/C4a is 0.002(1) around C4, and no deviation has been recorded for the fragment N1/N1^a/C2/C3 [0.000 (1)°]. The dihedral angle between the two planes is 27.80(5)°. The pyrrolidine ring N1/ C6/ C7/ C8/C9 is almost planar with a maximum deviation of 0.272(2)° around C8.

Table (2). Selected geometric parameters (Å, °) of the 2-[(dipyrrolidin-1-yl)methylene] malononitrile 2.

Bond	Bond length [Å]
N(1)–C(2)	1.3400(13)
N(1)–C(9)	1.4822(18)
C(2)–C(3)	1.429(2)
C(3)–C(4)	1.4148(16)
C(7)–C(8)	1.519(2)
N(1)–C(6)	1.4854(16)
N(5)–C(4)	1.1529(19)
C(3)–C(4)	1.4148(16)
C(6)–C(7)	1.522(2)
C(8)–C(9)	1.524(2)
C(2)–N(1)–C(6)	123.93(11)
C(2)–N(1)–C(9)	125.63(11)
C(6)–N(1)–C(9)	110.44(10)
N(1)–C(2)–C(3)	119.62(8)
N(1)–C(2)–N(1)a	120.76(14)
C(3)–C(2)–N(1)a	119.62(8)
C(2)–C(3)–C(4)	122.98(8)
C(2)–C(3)–C(4)a	122.98(8)
C(4)–C(3)–C(4)a	114.05(14)
N(5)–C(4)–C(3)	177.02(15)
C(2)–N(1)–C(9)–C(8)	162.79(12)
N(1)–C(2)–C(3)–C(4)a	27.70(9)
C(6)–N(1)–C(2)–C(3)	25.68(14)
C(6)– N(1)–C(2)–N(1)	154.32(11)
C(9)–N(1)–C(2)–C(3)	154.40(11)
C(9)–N(1)–C(2)–N(1)a	25.60(16)
C(2)–N(1)–C(6)–C(7)	169.68(11)
C(2)–N(1)–C(9)–C(8)	162.79(12)
N(1)–C(2)–C(3)–C(4)a	27.70(9)
C(6)–N(1)–C(2)–C(3)	25.68(14)

The dihedral angle between the pyrrolidine ring and N1/N1^a/C2/C3 is 33.06(8)°, and the dihedral angle between the pyrrolidine ring and N5/C2/C3/C4/N5a/C4a is 50.57(7)°.

Table (3). Plane deviations and angles [°] between selected planes in the structure of 2.

Plane	Atom with greatest deviation	Angle between planes
N1/N1a/C3/C3(i)	0.000 (1)	i & ii = 27.80(5)
N5/C2/C3/C4/N5a/C4a(ii)	C4; 0.002(1)	i & iii = 33.06(8)
N1/C6/C7/C8/C9(iii)	C8; 0.272(2)	ii & iii = 50.57(7)

The hydrogen bonding geometry of compound 2 is listed in Table 4. An intramolecular C(6) H(62) N(5) hydrogen bond has been observed in the structure of the compound. The C—H…N hydrogen bonds further stabilize the packing down the *c* direction, Figure 2.

Table (4). Hydrogen-bonding geometry (Å, º) for 2

D—H…*A*	*D*—H	H…*A*	*D*…*A*	*D*—H…*A*
C(6)--H(62)..N(5) [a]	1.02	2.62	3.3958(19)	134
C(6)--H(61)..N(5)[i ,b]	1.02	2.61	3.239(2	120
C(9)--H(92)..N(5)[ii, b]	1.02	2.61	3.494(2)	145

[a] Intramolecular, [b]Intermolecular; Symmetry codes: (i) 1-*x*,1-*y*,1-*z*; (ii) *x*,1-*y*,1/2+*z*

CONCLUSION

In summary, we have successfully synthesized and studied the crystal structure of 2-[(dipyrrolidin-1- yl) methylene] malononitrile 2**.** The percentage yield was 80%. The crystal data, X-ray data collection, data reduction, and structure refinement results of compounds were presented in this paper. The compound crystallized in an orthorhombic crystal system with a space group of *Pbcn*. In the title compound, the two cyanide groups and the two pyrrolidine rings adopted *trans* configurations across the C2=C3 bond. The crystal packing is stabilized by two intermolecular and one intramolecular C---H…N hydrogen bond, which form a one-dimensional polymeric chain along the axis.

REFERENCES

Al-Adiwish, W. M., Hamza, M. M., & Hamza, K. M. (2019). A Study X-ray Crystal Structure of Compound 2-[Methylthio (morpholino) methylene] malononitrile, C 9 H 11 N 3 OS. *American Journal of Quantum Chemistry and Molecular Spectroscopy, 3*(1), 12-16 .

Al-Adiwish, W. M., Tahir, M., Siti-Noor-Adnalizawati, A., Hashim, S. F., Ibrahim, N., & Yaacob, W. (2013). Synthesis, antibacterial activity and cytotoxicity of new fused pyrazolo [1, 5-a] pyrimidine and pyrazolo [5, 1-c][1, 2, 4] triazine derivatives from new 5-aminopyrazoles. *European journal of medicinal chemistry, 64*, 464-476 .

Al-Afaleq, E. I. (2001). A facile method for the synthesis of novel pyridinone derivatives via ketene N, S-acetals. *Synthetic communications, 31*(22), 3557-3567 .

Allen, F. H., Kennard, O., Watson, D. G., Brammer, L., Orpen, A. G., & Taylor, R. (1987). Tables of bond lengths determined by X-ray and neutron diffraction. Part 1. Bond lengths in organic compounds. *Journal of the Chemical Society, Perkin Transactions 2*(12), S1-S19 .

Altomare, A., Cascarano, G., Giacovazzo, C., Guagliardi, A., Burla, M., Polidori, G. t., & Camalli, M. (1994). SIRPOW. 92–a program for automatic solution of crystal structures by direct methods optimized for powder data. *Journal of Applied Crystallography, 27*(3), 435-436 .

Betteridge, P. W., Carruthers, J. R., Cooper, R. I., Prout, K., & Watkin, D. J. (2003). CRYSTALS version 12: software for guided crystal structure analysis.

Journal of Applied Crystallography, 36(6 .(

El-Saghier, A. M., Matough, F. S ،.Farhat, M. F., Saleh, N. A., Kreddan, K. M., El-Tier, S. O., & Hussien, H. B. (2008). Synthesis and Biological Evaluation of Some New Thienopyridine and Thienopyrimidine Derivatives. *Jordan Journal of Chemistry (JJC), 3*(3), 223-232 .

Elgemeie, G., Elghandour, A., Elzanate, A., & Ahmed, S. (1997). Synthesis of some novel α-cyanoketene S, S-acetals and their use in heterocyclic synthesis. *Journal of the Chemical Society, Perkin Transactions 1*(21), 3285-3290 .

Elgemeie, G. H., Ali, H. A., Elghandour, A .H., & Hussein, A. M. (2003). Synthesis of benzimidazole ketene N, S-acetals and their reactions with nucleophiles. *Synthetic communications, 33*(4), 555-562 .

Elgemeie, G. H., Elghandour, A. H., & Abd Elaziz, G. W. (2003). Novel synthesis of heterocyclic ketene N, N-, N, O-, and N, S-acetals using cyanoketene dithioacetals. *Synthetic communications, 33*(10), 1659-1664 .

Elgemeie, G. H., Elghandour, A. H., & Abd Elaziz, G. W. (2004). Potassium 2 ‐ Cyanoethylene ‐ 1 ‐ thiolate Derivatives: A New Preparative Route to 2 ‐ Cyanoketene S, N ‐ Acetals and Pyrazole Derivatives. *Synthetic communications, 34*(18), 3281-3291 .

Elgemeie, G. H., Elghandour, A. H., & Elaziz, G. W. A. (2007). Novel Cyanoketene N, S ‐ Acetals and Pyrazole Derivatives using Potassium 2 ‐ Cyanoethylene- - 1thiolates. *Synthetic communications, 37*(17), 2827-2834 .

Gouda, M., Berghot, M., Shoeib, A., & Khalil, A. (2010). Synthesis and antimicrobial of new anthraquinone derivatives incorporating pyrazole moiety. *European journal of medicinal chemistry, 45*(5 .1848-1843 ،(

Khalil, A., Berghot, M., & Gouda, M. (2009). Synthesis and antibacterial activity of some new heterocycles incorporating phthalazine. *European journal of medicinal chemistry, 44*(11), 4448-4454 .

Ma, Y., Wang, M., Li, D., Bekturhun, B., Liu, J., & Liu, Q. (2009). α-Alkenoyl ketene S, S-acetal-based multicomponent reaction: an efficient approach for the selective construction of polyfunctionalized cyclohexanones. *The Journal of Organic Chemistry, 74*(8), 3116-3121 .

Misra, N., Panda, K., Ila, H., & Junjappa, H. (2007). An efficient highly regioselective synthesis of 2, 3, 4-trisubstituted pyrroles by cycloaddition of polarized ketene S, S-and N, S-acetals with activated methylene isocyanides. *The Journal of Organic Chemistry, 72*(4), 1246-12 .51

Paris, T. J., Schwartz, C., Sundall, E., & Willand-Charnley, R. (2021). Rapid, One-Step Synthesis of α-Ketoacetals via Electrophilic Etherification. *The Journal of Organic Chemistry, 86*(21), 14797-14811 .

Paris, T. J., Schwartz, C., & Willand-Charnley, R. (2021). Electrophilic Etherification of α-Heteroaryl Carbanions with Monoperoxyacetals as a Route to Ketene O, O-and N, O-Acetals. *The Journal of Organic Chemistry, 86*(3), 2369-2384 .

Pro, C. (2010). Data Collection and Processing Software for Agilent X-Ray

Diffractometers. *Aglient Technologies: Yarnton, UK* .

Sommen, G., Comel, A., & Kirsch, G. (2003). Preparation of thieno [2, 3-b] pyrroles starting from ketene-N, S-acetals. *Tetrahedron, 59*(9), 1557-1564 .

Suryawanshi, S., Pandey, S., Bhatt, B & ،. Gupta, S. (2007). Chemotherapy of leishmaniasis Part VI: Synthesis and bioevaluation of some novel terpenyl S, N-and N, N-acetals. *European journal of medicinal chemistry, 42*(4), 511-516 .

Watkin, D., Prout, C., & Pearce, L. (1996). CAMERON, Chemical Crystallography Laboratory, *University of Oxford: Oxford*.

Zhang, L., Dong, J., Xu, X., & Liu, Q. (2016). Chemistry of ketene N, S-acetals: an overview. *Chemical Reviews, 116*(2), 287-322.

تحضير ودراسة التركيب البلوري للمركب 2-[ثنائي بيروليدين-1-يل ميثيلين] مالونونتريل

وداد ميلاد الأديوش*، وداد محمد برق ومريم صالح صالح

قسم الكيمياء، كلية العلوم، جامعة الزاوية، الزاوية- ليبيا

تاريخ الاستلام: 16 ديسمبر 2020/ تاريخ القبول: 03 يناير 2022

Doi:https://doi.org/10.54172/mjsc.v37i2.383

المستخلص : تهدف هذه الدراسة تحضير 2-[ثنائي بيروليدين-1-يل ميثيلين] مالونونتريل **2**، ودراسة تركيبه البلوري بواسطة الأشعة السينية. 2-[ثنائي بيروليدين-1-يل ميثيلين] مالونونتريل 2 تم تحضيره عن طريق الاستبدال المباشر لمجموعة الميثيل ثايو (SMe) في المركب 2-[ثنائي(ميثيل ثايو) ميثيلين] مالونونيتريل 1 مع بيروليدين كأمين أليفاتي ثانوي عن طريق تفاعل الإضافة والحذف المتعاقب تحت التقطير المرتد لمدة ساعتين. تم الحصول على المركب بإنتاجية عالية (80%). تم تحديد هيكل المركب 2 عن طريق إجراء تحليل حيود الأشعة السينية. تم الحصول علي البلورات المناسبة للمركب 2 عن طريق التبخر البطيء للمحلول الميثانولي للمركب حيث تبلور المركب في النظام البلوري المعيني القائم مع المجموعة الفراغية Pbcn. في الشكل البلوري للمركب، مجموعتي السيانيد، وحلقتين بيروليدين تشكل الهيئة الفراغية ترانس عبر رابطة $C_2=C_3$، أطوال، وزوايا الروابط بين حلقتين بيروليدين في المركب 2 $C_{12}H_{16}N_4$ كانت ضمن أطوال الروابط الطبيعية. أقصى انحراف لـ / N5 / C2 / C3 / C4 / $N5^a$ $C4^a$ هو (1) 0.002 حول C4 ولم يتم تسجيل أي انحراف للجزء [0.000(1) ^{o}] N1/ $N1^a$ / C2 / C3. الزاوية ثنائية السطوح بين حلقة البيروليدين والمستوى N1 / $N1^a$ / C2 / C3 هي °(8) 33.06، بينما الزاوية ثنائية السطوح بين حلقة البيروليدين، والمستوى $C4^a$ / $N5^a$ / C4 / C3 / C2 /N5 هي °(7) 50.57. البنية البلورية للمركب مرتبطة بواسطة رابطتين هيدروجينيتين بين الجزيئات وواحدة داخل الجزيئة C--N...H، والتي تشكل سلسلة بوليمرية أحادية البعد على طول المحور.

الكلمات المفتاحية : دراسة الأشعة السينية أحادية البلورة، التركيب البلوري، النظام البلوري المعيني، الاستبدال المباشر، عامل R = 0.040، wR = 0.110.

*1 وداد ميلاد الأديوش w.aladiwish@zu.edu.ly قسم الكيمياء، كلية العلوم، جامعة الزاوية، الزاوية- ليبيا.

Al-Mukhtar Journal of Sciences 37 (2): 113-119, 2022
ISSN: online 2617-2186 print 2617-2178
Journal Homepage https://omu.edu.ly/journals/index.php/mjsc/index

Water Quality Assessment of Lakes (Ain Al-Ghazala and Umm-Hufayn) for Fish Culture in the Eastern Coast of Libya

Amani F. Ali[1*] , Anwar A. R. Al-Mismari[2], Aldoushy A. Mahdy[3],Rashad E.M. Said[3] and Ashraf N. Masoud[2]

[1]*Department of Marine Resource, Faculty of Natural Resource, Tobruk University, Libya.*
[2]*Department of Environmental Science, Faculty of Natural Resource, Tobruk University, Libya.*
[3.]*Zoology Department, Faculty of Science, Al-Azhar University, Assiut ,Egypt*

Received: 12 August 2021/ Accepted: 14 March 2022
Doi: https://doi.org/10.54172/mjsc.v37i2.527

Abstract: Assessments of some physical and chemical properties were conducted for two Libyan water bodies (Ain Al- Ghazala and Umm-Hufayn). Of each ecosystem, ten water samples were taken from ten points for analysis. The results showed that the electric conductivity in Ain Al-Ghazala Bay waters is higher than that in the waters of Umm-Hufayn Lake. In the two areas, the hydrogen ion concentration pH recorded the highest value with a value of 8.3, with mean values of chloride (Cl) exceeding the internationally recorded limits. Furthermore, nitrites (NO_2), nitrate (NO_3), sulphate (SO_4), phosphate (PO_4), silicates (SiO_2), carbonate (CO_3), calcium (Ca), magnesium (Mg), sodium (Na), and potassium (K) were all greater in Ain Al-Ghazala Bay waters than in Umm-Hufayn Lake waters. In conclusion, more attention should be directed to the preservation of such natural resources.

Keywords: Water Quality, Physical and Chemical Properties, Ain Al-Ghazala Lagoon, Umm-Hufayn Lagoon.

INTRODUCTION

Water properties and quality are defined by specific physical, chemical, and biological properties and how these properties impact the survival, reproduction, growth, and management of aquatic life (Aduwo & Adeniyi, 2019). Water quality is the major limiting factor in the productivity of aquatic ecosystems, including fish resources. The health of an aquatic ecosystem depends on its physico-chemical and biological characteristics (Watson & Lawrence, 2003). The Libyan coast and lagoons are important for Mediterranean marine life biodiversity and productivity.(Haddoud & Rawag, 1995). The lakes may be used for recreation, and/or used as a component of hydropower generating systems. In developing countries, lakes are primarily used by the local inhabitants for transportation, fishing, washing, cooking, and irrigation practices (Okoro et al., 2014). Ain Al-Ghazala, is a long inlet with mainly rocky shores, lacking relevant tidal movements, but with characteristic extensive shallows occupied by Zosterabeds and mudflats (Team, 2010). The Umm-Hufayn lagoon is around 2 km2 in size and has a water depth of 0.5 to 3.0 m (Abdalhamid et al., 2018). It has a short passage connecting it to the sea, which is subject to tidal intrusions. Algal blooms,

***Corresponding author**: Amani Fitori *amanifitori1@gmail.com* Department of Marine Resource, Faculty of Natural Resource, Tobruk University, Libya.

anoxic conditions, and ocean acidification are caused by too much nitrogen and phosphorus, resulting in dead zones, fish kills, toxin generation, and changed plant species (Ngatia et al., 2019). About 75% of surface water may be contaminated by different kinds of pollutants. Pollutants may include heavy metals (Awoyemi et al., 2014), nutrients from industrial discharges (Mahananda et al., 2005), or agricultural activities. Higher concentrations of nutrients, e.g., phosphorus and nitrogen, may cause hypoxia and algal bloom (Garg et al., 2009); which may cause low light penetration, obstruction of oxygen levels, and loss of aquatic life and biodiversity (e.g., fish mortality) (Parashar et al., 2006).

The constant monitoring of water quality in lakes is essential and can be conducted by quantifying the level of physical and chemical parameters (Ademoroti, 1996). This paper's objective is to compare water quality between the two studied areas.

MATERIALS AND METHODS

Study area Ain Al- Ghazala Bay (Fig.1) is located west of Tobruk, about 60 km along the eastern extension of the Libyan coast in the Mediterranean Sea, with coordinates 32° 10' 42.49334" N**,** 23° 18' 37.80131" E. The shore is rocky, with sandy beaches interspersed. It is about 6 km long and 1.5 km wide, with depths ranging from 3.5 to 5 m and an area of 180 hectares. Almarakeb (Ulbah) island, located in front of the entrance, protects the bay from wave action and northern winds.

Lake Umm-Hufayn (Fig.1) originated from Bomba Bay 32° 33' 47.96503", 23° 5' 29.10995", about 80 km east of the city of Derna towards Tobruk, covers an area of about 2 km^2 and a depth of 0.5-3 m. During high tides, seawater enters the lake through the bay. Underground springs on the lake's inner shore provide fresh water, which helps to lessen its salinity.

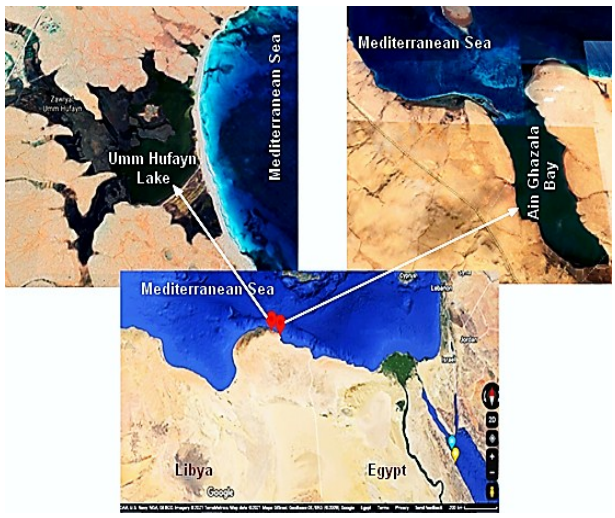

Figure (1).. Map showing the two studied areas, Umm Hufayn and Ain Al- Ghazala.

Water sampling: For chemical analysis, water samples were collected in polyvinyl chloride Van Dorn bottles at the two selected sites (10 points for each site). Some physicochemical parameters of water bodies at all studied sites were measured, including pH, by a multi-portable device (HACH, USA). Other Water samples were kept in a one-litre polyethylene bottle in an icebox and analyzed in the laboratory, Total dissolved salts TDS (mg/l), Conductivity EC (mS/cm), Total hardness TH (mg/l), Total Alkalinity TA (mg/l), Chloride Cl (mg/l), Nitrite NO_2 (mg/l), Nitrate NO_3 (mg/l), Sulfate SO_4 (mg/l), Phosphate PO_4 (mg/l), Silicate SiO_2 (mg/l) Carbonate CO_3 (mg/l), Bicarbonate, HCO_3 (mg/l), Calcium Ca (mg/l) Magnesium Mg (mg/l), Sodium Na (mg/l), Potassium K (mg/l) are measured according to the traditional manual methods (Beutler et al., 2014).

RESULTS

Table (1) shows the physicochemical parameters derived from the study of water samples. The results showed that the mean values of the water electric conductivity were higher in Ain Al- Ghazala water (62.500±1.141 mS/cm) than in those of Umm-Hufayn Lake (28.620±0.993 mS/cm). Total dissolved solids in Ain Al- Ghazala water (41.511 ±0.760mg/l) were more than twice as high as

in Umm-Hufayn (19.157±0.665 mg/l). TDS in this study were over the international permitted limit of 1mg/L. The pH values in Umm-Hufayn and Ain Al- Ghazala, respectively, were (8.14±.023) and (8.210±0.7), indicating that the water in Ain Al- Ghazala Lake is on the alkaline side. The greatest values of total alkalinity (6.822±0.190) and chloride (3.253±0.210) were found in Ain Al-Ghazala water, while these values were (1.576±0.054) and (3.185±0.110) in Umm-Hufayn respectively. In both areas, the mean chloride percentage exceeded the international standards. The findings also revealed that Lake Ain Al- Ghazala had higher nutrient levels of NO_3, NO_2, and PO_4 than Lake Umm-Hufayn. Phosphorus, like nitrogen, is a necessary component of all living organisms. Ain Ghazala Lake had greater SO_4, Ca, K, mg, Na, SiO_2, CO_3, and HCO_3 concentrations than Lake Umm-Hufayn. On the other hand, a T-test was used to demonstrate the differences in physicochemical parameters between the two assessed wetlands (Table 2). The T-test demonstrated the presence of greater and significant (Table 2) differences in the means of all parameters ($P<0.01$), except for pH (insignificant, $P> 0.05$).

Table: (1). Mean ±SD Water criteria sampled from the two investigated areas.

Water parameter	Ain AlGhazala	Umm Hufayn
Conductivity(mS/cm)	62.500±1.141	28.620±0.993
TDS (mg/l)	41.511±0.760	19.157±0.665
pH	8.21±0.07	8.14±.23
Hardness(mg/l)	7.302±0.132	3.427±0.118
Alkalinity (mg/l)	3.253±0.210	1.576±0.054
Chlorides (mg/l)	6.822±0.190	3.185±0.110
NO_2(mg/l)	0.223±0.004	0.112±0.003
NO_3(mg/l)	2.285±0.314	1.209±0.053
SO_4(mg/l)	2.341±0.340	1.485±0.050
PO_4(mg/l)	0.410±0.008	0.185±0.006
SiO_2(mg/l)	0.008±000	0.002±000
CO_3(mg/l)	0.064±0.001	0.017±0.008
HCO_3(mg/l)	3.085±0.067	1.547±0.053
Ca(mg/l)	6.116±0.114	2.89±0.100
Mg (mg/l)	1.042±0.370	0.543±0.018
Na(mg/l)	5.681±0.109	2.705±0.093
K(mg/l)	0.3007±0.024	0.173±0.006

DISCUSSION

Along the Libyan coast and offshore, there are a variety of natural aquatic environments. Despite their importance as natural resources, they have received little attention. Effective conservation and management are the most pressing issues facing marine biotopes. Recently, Elshakh et al. (2020) conducted an assessment to the fish *Liza aurata* collected from Umm Hufayn lagoon. The lagoon is a major artisanal fishing ground, an important wetland with high biodiversity, a refuge and breeding place for fish and turtles, as well as a nesting and resting location for local and migratory sea birds (Elshakh et al., 2020). In addition, *Chelonlabrosus* was recorded for the first time in Umm-Hufayn Lagoon (Elmor et al., 2020). This finding indicates that these species are highly adaptive to changing environmental conditions, implying that their presence is tied directly to their euryhaline character, a wide range of water parameters, and a diverse food menu. Umm-Hufayn is almost entirely exposed to juvenile eel migration, making it suitable for tilapias and mullets. It's vital to perform a thorough examination of the newly discovered critter, which could represent a threat to the fish population in the lagoon (Abdalhamid et al., 2018). When comparing the two water bodies, Ain Al-Ghazala waters were found to be slightly contaminated and of average quality, whereas Umm-Hufaynn waters were found to be slightly polluted and of average quality. In terms of statistical analysis (Table 2), T-tests revealed significant differences in water parameters between the two investigated areas ($p<0.01$), except for water pH ($p>0.5$). Ain Al-Ghazala has conductivity and total dissolved solids more than twice as high as Umm Hufayn. In fact, TDS are indicative of conductivity, namely, the higher TDS, the higher conductivity of water. Furthermore, hardness, alkalinity, chlorides, nitrates, sulphates, and bicarbonates were also dramatically higher at Ain Al-Ghazala when compared to Umm Hufayn.

The primary factors influencing lake water quality evaluation that should be managed are nitrate, phosphate, alkalinity, and total sus-

pended solids. The main reason for the difference in the physical, chemical, and biological properties between the two lakes is due to the increasing urbanization. The consequent discharge of harmful effluents from large cities is continually altering the water quality and productivity of Lakes Adverse changes in water quality of aquatic ecosystems in Ain Al-Ghazala and Umm-Hufayn Lake are reflected in the biotic community structure, and the most sensitive species often act as sentinels of water quality. Therefore, water quality monitoring is vital for the conservation of water resources and their sustainable use for irrigation and fish farming. The quality of surface water is mainly affected by natural processes (weathering and soil erosion) as well as anthropogenic inputs (municipal and industrial wastewater discharge). The anthropogenic discharges represent a constant polluting source, whereas surface runoff is a seasonal phenomenon, mainly affected by climatic conditions (Singh et al., 2004). The lagoon of Ain Al-Ghazala hosts a breeding site for the loggerhead sea turtle *Caretta caretta*. Mating occurs inside the lagoon (Pergent et al., 2007), while the egg deposition takes place outside along the sandy coastal region located to the east (Laurent et al., 1999). Lake Umm-Hufayn is home to a diverse range of fish, including mullet, sea bass, and tilapia, as well as being an important turtle hatching location and a haven for migratory birds (Abdalhamid et al., 2018).

Table (2). Differences in the means of water parameters, Independent Samples Test**,** T-test for Equality of Means

Water parameters		Sig.	t	Sig.	MD	Std. Error	95% CID	
							Lower	Upper
EC	EVA	.40	69.84	.00	33.42	.47	32.42	34.43
	EVNA		69.84	.00	33.42	.47	32.42	34.43
TDS	EVA	.43	70.01	.00	22.38	.31	21.71	23.06
	EVNA		70.01	.00	22.38	.31	21.71	23.06
pH	EVA	.18	.91	.37	.07	.07	-.09	.23
	EVNA		.91	.38	.07	.07	-.09	.23
Hrds.	EVA	.41	68.22	.00	3.87	.05	3.75	3.99
	EVNA		68.22	.00	3.87	.05	3.75	3.99
Alk.	EVA	.00	23.82	.00	1.67	.07	1.52	1.82
	EVNA		23.82	.00	1.67	.07	1.52	1.83
Cl	EVA	.12	51.54	.00	3.63	.07	3.49	3.78
	EVNA		51.54	.00	3.63	.07	3.48	3.78
NO_2	EVA	.51	61.63	.00	.10	.00	.10	.11
	EVNA		61.63	.00	.10	.00	.10	.11
NO_3	EVA	.07	10.65	.00	1.06	.10	.85	1.27
	EVNA		10.65	.00	1.06	.10	.84	1.29
SO_4	EVA	.39	52.41	.00	1.27	.02	1.24	1.32
	EVNA		52.41	.00	1.27	.02	1.24	1.32
PO_4	EVA	.37	68.25	.00	.22	.00	.21	.23
	EVNA		68.25	.00	.22	.00	.21	.23
SiO_2	EVA	.30	15.25	.00	.00	.00	.00	.00
	EVNA		15.25	.00	.00	.00	.00	.00
CO_3	EVA	.39	80.12	.00	.04	.00	.04	.04
	EVNA		80.12	.00	.04	.00	.04	.04
HCO_3	EVA	.21	57.10	.00	1.53	.02	1.48	1.59
	EVNA		57.10	.00	1.53	.02	1.48	1.59
Ca	EVA	.40	68.19	.00	3.28	.04	3.18	3.38
	EVNA		68.19	.00	3.28	.04	3.18	3.38
Mg	EVA	.11	23.93	.00	.60	.02	.55	.66
	EVNA		23.93	.00	.60	.02	.55	.66
Na	EVA	.39	65.30	.00	2.97	.04	2.87	3.07
	EVNA		65.30	.00	2.97	.04	2.87	3.07
K	EVA	.36	41.80	.00	.13	.00	.13	.14
	EVNA		41.80	.00	.13	.00	.13	.14

EC: electric conductivity, TDS: total dissolved solids, Hrds.: hardness, Alk.: alkalinity, EVA: Equal variances assumed, EVNA: Equal variances not assumed, LTEV: Levene's Test for Equality of Variances, 95%, MD: Mean Difference, CID: Confidence Interval of the Difference

CONCLUSION

The study found that the ecological characteristics of these lakes vary greatly. Some elements are over the allowable limits based on the standard limitations of the aquatic ecosystem. As a result, further research is needed to assess the anthropogenic activities that degrade water quality, and special care should be given to water management and the protection of the environment all around the lakes. The dumping of garbage and other urban waste products around the site must be strictly avoided, given the highly sensitive ecological balances that should be maintained. Urgent action should be taken to protect the lakes. Now that there is a definite underway to develop a hatchery and aquafarming complex at Ain Al- Ghazala and Umm-Hufayn lagoon, careful consideration should be given to the need for embarking on any additional large-scale capacity building for the national aquaculture sector in the near term.

REFERENCES

Abdalhamid, A., Ali, R., & El-Mor, M. (2018). Ali, SM and Elawad, AN (2018). Some Ecological and Biological Studies on the European eel Anguilla anguilla (Linnaeus, 1758) in Umm Hufayan brackish lagoon, eastern Libya Mediterranean Sea. *Bulletin de l'Institut Scientifique, Rabat, Section Sciences de la Vie*(40), 23-30.

Ademoroti, C. (1996). Standard methods for water and effluents analysis: Foludex Press Ltd., Ibadan.

Aduwo, A. I., & Adeniyi, I. F. (2019). The Physico-chemical water quality of the Obafemi Awolowo University teaching and research farm lake, OAU Campus, Ile-Ife, Southwest, Nigeria. *Journal of Environmental Protection, 10*(07), 881.

Awoyemi, O. M., Achudume, A. C., & Okoya, A. A. (2014). The physicochemical quality of groundwater in relation to surface water pollution in Majidun area of Ikorodu, Lagos State, Nigeria. *American Journal of Water Resources, 2*(5), 126-133.

Beutler, M., Wiltshire, K., Meyer, B., Moldaenke, C., Luring, C., Meyerhofer, M., & Hansen, U. (2014). APHA (2005), Standard Methods for the Examination of Water and Wastewater, Washington DC: American Public Health Association. Ahmad, SR, and DM Reynolds (1999), Monitoring of water quality using fluorescence technique: Prospect of on-line process control, Water Research, 33 (9), 2069-2074. Arar, EJ and GB Collins (1997), In vitro determination of chlorophyll a and pheophytin a in. *Dissolved Oxygen Dynamics and Modeling-A Case Study in A Subtropical Shallow Lake, 217*(1-2), 95.

Elmor, M. E., Ali, A. F., & Buzaid, E. M. (2020). First observation of Chelon labrosus (Risso, 1827) from Um-Hufayan Lagoon eastern Libya. *Al-Azhar Bulletin of Science, 31*(2-C), 1-9.

Elshakh, A. S., Ali, R. A. S., Ali, S. M., & Hussain, N. S. (2020). Some morphometric traits of *liza aurata* (risso, 1810) in Umm Hufayn brackish lagoon, eastern libya Mediterranean sea coast. *International Journal of Fisheries and Aquaculture Research, 7*(1).

Garg, R., Rao, R., & Saksena, D. (2009). Water quality and conservation management of Ramsagar reservoir, Datia, Madhya Pradesh. *Journal of Environmental Biology, 30*(5), 909.

Haddoud, D., & Rawag, A. (1995). Marine protected areas along Libyan coast. *DA*

Haddoud and AA Rawag. Tajura: Marine Biology Research Centre, 23-31.

Laurent, L., Bradai, M., Hadoud, D., El Gomati, H., & Hamza, A. (1999). Marine Turtle Nesting Activity Assessment on Libyan Coasts, Phase 3: Survey of the Coast to the West of Misratah. *RAC/SPA and UNEP, Tunis*.

Mahananda, H., Mahananda, M., & Mohanty, B. (2005). Studies on the physico-chemical and biological parameters of a fresh water pond ecosystem as an indicator of water pollution. *Ecology environment and conservation, 11*(3/4), 537.

Ngatia, L., Grace III, J. M., Moriasi, D., & Taylor, R. (2019). Nitrogen and phosphorus eutrophication in marine ecosystems. *Monitoring of marine pollution*, 1-17.

Okoro, B., Uzoukwu, R., & Chiomezie, N. (2014). River basins of Imo State for sustainable water resources management. *Journal of Civil and Environmental Engineering, 4*(1), 1-8.

Parashar, C., Dixit, S., & Shrivastava, R. (2006). Seasonal variations in physico-chemical characteristics in upper lake of Bhopal. *Asian J. Exp. Sci, 20*(2), 297-302.

Pergent, G., Djellouli, A., Hamza, A., Ettayeb, K., Alkekli, A., Talha, M., & Alkunti, E. (2007). Structure of Posidonia oceanica meadows in the vicinity of Ain al-Ghazala lagoon (Libya): the «macroatoll» ecomorphosis. Third Mediterranean symposium on marine vegetation. RAC/SPA Publ., Marseilles,

Team, E.-R. S. W. C. (2010). *Atlas of Wintering Waterbirds of Libya 2005-2010*.

Watson, S. B., & Lawrence, J. (2003). Overview-Drinking water quality and sustainability. *Water Quality Research Journal, 38*(1), 3-13.

تقييم جودة مياه البحيرات (بحيرة عين الغزالة وبحيرة أم حفين)، لاستزراع الأسماك بالساحل الشرقي، ليبيا

أماني فيتوري علي[1] ، أنور عبد الرحيم صالح[2]،الدوشي عبدالكريم مهدي[3] ، رشاد السيد محمد سعيد[3] واشرف ناجي مسعود[2]

[1]قسم الموارد البحرية، كلية الموارد الطبيعية وعلوم البيئة، جامعة طبرق، طبرق، ليبيا
[2]قسم علوم البيئة، كلية الموارد الطبيعية وعلوم البيئة، جامعة طبرق، طبرق، ليبيا
[3]قسم علم الحيوان، كلية العلوم، جامعة الأزهر، أسيوط ،مصر

تاريخ الاستلام: 12 أغسطس 2021 / تاريخ القبول: 14 مارس 2022
Doi:https://doi.org/10.54172/mjsc.v37i2.527

المستخلص : أجريت تقييمات لبعض الخصائص الفيزيائية والكيمائية في اثنين من المسطحات المائية الليبية (عين الغزالة وأم حفين). لكل نظام بيئي، تم اخذ عشر عينات مائية من عشر نقاط لغرض التحليل. وأظهرت النتائج أن الموصلية الكهربائية في مياه خليج عين الغزالة أعلى منها في مياه بحيرة أم حفين. في كلا المنطقتين، سجل الأس الهيدروجيني لتركيز أيون الهيدروجين أعلى قيم بقيمة 8.3 مع قيم متوسطة للكلوريد (Cl) تجاوزت الحدود المسجلة دوليًا. علاوة على ذلك، فإن النتريتات (NO2)، والنترات (NO3)، والكبريتات SO4، والفوسفات (PO4)، والسيليكات (SiO2)، والكربونات (CO3)، والكالسيوم (Ca)، والمغنيسيوم (Mg)، والصوديوم (Na)، والبوتاسيوم (K) كانت جميعها أعلى في مياه خليج عين الغزالة عنها في مياه بحيرة أم حفين. اخيرا، ينبغي اعطاء المزيد من الاهتمام إلى الحفاظ على هذه الموارد الطبيعية.

الكلمات المفتاحية : جودة المياه، الخصائص الفيزيائية والكيمائية، بحيرة عين الغزالة، بحيرة أم حفين.

*[1] أماني فيتوري amanifitori1@gmail.com قسم الموارد البحرية، كلية الموارد الطبيعية وعلوم البيئة، جامعة طبرق، طبرق، ليبيا.

Al-Mukhtar Journal of Sciences 37 (2): 120-126, 2022
ISSN: online 2617-2186 print 2617-2178
Journal Homepage https://omu.edu.ly/journals/index.php/mjsc/index

Determination of Heavy Metals in Henna Leaves and Cosmetic Henna Products Available in Zliten, Libya

Ismail A. Ajaj[1], Wafa K. Amhimmid [2*], Hala Ismail[1], Tahani Al-Arabi[1] and Khawla Al-Oraibi[1]

[1] *Chemistry Department, Alasmarya University , Zliten, Libya*
[2]*Chemistry Department, Azzaytuna, University, Tarhuna Libya*

Received: 06 November 2021/ Accepted: 18 May 2022
Doi: https://doi.org/10.54172/mjsc.v37i2.372

Abstract: Henna is widely used by Libyan women as a cosmetic, which may contain lead (pb), cadmium (Cd) and other toxic heavy metals. The purpose of this study was to determine heavy metal content of seven henna products, imported and locally produced in Zliten, Libya. An analytical method was performed using Atomic Absorption Spectrophotometer (AAS). In terms of heavy metal content determination, the results revealed a significant difference between henna leaves and cosmetic henna samples. The premixed henna sample H2 had the highest heavy metal concentrations with a high level of lead (6.952ppm), exceeding the WHO's maximum limit and the (ASEAN) Guidelines on Limits of Contaminants for Cosmetics Heavy metal maximum limits, Lead (Pb) is 1 ppm. Nickel (Ni) levels in (H4=5.201ppm) and (H6=2.023ppm) henna samples were found to be above the WHO's limit of 1.68ppm. The results indicated that such cosmetics expose consumers to high levels of Pb and Cu, and hence to potential health risks. Thus، investigating the sources and effects of heavy metals in such cosmetics is strongly advised.

Keywords: Heavy metal, Henna leaves, Henna Products, Toxic levels.

INTRODUCTION

Henna, scientifically known as Lawsonia inermis, is a plant in the Lythraceae family. It grows best in tropical climates across all of Africa, northern Australia, and southwest Asia (Chaudhary et al., 2010; Gevrenova, 2010), and it is well known for its cosmetic and therapeutic properties. According to ethnobotanical and historical evidence, henna was one of the first plants to be used for cosmetic purposes (Ozbek, 2018). Henna painting was done in ancient Egypt and its neighboring countries. Henna is extremely popular in Libya because it is part of the culture and traditions. The Libyan market offers a wide range of henna products in a variety of colors. Some are produced locally, while others are imported from Sudan, Yemen, Tunisia, India, and Pakistan. Unfortunately, in recent years, henna has become a potentially life-threatening substance for Libyan women, particularly in the eastern region of the country, where more than 550 cases of henna poisoning have been reported, with 57 deaths, according to the Libyan Ministry of health. Until today, scientific information about the true causes of these widespread poisoning and death cases remained unknown. Despite the seriousness of the problem, published studies on henna in Libya are rare (Kumar & Kathireswari, 2016). Therefore, it is necessary to determine the levels of heavy metals in henna leaves and henna products in order

***Corresponding author:** Wafa K. Amhimmid: khlwafaa321@gmail.com, Chemistry Department, Azzaytuna, University, Tarhuna Libya

to identify the heavy metals ratio and protect henna users from the toxic effects of heavy metals.

Henna contains tannin product called Lawsone (2-hydroxy-1,4 naphthoquinone), which is responsible for the henna dye at concentrations ranging from 1.0 to 1.5%. Lawsone is extracted from henna leaves (Singh et al., 2005). Lawsone is a compound that imparts the characteristic red-orange pigmentation that makes the skin, nails, and hair look beautiful and appealing (DeLeo, 2006). The henna plant as a whole contains xanthones, coumarins (fraxetin and scopletin), flavanoides, luteolins, apigenin and its glycosides, and steroids (β-sitosterol). In addition to organic compounds, henna plants absorb heavy metal ions from the soil and later are accumulated in other parts such as leaves, the heavy metals that are available for plant uptake are those that are present as soluble components in soil solution or those that are easily solubilized by root exudates, however, excessive amounts of these metals can be toxic to plants. Plants' ability to accumulate essential metals also allows them to acquire nonessential metals. metals cannot be broken down, so when concentrations within the plant exceed optimal levels, they adversely affect the plant both directly and indirectly (Khattak & Khattak, 2011).

The chemical structure of the henna dye molecule places it in the class of dyes known as α-hydroxy-naphthoquinones. There are very rare reactions to the lawsone compound in henna leaves, which are mainly caused by naphthoquinone sensitivity (Kang & Lee, 2006). To make it more permanent or stronger, marketed henna is often mixed with various herbs and different chemical additives (which contain high levels of trace elements) and synthetic dyes such as para-phenylenediamine (PPD) (Aktas Sukuroglu et al., 2017). However, such additives have toxic side effects ranging from mild irritation to more severe allergic reactions exhibited through blisters, lesions, and sores on the skin, Natural henna is generally safe and well-tolerated in humans, but henna containing additives may cause side effects or even death (Fahad, 2016; Swift, 1997). Heavy metal contamination in cosmetic products is a significant environmental and health concern because the metals are toxic (Alissa & Ferns, 2011). Some of the toxic effects of lead include hematological, cardio-vascular and neurobehavioral complications such as encephalopathy, depression and malaise (Control & Prevention, 2005; Kollmeier et al., 1990). Cadmium has been linked to oestomalacia as well as respiratory effects such as pulmonary fibrosis, pneumonitis, emphysema and lung cancer. Nickel is a strong allergen and the primary cause of skin sensitivity (Bobaker et al., 2019).

Figure: (1). shows the Adverse effects of premixed Henna products

The current study is primarily motivated by the urge to determine the heavy metal concentrations in the henna merchandise in the city of Zliten, Libya.

MATERIALS AND METHODS

Sample collection: In this study, two types of natural henna were used; the first was collected from a henna tree on one of Zliten's farms, and the second was prepared by drying and grinding the leaves. The other sample was a pre-prepared natural henna from an herbalist shop. And five types of commercial henna traded on the market were used. However, all henna products are sold without information about their chemical contents. and placed in bags weighing approximately 100

grams.

Table: (1). shows the names of henna samples and their symbols

Code	Sample
H1	Natural henna from the henna tree
H2	Natural henna from an aromatic store
H3	Premium Crown Henna
H4	Bride's henna
H5	Henna Gulf Cup
H6	Royal Al Haramain Henna
H7	Herbal henna

Sample Digestion: Using the dry burning method by weighting 5 grams per natural henna leaf and sold henna and placing it in an incineration oven at 450-500 ºC for 4-6 hours. The ashes were then washed with 5.1% nitric acid and the volume was completed up to 50 ml. The extract was ready to determine the concentration of heavy elements in samples studied using an Atomic Absorption Spectrophotometer,(AAS) Perkin Elmer Model 2380.

Figure: (2) The Atomic Absorption Spectrophotometer (AAS)

The pH values were measured by taking 0.5g of each henna sample and adding 70ml of distilled water into a 250ml flask with stirring until the henna is well combined with the water. A pH test was then performed using a pH meter (Fig.3).

Figure: (3). The PH device used to measure acidity in the Henna samples.

RESULTS

pH measurement: As shown in figure (4) below, the pH values of Henna samples were acidic in the range between 3.6 and 5.3.

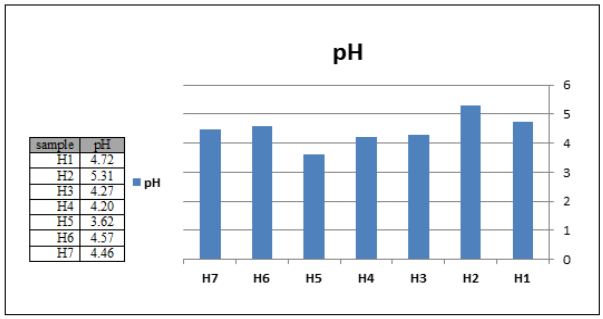

Figure: (4). pH values of Henna samples

Low pH (acidic) mixes are rich in hydrogens, which keep aglycones relatively stable until it is time to use the dye. This hydrogen-rich environment provided by the acid liquid allows for a longer and fuller dye-release as well as a more stable bond to keratin aglycones to bond to the keratin of the hair through a Michael Addition.

The low pH level of an acidic henna paste allows the aglycones to remain stable for a longer period of time. This allows for a slow, steady dye-release for the optimal amount of available aglyones. Mixing henna without an acid (such as using only water) will cause the paste to have a weaker dye release which demises faster. The optimal pH level for a henna mix is right around 5.5, which can be achieved with a number of fruit juices, or the use of a fruit acid powder and distilled water.

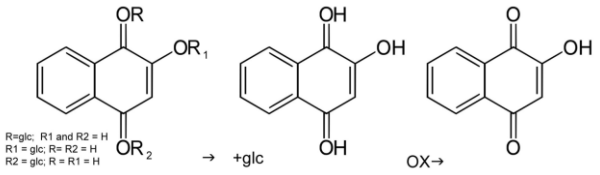

Figure (5). Hennocide precursors convert into an aglycone state in a low pH medium, and eventually oxidize to a stable molecule.

Heavy metals determination: Table (2) shows the results of AAS analysis of ten heavy metals in Henna samples, including Aluminum, Arsenic, Silver ,cadmium, chromium, copper, cobalt, lead, Nickel, and zinc. . The prepared standards of each metal and their corresponding absorbencies were used to plot calibration curves. The product-moment correlation coefficient factor and the equation for the line of regression were derived from calibration curve of each metal.

$$\text{Actual concentration} = \frac{Concentration\ \left(\frac{\mu g}{ml}\right)\ X\ Volume\ digested\ (ml)}{Weight\ of\ sample\ (g)} \ldots Eq\ (1)$$

The actual concentration of heavy metals in henna leaf samples obtained from AAS was derived using Equation (1) For dilutions, the actual weight was obtained by multiplying the readout results from AAS with the dilution factor.

Table:(2). Concentration of Heavy Metals in Henna Samples

Metal	Sample (Concentration ppm)						
	H1	H2	H3	H4	H5	H6	H7
Al	496.9	53.8	81.52	737.8	285.1	754.8	754.8
As	< 0.02	< 0.02	< 0.02	< 0.02	< 0.02	< 0.02	< 0.02
Ag	2.210	1.064	1.708	<0.002	<0.002	<0.002	<0.002
Cd	<0.002	<0.002	<0.002	<0.002	<0.002	<0.002	<0.002
Cr	0.562	<0.002	<0.002	0.678	0.063	3.69	0.193
Cu	4.273	7.570	6.628	5.96	5.014	5.078	5.208
Co	< 0.005	< 0.005	< 0.005	< 0.005	< 0.005	< 0.005	< 0.005
Pb	< 0.03	6.952	< 0.03	< 0.03	< 0.03	< 0.03	< 0.03
Ni	0.669	1.642	< 0.01	5.201	0.874	2.023	0.395
Zn	10.219	4.736	21.72	-	-	-	10.99

DISCUSSION

Seven different cosmetic henna products were tested in this study to determine the concentration of some heavy metals. Aluminum and copper metals were detected in all samples, while zinc was detected in four. Although some metals, such as chromium, copper, aluminum, and zinc, play important biochemical roles in many organisms at low concentrations, their toxic effects are observed at high concentrations. All of these metals can damage or impair central nervous system functions, as well as blood composition, lungs, kidneys, liver, and other vital organs. Long-term exposure may cause slow-progressive physical, muscular, and neurological degeneration processes such as Alzheimer's disease, Parkinson's disease, muscular dystrophy, and multiple sclerosis. Despite the fact that EU regulation suggests that the concentration of some heavy metals, such as chromium, in color additive cosmetics should be 1.0 mg/kg (Borowska & Brzóska, 2015), one sample [H6=3.69ppm] had a chromium concentration higher than the EU standard in cosmetic products. The presence of chromium in the body facilitates glucose entry into cells (Krejpcio, 2001). On the other hand, exposure to high levels of chromium, on the other hand, has been linked to kidney and lung damage, as well as other cancers. Chromium has also been linked to skin effects such as eczema and other skin inflam-

mations (Umar & Caleb, 2013).

Table 2 shows that the lead content of one sample exceeded the WHO's recommended maximum limit for cadmium in cosmetics. Zinc was detected in four samples. According to (Zafar Alam et al., 2009), zinc oxide was probably used in cosmetics due to its powerful natural sunblock property. Furthermore, zinc is also required for oxygen metabolism and mitochondrial function (Popoola et al., 2013). These toxic metals may enter the products when low-quality raw materials are used.

CONCLUSION

According to the findings of this study, henna leaves from Zliten are a good raw material for henna products due to their low levels of lead, cadmium and nickel in comparison to WHO standard limits. Henna leaves had lower significant levels of Pb, Cd and Ni as raw materials than henna products, but more of these metals were added during the manufacturing process. the concentrations of Lead and copper in the H2 premixed henna sample exceeded the WHO's maximum allowable limits. Therefore it conceder dangerous product. As a result, the general public should be educated about the dangers of long-term use of toxic cosmetic products. Extensive and continuous use of these cosmetic products may cause the slow release of heavy metals and endangering consumers. National standard legislations for cosmetic products should be available to monitor the safety of these products before they are imported and reach consumers. However, more research is needed to assess the metals concentrations in various types of cosmetics and body care products in order to protect consumer health.

REFERENCES

Aktas Sukuroglu, A., Battal, D., & Burgaz, S. (2017). Monitoring of Lawsone, p‐phenylenediamine and heavy metals in commercial temporary black henna tattoos sold in Turkey. *Contact dermatitis, 76*(2), 89-95 .

Alissa, E. M., & Ferns, G. A. (2011). Heavy metal poisoning and cardiovascular disease. *Journal of toxicology, 2011* .

Bobaker, A. M., Alakili, I., Sarmani, S. B., Al-Ansari, N., & Yaseen, Z. M. (2019). Determination and assessment of the toxic heavy metal elements abstracted from the traditional plant cosmetics and medical remedies: case study of Libya. *International journal of environmental research and public health, 16*(11), 1957 .

Borowska, S., & Brzóska, M. M. (2015). Metals in cosmetics: implications for human health. *Journal of applied toxicology, 35*(6), 551-572 .

Chaudhary, G., Goyal, S., & Poonia, P. (2010). Lawsonia inermis Linnaeus: a phytopharmacological review. *Int J Pharm Sci Drug Res, 2*(2), 91-98 .

Control, C. f. D., & Prevention. (2005). Preventing lead poisoning in young children .*http://www. cdc. gov/nceh/lead/Publications/PrevLeadPoisoning. pdf* .

DeLeo, V. A. (2006). p-Phenylenediamine. *Dermatitis, 17*(2), 53-55 .

Fahad, A. S. (2016). Henna beyond skin arts: literatures review .

Gevrenova, R. (2010). Determination of natural colorants in plant extracts by high performance liquid chromatography. *Journal of the Serbian Chemical Society, 75*(7), 903-915 .

Kang, I. J., & Lee, M. H. (2006). Quantification of para‐phenylenediamine and heavy metals in

henna dye. *Contact dermatitis, 5* ،(1)5 .29-26

Khattak, M. I., & Khattak, M. I. (2011). Study of heavy trace metals in some medicinal–herbal plants of Pakistan. *Pak. J. Bot, 43*(4), 2003-2009 .

Kollmeier, H., Seemann, J., Wittig, P., Rothe, G., & Müller, K.-M. (1990). Cadmium in human lung tissue. *International archives of occupational and environmental health, 62*(5), 373-377 .

Krejpcio, Z. (2001). Essentiality of chromium for human nutrition and health. *Polish Journal of Environmental Studies, 10*(6), 399-404 .

Kumar, K. S., & Kathireswari, P. (2016). Biological synthesis of Silver nanoparticles (Ag-NPS) by Lawsonia inermis (Henna) plant aqueous extract and its antimicrobial activity against human pathogens. *Int. J. Curr. Microbiol. App. Sci, 5*(3), 926-937 .

Ozbek, N. (2018). Elemental analysis of henna samples by MP AES. *Journal of the Turkish Chemical Society, Section A: Chemistry, 5*(2), 857-868 .

Popoola, O., Bisi-Johnson, M., Abiodun, A., & Ibeh, O. (2013). Heavy metal content and antimicrobial activities of some naturally occurring facial cosmetics in Nigeria. *Ife journal of science, 15*(3), 637-644 .

Singh, M., Jindal, S., Kavia, Z., Jangid, B., & Khem, C. (2005). Traditional methods of cultivation and processing of henna. *Henna, cultivation, improvement and trade*, 21-34 .

Swift, J. A. (1997). *Fundamentals of human hair science*. Micelle Press .

Umar, M., & Caleb, H. (2013). Analysis of metals in some cosmetic products in FCT-Abuja, Nigeria. *International Journal of Research in Cosmetic Science, 3*(2), 14-18 .

Zafar Alam, M ،.SMS, Z., Khan, U., Obaid, A., Sarwat, J., Aftab, S., Rabail, Z., & Misbah, Z. (2009). Kohl [SURMA]: retrospect and prospect .

تقدير العناصر الثقيلة في أوراق الحناء ومنتجات الحناء التجميلية في مدينة زليتن، ليبيا

إسماعيل عبدالرحمن عجاج[1]، وفاء خليفة أمحمد*[2]، هالة إسماعيل[1]، تهاني العربي[1] ، خولة العريبي[1]

[1] قسم الكيمياء، الجامعة الأسمرية، زليتن ، ليبيا

[2] قسم الكيمياء ، جامعة الزيتونة، ترهونة، ليبيا

تاريخ الاستلام: 06 نوفمبر 2021 / تاريخ القبول: 18 مايو 2022

Doi: https://doi.org/10.54172/mjsc.v37i2.372

المستخلص : تستخدم النساء الليبيات الحناء على نطاق واسع مستحضرا تجميلا، والتي قد تحتوي على الرصاص(Pb)، والكادميوم (Cd)، والعناصر الثقيلة السامة الأخرى. والغرض من هذه الدراسة تحديد محتوى العناصر الثقيلة من سبع عينات لمنتجات الحناء المستوردة، والمنتجة محليا المتداولة في مدينة زليتن، ليبيا. تم إجراء التحاليل باستخدام مطياف الامتصاص الذري (AAS). و كشفت النتائج عن وجود فرق كبير بين أوراق الحناء، وعينات الحناء التجميلية. عينة الحناء المصنّعة H2 أظهرت أعلى تركيزات المعادن الثقيلة؛ نتيجة تلوثها بمستوى عال من الرصاص (6.952ppm)، متجاوزة الحد الأقصى لمنظمة الصحة العالمية وهو 2 ppm، و كذلك متجاوزة معايير المنظمة الأسيوية (ASEAN)، وبشأن حدود الملوثات لمستحضرات التجميل الحد الأقصى للمعادن الثقيلة الرصاص هو 1 ppm. ومستويات النيكل (Ni) في عينات الحناء التجميلية (H4 = 5.201ppm)، و (H6 = 2.023ppm) لتكون فوق الحد الأقصى المسموح به لمنظمة الصحة العالمية، وهو 1.68 ppm. تركيزات كل من As , Co, Cu و Cd كانت في جميع العينات أقل من الحد المسموح به. وأشارت النتائج إلى أن مثل هذه المستحضرات التجميلية تعرض المستهلكين لمستويات عالية من العناصر الثقيلة السامة، وبالتالي إلى مخاطر صحية محتملة. لذا نوصي بشدة بضرورة إجراء المزيد من الدراسات لتحديد مصادر العناصر الثقيلة السامة في منتجات الحناء، والمستحضرات التجميلية المصنعة منها.

الكلمات المفتاحية : العناصر الثقيلة، أوراق نبات الحناء، منتجات الحناء، معدلات التسمم.

* وفاء خليفة أمحمد، khlwafaa321@gmail.com ، قسم الكيمياء ، جامعة الزيتونة ، ترهونة ، ليبيا.

Al-Mukhtar Journal of Sciences 37 (2): 127-137, 2022
ISSN: online 2617-2186 print 2617-2178
Journal Homepage https://omu.edu.ly/journals/index.php/mjsc/index

Determining the Prevalence of Bacterial Vaginosis and their Patterns of Susceptibility to Antibiotics among Benghazi Women, Libya

Noor alhooda M. Al-awkally[1*], Hamza K. Ibrahim[2], Nessren F. Mousa [3], Mareei. A. Ali [1], Abdlmanam S. Fakron [4], Nesrine M. Al-awkally [5], Muftah A. Nasib [4], Alreda M. Al-Awkally [6] & Fathia M. SenossI [7]

[1]*Department of Medical laboratory, Higher Institute of Science and Technology, Suluq, Libya*
[2]*Department of pharmacy, Higher Institute of medical Technology, Bani Waleed, Libya*
[3]*Department of Statistics, Faculty of arts and sciences, University of Benghazi, Libya*
[4] *Department of Microbiology, Faculty of Science, Omar Al Mukhtar University, Libya*
[5]*Department of Surgery, Alhaowari hospital, Benghazi, Libya*
[6] *Central Pharmacy, Ministry of health, Darna, Libya*
[7] *Department of Zoology, Faculty of Art and Science, Benghazi University, Libya*

Received: .07 December 2021/ Accepted: 16 March 2022
Doi: https://doi.org/10.54172/mjsc.v37i2.366

Abstract: Vaginal discharge in women is occasionally caused by aerobic bacterial organisms. The study aimed to determine the etiology of female vaginosis and their antibiotic sensitivity pattern. HV culture results, age, and sex of all female patients with suspected bacterial vaginosis were collected. High vaginal swabs were inoculated into MacConkey agar, 5% blood agar, and chocolate agar and then incubated at 37°C in the presence of 5% CO_2 for 24-48 h. The antimicrobial susceptibility testing was performed by the disk diffusion method. Ten different antibiotic discs were used: Amikacin, Augmentin, Ceftazidime, Ceftriaxone, Ciprofloxacin, Gentamicin, Levofloxacin, Meropenem, Septrin, and Clindamycin. After 24 hours, zones were measured in mm, and zone interpretations were in accordance with the National Committee for Clinical Laboratory Standards criteria guidelines. A total of 215 females were included in the study, the incidence of bacterial vaginosis was 18.6% (40/215). Females between 33 and 45 years old had a somewhat high prevalence (19/40:47.5%) of bacterial vaginosis. The most frequent isolates were 45% (18/40) *Escherichia coli* followed by 15% (6/40) *Strep pneumonia*. The in vitro susceptibility tests of the most common isolates showed high resistance levels to commonly used antibiotics such as Augmentin and Gentamycin. Whereas highly sensitive rates were observed for Ceftriaxone 70%, followed by Ciprofloxacin 57.5%. Ceftriaxone and Ciprofloxacin showed the best antibiotic sensitivity. Additional studies are necessary to recognize those bacterial species that cause vaginal infections and determine the susceptibility of those species to recently used antibiotics.

Keywords: Al saleem medical laboratory; Augmentin; Ceftriaxon; *E. coli*; *Strep pneumoniae.*

INTRODUCTION

The vagina is sterile at birth. After a few days, when maternal estrogen increases the glycogen levels of the epithelial cells, the baby's vagina is colonized by lactobacilli from the mother (Forsum *et al*., 2005). Protection of the vaginal mucosa depends on the specif-

***Corresponding author:** Noor alhooda M. Al-awkally: *noornooor1973@gmail.com* , Department of Medical laboratory, Higher Institute of Science and Technology, Suluq, Libya.

ic recognition of structures on the lactobacilli surface (adhesions) and the vaginal epithelium (receptors). This adhesion-receptor interaction results in forming a biofilm that exerts a local protective action against colonization by undesirable microorganisms (Boris et al., 1998; Szöke *et al.,* 1996). The physiologic pH of the vagina ranges from 3.8 to 4.5 (Watts *et al*., 2005). By using glycogen from the vaginal epithelium as substrate, lactobacilli produce organic acids, thus keeping the vaginal pH below 4.5. This acid environment partially or fully inhibits the development of most bacteria from both the digestive tract and the environment. This is considered a very efficient mechanism of mucosal protection (Martin *et al*., 2008)**.**

Besides *Lactobacillus* spp., other bacteria are frequently found in the vaginal microbiota of healthy women such as Streptococcus, Corynebacterium, Staphylococcus, Escherichia, Klebsiella, Proteus, Mycoplasma, Ureaplasma, Atopobium, Peptococcus, Peptostreptococcus, Clostridium, Bifidobacterium, Propionibacterium, Eubacterium, Bacteroides, Prevotella and Gardnerella vaginalis (Martin *et al*., 2008). Bacterial vaginosis (BV) is caused by an imbalance of the organisms (flora) that naturally exist in the vagina. BV is among the diseases most frequently associated with vaginitis. The other diseases are vulvovaginal candidiasis, and trichomoniasis. Vaginitis is usually characterized by vaginal discharge, vulvar itching, irritation, or odor (Prospero. 2014).

Vaginitis is the infection and inflammation of the vagina and is commonly encountered in clinical medicine (polat *et al*., 2021). Vaginal infections with bacterial vaginosis are a worldwide health problem for women (Go *et al*., 2006). Infections of the reproductive tract or genitourinary tract infections are a common problem of female sexual health and a significant risk of morbidity. Sexually transmitted diseases in women occur when there is an introduction of sexually transmitted organisms into the vagina, mostly through sexual activity. (Workowski & Berman, 2010) Aerobic vaginitis, like bacterial vaginosis, causes depletion of normal bacteria flora *Lactobacillus*. It is clinically characterized by the red and inflamed vagina, yellowish vaginal discharge with burning sensation and dyspareunia (Mumtaz l*et al*., 2008). Bacterial vaginosis and candidiasis are responsible for most vaginal infections in women of reproductive age. (polat *et al*., 2021 and Spinillo *et al.*, 1997).

They are commonly seen in females of reproductive age and typically present with vaginal discharge (Mylonas & Friese, 2007). Vaginal discharges are biological fluids contained within or expelled from the vagina (Ullah and Sana. 2014). Sometimes certain enteric bacteria like *Proteus* spp and *E. coli* may be found there. A vagina is an existing place for certain microbes. It is colonized with *E. coli,* Staphylococci, and Streptococci after delivery (Alawkally *et al*., 2022; Tripathi. 2003). Therefore, this study aimed to determine the etiology of female vaginosis and their antibiotic sensitivity pattern in Al Saleem Medical Laboratory, Benghazi, Libya.

MATERIALS AND METHODS

Specimen Collection and Processing: The study population included was 215 females, ranging in age from 20 to 58 years. Patients vaginal swabs were collected as each physician ordered. High vaginal (HV) culture results and age of all female patients with supposed bacterial vaginosis between February 2020 and November 2021 were retrieved. The information obtained comprises the presence of vaginal irritation, itching, and abnormal vaginal discharge. Vaginal swab samples were obtained from patients attending the Microbiology Laboratory of Al Saleem Medical Laboratory to diagnose bacterial vaginosis.

Culture and Sensitivity: High vaginal swab specimens were inoculated into MacConkey agar, 5% blood agar, and chocolate agar**.** The inoculated media were incubated at 37 °C aerobically for 24–72 hours. Conventional

phenotypic and biochemical methods made identification of the cultured isolate. (Fakron *et al*., 2022). McFarland's Standards are used as the reference to adjust the turbidity of the liquid/ bacterial suspension in the vial or tube in the microbiology laboratory before swab on Muller Hinton Agar media. It helps maintain and/or ensure that the number of bacteria will be within a given range to standardize microbial testing. The most commonly used concentration for antimicrobial susceptibility testing and the culture media performance testing is usually done by 0.5 McFarland standards in the microbiological laboratories (Fakron *et al*., 2022).

However, the used concentration for the antimicrobial susceptibility testing and the culture media performance testing is done by 0.5 McFarland standards in the microbiological laboratory (Jan. 2016). According to the manufacturer's instructions, the results were considered resistant (R) and susceptible (S), with intermediately resistant strains collected together as drug-resistant (Noor-alhooda *et al*., 2019**)**.

The following antimicrobial agents were employed: Amikacin-AK (30µg), Augmentin-AUG (30ug), Ceftazidime-CAZ (30mcg), Ceftriaxone-CRO (30µg), Ciprofloxacin-CIP (5µg), Gentamicin-GN (10µg), Levofloxacin-LEV, Meropenem-MER (30µg), Septrin-SXT (25ug) and Clindamycin (2µg) (Oxoid, England). Antimicrobial susceptibility testing was performed by the disc diffusion method.

Methodology: Entire data from the investigation were entered and analyzed using SPSS version 20.

RESULTS

Distribution of the growth of positive cases: A total of 215 females were included in the study. The incidence of bacterial vaginosis was 18.6% (40/215).

Table: (1). Distribution of the growth of positive cases.

High Vaginal Swab	Growth	No growth
Growth	40	18.6%
No growth	175	81.3%
Total	215	100%

Distribution of the growth of positive cases by age group: Bacterial vaginosis (BV) and its association with age are presented in Table 2. Females between 33 and 45 years old had a somewhat high prevalence (19/40: 47.5%) of bacterial vaginosis. In the age group 46-58 years (n=13), the incidence of BV is somewhat reduced to (32.5%).

Table: (2). Distribution of the growth of positive cases by age group

Age	Frequency	Percent
20-32	8	20
33-45	19	47.5
46-58	13	32.5
Total	40	100.0

Distribution of organisms from HVS samples: The most commonly isolated were gram-negative organisms. The most frequent isolates were 45% (18/40) *Escherichia coli* followed by 15% (6/40) *Strep pneumonia*, *Staph aureus* and *Strep agalactia* 12.5% (5/40) equally, *Klebsiella pneumonia* 7.5% (3/4), *Klebsiella* spp 5% (2/40) *and Pseudomonas aeruginosa* 2.5 % (1/40).

Table: (3). Types of Organisms isolated in Blood Culture

Bacteria	Frequency	%
E. coli	18	45.0
Klebsiella pneumonia	3	7.5
Klebsiella spp	2	5.0
Pseudomonas aeruginosa	1	2.5
Staph aureus	5	12.5
Strep agalactia	5	12.5
Strep pneumonia	6	15.0
Total	40	100.0

Prevalence of Bacterial infection in women age groups: A significant role in the etiology of vaginosis in female patients in this study was played by *E. coli* (45%). Vaginosis in the

present study was relatively higher among age groups of 33-45years compared to others.

Table:(4). Types of bacteria isolated according to the age group

Bacteria	Age			Total
	20-32	33-45	46-58	
E. coli	3	10	5	18
Klebsiella pneumonia	0	2	1	3
Klebsiella spp	1	1	0	2
Pseudomonas aeruginosa	0	1	0	1
Staph aureus	1	2	2	5
Strep agalactia	0	4	1	5
Strep pneumonia	0	4	2	6
Total	5	24	11	40

Antibiotic sensitivity, resistance and intermediate sensitivity of bacteria isolated from blood cultures: The in vitro susceptibility tests of the most common isolates showed high levels of resistance to commonly used antibiotics such as Augmentin, Gentamycin, and Septrin. All isolates were highly sensitive to Ceftriaxone 70%, followed by Ciprofloxacin 57.5%.

Antimicrobial susceptibility profiles of bacterial isolates from vaginal specimen: The antibiotic resistance patterns of *E. coli* showed higher resistance towards Augmentin, and *E. coli* strains were more sensitive to Ceftriaxone, Levofloxacin, and Ciprofloxacin. The antibiotic sensitivity patterns of *Strep pneumonia* showed higher resistance towards Levofloxacin and Gentamycin, and *Strep pneumonia* showed sensitivity to Augmentin and Ceftriaxone.

***Note*:** I; Intermediate, R; Resistant, S; Sensitive, AUG; Augmentin, MER; Merapenem, CRO; Ceftriaxone, CAZ; Ceftazidime, LEV; Levofloxacin, CN; Gentamycin, CIP, Ciprofloxacin, AK; Amikacin, SXT; Septrin, DA, Clindamycin.

Table: (5). Antibiotic sensitivity, resistance, and intermediate sensitivity of bacteria isolated from blood culture.

Drug	Susceptibility pattern	Frequency	%
Augmentin	Miss	1	2.5
	I	5	12.5
	R	14	35.0
	S	20	50.0
	Total	40	100.0
Merapenem	Miss	25	62.5
	R	2	5.0
	S	13	32.5
	Total	40	100.0
Ceftriaxone	Miss	5	12.5
	I	1	2.5
	R	6	15.0
	S	28	70.0
	Total	40	100.0
Ceftazidime	Miss	25	62.5
	I	2	5.0
	R	5	12.5
	S	8	20.0
	Total	40	100.0
Levofloxacin	Miss	8	20.0
	I	4	10.0
	R	8	20.0
	S	20	50.0
	Total	40	100.0
Gentamycin	Miss	6	15.0
	I	2	5.0
	R	18	45.0
	S	14	35.0
	Total	40	100.0
Ciprofloxacin	Miss	3	7.5
	I	8	20.0
	R	6	15.0
	S	23	57.5
	Total	40	100.0
Amikacin	Miss	16	40.0
	I	5	12.5
	R	8	20.0
	S	11	27.5
	Total	40	100.0
Ssptrin	Miss	17	42.5
	R	15	37.5
	S	8	20.0
	Total	40	100.0
Clindamycin	Miss	25	62.5
	R	5	12.5
	S	10	25.0
	Total	40	100.0

Table: (6). Antimicrobial susceptibility profiles of bacterial isolates from vaginal specimen Augmentin

Bacteria	Not available (NA)	I	R	S	Total
E. coli	0	3	10	5	18
Klebsiella pneumonia	0	1	0	2	3
Klebsiella spp	1	0	1	0	2
Pseudomonas aeruginosa	0	0	1	0	1
Staph aureus	0	0	0	5	5
Strep agalatia	0	0	2	3	5
Strep pneumonia	0	1	0	5	6
merapenem					
E. coli	11	0	0	7	18
Klebsiella pneumonia	3	0	0	0	3
Klebsiella spp	0	0	0	2	2
Pseudomonas aeruginosa	1	0	0	0	1
Staph aureus	3	0	1	1	5
Strep agalactia	3	0	1	1	5
Strep pneumonia	4	0	0	2	6
Ceftriaxone					
E. coli	0	1	2	15	18
Klebsiella pneumonia	1	0	0	2	3
Klebsiella spp	0	0	2	0	2
Pseudomonas aeruginosa	0	0	1	0	1
Staph. aureus	1	0	0	4	5
Strep agalactia	1	0	1	3	5
Strep pneumonia	2	0	0	4	6
Ceftazidime					
E. coli	10	1	1	6	18
Klebsiella pneumonia	2	0	0	1	3
Klebsiella spp	1	0	1	0	2
Pseudomonas aeruginosa	0	0	1	0	1
Staph aureus	5	0	0	0	5
Strep agalactia	2	0	2	1	5
Strep pneumonia	5	1	0	0	6
Levofloxacin					
E. coli	3	1	2	12	18
Klebsiella pneumonia	0	1	2	0	3
Klebsiella spp	0	0	0	2	2
Pseudomonas aeruginosa	0	1	0	0	1
Staph. aureus	4	0	0	1	5
Strep agalactia	1	0	1	3	5
Strep pneumonia	0	1	3	2	6
Gentamycin					
E. coli	4	1	6	7	18
Klebsiella pneumonia	0	1	1	1	3
Klebsiella spp	0	0	2	0	2
Pseudomonas aeruginosa	0	0	1	0	1
Staph. aureus	1	0	3	1	5
Strep agalactia	1	0	2	2	5
Strep pneumonia	0	0	3	3	6
Ciprofloxacin					
E. coli	0	2	3	13	18
Klebsiella pneumonia	1	1	1	0	3
Klebsiella spp	1	0	0	1	2
Pseudomonas aeruginosa	0	0	0	1	1
Staph aureus	0	1	1	3	5
Strep agalactia	1	1	0	3	5
Strep pneumonia	0	3	1	2	6

Amikacin					
E. coli	3	4	5	6	18
Klebsiella pneumonia	2	1	0	0	0
Klebsiella spp	1	0	0	1	1
Pseudomonas aeruginosa	0	0	0	1	1
Staph. aureus	3	0	1	1	1
Strep agalactia	4	0	0	1	1
Strep pneumonia	3	0	2	1	1
Septrin					
E. coli	6	0	5	7	18
Klebsiella pneumonia	1	0	2	0	3
Klebsiella spp	2	0	0	0	2
Pseudomonas aeruginosa	1	0	0	0	1
Staph. aureus	3	0	2	0	5
Strep agalactia	1	0	4	0	5
Strep pneumonia	3	0	2	1	6
Total	17	0	15	5	40
Clindamycin					
E. coli	9	0	4	5	18
Klebsiella pneumonia	2	0	0	1	3
Klebsiella spp	2	0	0	0	2
Pseudomonas. aeruginosa	1	0	0	0	1
Staph aureus	3	0	0	2	5
Strep agalactia	5	0	0	0	5
Strep pneumonia	3	0	1	2	6
Total	25	0	5	10	40

Distribution of growth positive cases by years: 60% of positive cases were recorded in 2021.

Table: (7). Distribution of growth of positive cases by years.

Year	Frequency	%
2020	16	40.0
2021	24	60.0
Total	40	100.0

Distribution of the growth of positive cases by seasons: 30% of the cases were recorded in the winter and 22.5% in summer.

Table: (8). Distribution of the growth of positive cases by seasons.

Season	Frequency	%
12-2	12	30.0
3-5	7	17.5
6-8	9	22.5
9-11	12	30.0
Total	40	100.0

Distribution of isolates by years: According to table 9, 32.5% incidence of *E. coli* was recorded in 2021.

Table: (9). Distribution of isolates by years

Bacteria/year	2020	2021	Total
E. coli	5	13	18
Klebsiella pneumonia	1	2	3
Klebsiella spp	0	2	2
Pseudomonas aeruginosa	1	0	1
Staph aureus	2	3	5
Strep agalactia	3	2	5
Strep pneumonia	4	2	6
Total	16	24	40

Distribution of isolates by months: The rate of isolation of *E. coli* was highest in months 2-12, followed by months 3-5.

Table: (10). Distribution of isolates by months

Months					
Bacteria	2-12	3-5	6-8	9-11	Total
E. coli	9	6	1	2	18
Klebsiella pneumonia	0	1	0	2	3
Klebsiella spp	0	0	2	0	2
Pseudomonas aeruginosa	0	0	0	1	1
Staph aureus	2	0	1	2	5
Strep agalactia	0	0	2	3	5
Strep pneumonia	1	0	3	2	6
Total	12	7	9	12	40

DISCUSSION

In bacterial vaginosis (BV), a condition characterized by an increased vaginal pH and milky discharge, the normal vaginal flora is substituted by a diverse flora of aerobic, anaerobic, and microaerophilic species (Mumtaz et al., 2008). In the current study, the overall prevalence rate of bacterial vaginosis was 18.6%. An earlier study done by (Mohammed et al., 2016) reported prevalence rates of bacterial vaginosis in 15.4%–19.4%. Lower prevalence rates of bacterial vaginosis than those in this study were reported from Botswana (38%) (Das et al., 1996).

In the present study, the most common BV was *E. coli,* with 34%, according to Table 10. The incidence of *E. coli* is the highest among all cases. Similar studies were conducted in India by (Donders et al., 2009; Orish et al., 2016; Ravishankar & Prakash, 2017) also imply that the cause of vaginitis is *E. coli*. It is mentioned as one of the most common causes of vaginitis and is sometimes isolated alone. In the studies prepared by Ravishankar and Das et al., 1996; Ravishankar & Prakash, 2017) (44%) *E. coli* was the most common isolated organism.

Strep pneumoniae, however, is not a part of the normal vaginal flora. It is presumed that Pneumococci cannot persist at normal vaginal pH. But during pregnancy and puerperium, changes in vaginal pH may temporarily permit it to occur as a vaginal commensal (Galea et al., 2014). Primary pneumococcal infection of the female genital tract may occur through the insertion of an intrauterine device such as the use of tampons or the postpartum period (Hutchison et al., 1984), or as a normal respiratory commensal during orogenital sexual practices. Infection transmittable via gastrointestinal tract Pneumococci has rarely been isolated as an intestinal pathogen (Petti et al., 2002). But it may colonize the perineum and introitus vaginae giving rise to bartholinitis, colonization of vagina and cervix leading to infection or infection via lymphatics, or infections via the bloodstream (Adnan et al., 2008).

The second most common isolates in the current study are *strep pneumonia* 15%. The isolation rate was highest among 33-45-year-olds (19/40:47.5%), followed by 46-58 years of age (13/40:32.5%). The maximum number of infections was found in the 31–40 year age group 101/258). Because of the prevalent use of antibiotics, especially in developing countries, the resistance profile of microorganisms is changing, as evidenced by the increasing rate of antibiotic resistance among bacterial populations (Farrar, 1985).

The in vitro sensitivity tests of the most common isolates showed high resistance levels to commonly used antibiotics such as Augmentin, Gentamycina, and Septrin. Ceftriaxone is a third-generation cephalosporin that was more effective. This high antibacterial susceptibility by the cephalosporin was found to be in accordance with the works of Ravishankar and Mumtaz and his colleagues (Ravishankar & Prakash, 2017). All isolates were highly sensitive to Ceftriaxone followed by Ciprofloxacin. This high antibacterial sensitivity by the Ceftriaxone is in accordance with the work of (Mumtaz *et al.,* 2008) 32.5% and Levofloxacin 30%.

In the antibiogram study, isolates belonging to *E. coli* are highly sensitive to Ciprofloxacin. As similar to a study done by Bibi Ayesha *et al*., 2014), (Abera & Kibret, 2011; Mumtaz *et al*., 2008) showing that *E. coli* is highly sensitive to Ciprofloxacin 21%. In this study, *E.coli* showed high levels of resistance (25 %) to Augmentin 25%. This study establishes that *E. coli* was more resistant to Augmentin 30% (Singh *et al.,* 2016). High-risk groups could be targeted more efficiently. This study is a step in familiarizing sensitivity and resistance patterns to used antibiotics, preventing resistance and thus preventing chronic sequelae. Thus, the present study raises the question of changing the syndromic protocol to treatment based on culture sensi-

tivity. Substantial health gains with a reduction of the disease burden among women should be the long-term goal of treatment which should be intended with knowledge of cultural sensitivity.

CONCLUSION

Comprehensive healthcare education aimed at reducing bacterial vaginosis is favorable. The most common bacterial vaginosis were *Escherichia coli* and *Streptococcus pneumonia*. Infection should be screened and vaccinated, especially if the women were infected with *Streptococcus pneumonia*. Ceftriaxone and Ciprofloxacin showed the best antibiotic sensitivity. Females with vaginitis should frequently be cultured with vaginal samples, and the drug sensitivity pattern of each isolate should be recognized. Further studies are encouraged to identify other bacterial species involved in vaginal infections and determine the susceptibility of these species to newly introduced antibiotics.

REFERENCES

Abera, B., & Kibret, M. (2011). Bacteriology and antimicrobial susceptibility of otitis media at dessie regional health research laboratory, Ethiopia. *Ethiopian Journal of Health Development, 25*(2), 161-167 .

Adnan, E. K., Aymen H, E. E., & Nasser Yehia A, A. (2008). *Streptococcus pneumoniae* as a cause of early onset neonatal sepsis: first report from Kuwait .

Agarwal, S K et al. (2900). "Antifungal activity of anthraquinone derivatives from Rheum emodi." *Journal of ethnopharmacology* vol. 72,1-2 43-6. doi:10.1016/s0378-8741(00)00195-1

Alawkally, Noor Alhooda & Nag, Miftah & Ali, Maree & Al-Awkally, Nesrine & Al-Awkally, Abeer & Al-Awkally, Alreda. (2022). Antibiotic sensitivity of *Escherichia coli* isolated from different clinical specimens of patient human in Al-jala hospital-Benghazi Libya. International Journal of Current Research in Science Engineering & Technology. 8. Pages: 509-517

Bibi Ayesha.، Sana Jabeen., Muhammad Ismail., Sayyed Salman., Sana Ullah, Zeeshan Niaz., Tauseef Ahmad. (2014). Isolation, Identification And Antibiotic Susceptibility Testing Of Microorganisms From Female Patients Of Ayub Medical Complex Through High Vaginal Swab. Sci.Int.(Lahore),26(4),1581-1586, ISSN 1013-5316; Coden: Sinte 8

Boris, S., Suárez, J. E., Vázquez, F., & Barbés, C. (1998). Adherence of human vaginal lactobacilli to vaginal epithelial cells and interaction with uropathogens. *Infection and immunity, 66*(5), 1985-1989 .

Das, C., Pattnaik, P., & Sahoo, P. (1996). Prevalence of vaginal infection in preterm labour. *Antiseptic, 93*(4), 140-143 .

Donders, G., Van Calsteren, K., Bellen, G., Reybrouck, R., Van den Bosch, T., Riphagen, I., & Van Lierde, S. (2009). Predictive value for preterm birth of abnormal vaginal flora, bacterial vaginosis and aerobic vaginitis during the first trimester of pregnancy. *BJOG: An International Journal of Obstetrics & Gynaecology, 11* .1324-1315 ،(10)6

Farrar, W. E. (1985). Antibiotic resistance in developing countries. *The Journal of infectious diseases, 152*(6), 1103-1106 .

Fakron, A., Alawkally, N., El- warred, S., Aldouakali Ali , M., El-amari , M., Awkally, A., Soutiyah, M., Suliman, N. and Ibrahim, H. (2022). Risk Factors for Ciprofloxacin and Gentamycin

Resistance among Gram Positive and Gram Negative Bacteria Isolated from Community-Acquired Urinary Tract Infections in Benghazi city. *Scientific Journal for the Faculty of Science-Sirte University*. 2, 1 (Apr. 2022), 76-87. DOI:https://doi.org/10.37375/sjfssu.v2i1.204.

Forsum, U., Holst, E., Larsson, P.-G., Vasquez, A., Jakobsson, T., & Mattsby-Baltzer, I. (2005). Bacterial vaginosis–a microbiological and immunological enigma. *Apmis, 113*(2), 81-90 .

Galea, G., Abela, R., Deguara, C., Cuschieri, P., & Brincat, M. P. (2014). Puerperal Streptococcus *pneumoniae endometritis*: a case report and literature review .

Go, V. F., Quan ،V. M., Celentano, D. D., Moulton, L. H., & Zenilman, J. M. (2006). Prevalence and risk factors for reproductive tract infections among women in rural Vietnam. *Southeast Asian Journal of Tropical Medicine and Public Health, 37*(1), 185 .

Hutchison, C., Kenney, A., & Eykyn, S. (1984). Maternal and neonatal death due to pneumococcal infection. *Obstetrics and gynecology, 63*(1), 130-131 .

Noor-alhooda Milood Al-awkally, Maree DokallyAli, ReedaMiloud Al-awkally, Abeer Miloud AL-awkally, Fowziya M. Ali and Ahmed Abouserwel. (2019). Antibiotic Susceptibility and Resistant Pattern of Isolates of Pseudomonas aeruginosa recovered from Infected Swabs, Abscess, Burn, Medical Tips and Blood from Patients at 4 Geographical Locations in Libya (Al-Bayda, Shahat, Derna and Benghazi). Int.J.Curr.Microbiol.App.Sci. 8(10): 143-149. doi:https://doi.org/10.20546/ijcmas.2019.810.015

Martin, R., Soberon, N., Vazquez, F., & Suárez, J. E. (2008). Vaginal microbiota: composition, protective role, associated pathologies, and therapeutic perspectives. *Enfermedades Infecciosas y Microbiología Clínica, 26*(3), 160-167 .

Mohammed, M. A., Alnour, T. M., Shakurfo, O. M., & Aburass, M. M. (2016). Prevalence and antimicrobial resistance pattern of bacterial strains isolated from patients with urinary tract infection in Messalata Central Hospital, Libya. *Asian Pacific journal of tropical medicine, 9*(8), 771-776 .

Mumtaz, S., Ahmad, M., Aftab, I., Akhtar, N., ul Hassan, M., & Hamid, A. (2008). Aerobic vaginal pathogens and their sensitivity pattern. *J Ayub Med Coll Abbottabad, 20*(1), 113-117 .

Mylonas, I., & Friese, K. (2007). Genital discharge in women. *MMW Fortschritte der Medizin, 149*(35-36), 42-46; quiz 47 .

Orish, V. N., Ofori-Amoah, J., François, M., Silverius, B. K & ،.Mensah, E. K. (2016). Microbial and antibiotic sensitivity pattern of high vaginal swab culture results in sekondi-takoradi metropolis of the western region of ghana: retrospective study. *European Journal of Clinical and Biomedical Sciences, 2*(5), 45.50-

Polat IH, Marin S, Ríos J, et al. (2021). Exploratory and confirmatory analysis to investigate the presence of vaginal metabolome expression of microbial invasion of the amniotic cavity in women with preterm labor using high-performance liquid chromatography. Am J Obstet Gynecol ;224:90.e1-9.

Petti, C. A., Ignatius Ou, S.-H., & Sexton, D. J. (2002). Acute terminal ileitis associated with *pneumococcal bacteremia*: case report and review of pneumococcal gastrointestinal diseases. *Clinical Infectious Diseases, 34*(10), e50-e53 .

Ravishankar, N., & Prakash, M. (2017). Antibiogram of bacterial isolates from high vaginal swabs of pregnant women from tertiary care hospital in Puducherry. *India IJCMAS, 6*, 964-972 .

Singh ،S., Swain, S., Das, L., Das, P. C., & Sahoo, S. (2016). Isolation and characterization of organisms in high vaginal swab culture in preterm pregnancy (28-37 week). *International Journal of Reproduction, Contraception, Obstetrics and Gynecology, 5*(11), 385 .3859-3

Spinillo, A., Bernuzzi, A. M., Cevini, C., Gulminetti, R., Luzi, S., & De Santolo, A. (1997). The relationship of bacterial vaginosis, Candida and Trichomonas infection to symptomatic vaginitis in postmenopausal women attending a vaginitis clinic. *Maturitas, 27*(3), 253-260 .

Szöke, I., Pascu, C., Nagy, E., LJUNG, A., & Wadstrom, T. (1996). Binding of extracellular matrix proteins to the surface of anaerobic bacteria. *Journal of medical microbiology, 45*(5), 338-343 .

Tripathi, G. (2003). *Potentials Of Living Resources*. Discovery Publishing House

Ullah, Sana. (2014). Isolation, Identification and Antibiotic Susceptibility Testing of Microorganisms from Female Patients of Ayub Medical Complex Through High Vaginal Swab. Science International. 26. 1581-1587.

Watts DH, Fazzari M, Minkoff H, Hillier SL, Sha B, Glesby M, Levine AM, Burk R, Palefsky JM, Moxley M, Ahdieh-Grant L, Strickler HD. (2005). Effects of bacterial vaginosis and other genital infections on the natural history of human papillomavirus infection in HIV-1-infected and high-risk HIV-1-uninfected women. J Infect Dis. 2005 Apr 1;191(7):1129-39. doi: 10.1086/427777. Epub 2005 Feb 21. Erratum in: J Infect Dis. Sep 1;192(5):943. Fazarri, Melissa [corrected to Fazzari, Melissa]. PMID: 15747249.

Workowski, K. A., & Berman, S. M. (2010). Sexually transmitted diseases treatment guidelines .

تحديد مدى انتشار التهاب المهبل البكتيري وأنماط تحسسها للمضادات الحيوية بين نساء بنغازي ، ليبيا

نور الهدى ميلود العوكلي[1]، حمزة خليفة أبراهيم[2]، نسرين فرج موسى[3]،مرعي الدوكالي علي[1] ،عبد المنعم سعد فكرون[4]، نسرين ميلود العوكلي[5]، مفتاح عبدالواحد نصيب[4]، الرضا ميلود العوكلي[6]، وفتحيه مسعود السنوسي[7]

[1] قسم المختبرات الطبية، المعهد العالي للعلوم والتكنولوجيا، سلوق، ليبيا

[2] قسم الصيدلة، المعهد العالي للعلوم والتكنولوجيا، بني وليد، ليبيا

[3] قسم الإحصاء، كلية الآداب والعلوم، جامعة بنغازي، ليبيا

[4] قسم الأحياء الدقيقة، كلية العلوم، جامعة عمر المختار، ليبيا

[5] قسم الجراحة، مستشفى الهواري، بنغازي، ليبيا

[6] الصيدلية المركزية، وزارة الصحة، درنة . ليبيا

[7] قسم علم الحيوان، كلية الآداب والعلوم، جامعة بنغازي، ليبيا

تاريخ الاستلام: 07 ديسمبر 2021/ تاريخ القبول: 16 مارس 2022

Doi:https://doi.org/10.54172/mjsc.v37i2.366

المستخلص : تحدث الإفرازات المهبلية عند النساء أحيانًا بسبب الكائنات البكتيرية الهوائية. هدفت الدراسة إلى تحديد مسببات التهاب المهبل الأنثوي، ونمط حساسيتها للمضادات الحيوية. تم جمع نتائج مزارع أعلى عنق المهبل، وعمر، وجنس جميع المرضى الإناث المصابات بالتهاب المهبل الجرثومي المفترض. تم زرع مسحات أعلى المهبل في وسط أجار ماكونكي، و 5 ٪ أجار الدم، وأجار الشوكوليت ثم تم تحضينها عند 37 درجة مئوية في وجود 5 ٪ من ثاني أكسيد الكربون لمدة 24–48 ساعة. تم إجراء اختبار الحساسية لمضادات الميكروبات عن طريق طريقة انتشار القرص. تم استخدام عشرة أقراص مضادات حيوية مختلفة: أميكاسين ، أوجمنتين ، سيفتازيديم ، سيفترياكسون ، سيبروفلوكساسين ، جنتاميسين ، ليفوفلوكساسين ، ميروبينيم ، سبترين وكليندامايسين. بعد 24 ساعة ، تم قياس المناطق بالملليمتر ، وكانت تفسيرات المناطق من قبل اللجنة الوطنية لمعايير معايير المختبرات السريرية. تم اشتمال إجمالي 215 أنثى في الدراسة، وبلغت نسبة الإصابة بالتهاب المهبل الجرثومي 18.6٪ (215/40). كان معدل انتشار التهاب المهبل البكتيري بين الإناث بين 33، و 45 عامًا مرتفعًا إلى حد ما (40/19: 47.5٪). كانت العزلات الأكثر شيوعاً 45٪ (40/18) الإشريكية القولونية تليها 15٪ (40/6) بكتيريا الالتهاب الرئوي العقدي. أظهرت اختبارات الحساسية في المختبر للعزلات الأكثر شيوعًا مستويات مقاومة عالية للمضادات الحيوية الشائعة الاستخدام مثل أجومنتين، و جنتامايسين. في حين لوحظت معدلات حساسية عالية لسيفترياكسون 70٪، يليه سيبروفلوكساسين 57.5٪. أظهر سيفترياكسون، وسيبروفلوكساسين أفضل تحسس في المضادات الحيوية. من الضروري إجراء دراسات إضافية للتعرف على تلك الأنواع البكتيرية التي تسبب الالتهابات المهبلية، وتحديد مدى تحسس هذه الأنواع للمضادات الحيوية المستخدمة مؤخرًا.

الكلمات المفتاحية : مختبر السليم الطبي، أجومنتين، سفترياكسون، الإشريكية القولونية، بكتيريا الالتهاب الرئوي العقدي.

*[1] نور الهدى ميلود العوكلي: noornooor1973@gmail.com قسم المختبرات الطبية ، المعهد العالي للعلوم والتكنولوجيا ، سلوق ، ليبيا.

Al-Mukhtar Journal of Sciences 37 (2): 138-149, 2022
ISSN: online 2617-2186 print 2617-2178
Journal Homepage https://omu.edu.ly/journals/index.php/mjsc/index

Morphological Description of Some Megachilidae Species in Aljabal Alakhder, Libya

Marwah Y. H. Almabrouk[1]*, Ali A. Bataw[2] , Mansour s. a. Attia [2], Asrana R. Mohammrd [2], Muna M, Algbali[2]

[1]*Department of Zoology, Faulty of Science and Arts, Alabiar, University of Benghazi, Libya*
[2]*Department of Zoology, Faculty of Science, Omar Al Mukhtar University, Libya*

Received: 08 December 2021/ Accepted: 19 May 2022
Doi: https://doi.org/10.54172/mjsc.v37i2.373

Abstract: Bees are a large and diverse species of insects belonging to the Hymenoptera order. The family Megachilidae represents a large part of most of the bee fauna all over the world as a result of their importance as pollinators. The study aimed to describe the morphological characteristics of three species of wild bees belonging to *Megachile parientina* (Geoffroy, 1785), *Rhodanthidium sticticum* (Fabricius, 1787), and *Anthidium diadema* Latreille, 1809 in Aljabal Alakder, Libya. Specimens were collected by hand net from different locations in the Aljabal Alakder area (Albayda and Alwastia). The morphological characters were described by using the OPTIC microscope. Measurements were taken at full body length (in cm), front wings length, thorax and abdomen width, body color was taken (head, abdomen, thorax, wings), and the study described in details the morphology of mouthparts, wings venation, antenna and abdominal structure for all species. The morphological structures vary between the different species in color, size, and wings. The body length of *M. parientina* was 19 mm, *R. sticticum* was 12 mm, and *A. diadema* was 13 mm. The study's conclusion insists on the importance of morphological description studies to facilitate the identification of wild bees species in Libya.

Keywords: Wild Bees, Megachilidae, Morphological Description, Aljabal Alakader, Libya.

INTRODUCTION

The importance of bees as key ecosystem service providers cannot be overemphasized. There are 20,000 bee species in the world that provide pollination services for many wild and cultivated plants for reproduction(Khalifa et al., 2021). The bee family Megachilidae is found in a wide diversity of habitats on all continents except Antarctica (Litman et al., 2011).The genus Megachile Latreille, 1802 represents a large part of most of the bee fauna (Michener, 2007). There are around 1400 species in this genus (Ascher & Pickering, 2020), divided into 55 subgenera (Michener, 2007; Trunz et al., 2016).

The Mediterranean region, especially North Africa, contains a wide diversity of bee species (Ascher & Pickering, 2020; Grace, 2010; Guiglia, 1942; Shebl et al., 2021), distributed in a wide variety of habitats (Gonzalez et al., 2012; Sakenin et al., 2020). *Megachile* species are solitary, and many species are highly seasonal. Their preferred host plants have a

***Corresponding author:** Marwah Y. H. Almabrouk: marwaalgadi92@gmail.com Department of Zoology, Faulty of Science and Arts, Alabiar, University of Benghazi, -Libya

short flowering season, and this species is an important pollinator for grasses, crops, and fruit plants in different parts of the world (Zakikhani et al., 2021).These solitary bees are both ecologically and economically relevant; they include many pollinators of natural, urban, and agricultural vegetation (Gonzalez et al., 2012). Some species are effective pollinators (Bosch & Blas, 1994; Vicens & Bosch, 2000), and a polylectic pollinator that is native to North Africa (Henson et al., 2019).

The Megachilidae is one of two families of long-tongued bees characterized by having two marginal cells, and the stigma is small in the front wings (Michener, 2007). The pollen-collecting scopa of all nonparasitic females is located on the abdominal sterna (Özbek & Zanden, 1992; Stephen et al., 1969). Most Megachile nest opportunistically in a variety of pre-existing cavities that they line with external materials such as resin or neatly cut and folded leaves, and these are potentially manageable through deployment of trap-nests. Others, such as species of subgenus Creightonella instead, excavate burrows in soil that they line with folded leaves (Michener, 2007).

The taxonomic keys of bees give important to the morphological characters, in particular, distinctive characters (Praz, 2017).Libya possesses an extensive and rich bee fauna (Zavattari, 1934); few studies were conducted in Libya and investigated the presence and taxonomic characteristics of wild bees, but in spite of these findings, the faunistic data on wild bees in Libya is still not complete (Almabrouk & Bataw, 2019). Until recently, little was known about Apoidea fauna in Libya, and findings were fragmentary. Since the works of (Guiglia, 1942; Zavattari, 1934), no taxonomic studies of bees has been published for Libya. Recently studies were performed by (Almabrouk & Bataw, 2019).

Therefore, it is necessary to plan a comprehensive project to sample many localities and provide a need to focus on the taxonomy, diversity, ecology, and biology of native bees, The study aims to identify and describe the morphological characteristics of some species of Megachilidae bee species in northeastern Libya to facilitate further studies concerning the distribution map of Libyan bee pollinator species and their conservation.

MATERIALS AND METHODS

The specimens were collected from two nature areas in northeastern Libya (Albayda 32°45′40.4″N: 21°44′51.4″E (619m) and Alwastia 32°51′080.83″N: 21°43′91″E (336m)) from March 2014 to May 2018. The areas are characterized by a rich fauna of wildflowers and economic plants.

The bees were collected by a net and placed in glass bottles with wet papers containing some drops of ethyl acetate alcohol to kill bees, then pinned and labeled for each specimen with bee special information (the area from which the bees were collected, date of collection, name of collector) and stored in wooden boxes in entomology laboratory of the Zoology Department, Faculty of Science, Omar Al Mukhtar University. The available keys were used for bees' identification: (Michener, 2007; Michener & Griswold, 1994; Praz, 2017). Identifications were confirmed with help of bee specialists (e.g. Georg Els, Robert Stuart - NHM UK). The various body characteristics of specimen bees were measured and described according to terminology used by Michener (2007). A stereomicroscope (OPTECH, modular stereomicroscope, Optical Technology, Germany) was used in the description process supplied with an Olympus digital camera.

RESULTS

***Megachile (chalicodama) parietina* (Geoffry, 1785)**

Examined material: ♀ 2 Alwasita, 16.iii.2017; Albaida, 16.iv.2014, 27.iii.2018,

1.iv.2018, 2.iv.2018, 3.iv.2018, 4.iv.2018, 6.iv.2018, 11.iv.2018, 15.v.2018.
Measurements: 19 mm body length.

Head: black, triangular-shaped, slightly narrower than body, with long black setae, densely punctate, vertex curved to the inside with long black setae erected to the outside (Fig. 1).

Figure (1). The head of (♀) *Megachile parientina* (♀).

Compound eyes: bright black, with densely long black setae between compound eyes, paraocular carina clear, genal area narrow.
Ocelli: arranged in a triangle shape, dark brown, lateral ocelli at same level of posterior margin of compound eyes (Fig. 2).

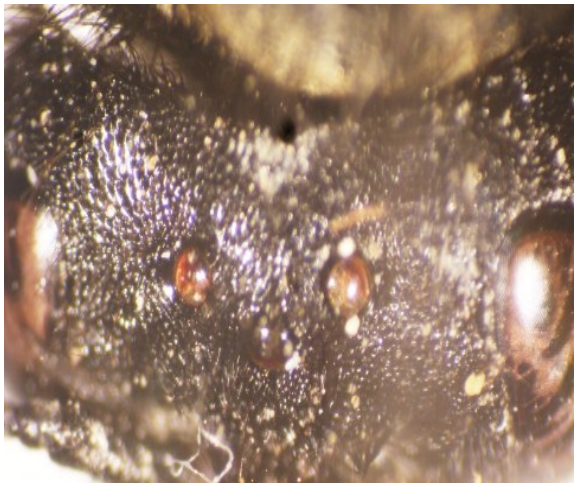

Figure (2). Ocelli of *Megachile parientina* (♀).

Clypeus: black, the end of the apical ciliated with dark brown setae, densely punctate.
Mandibles*:* rectangular, wider at apical, black with long little light brown setae, inner mandible with cutting edge (Fig.3).

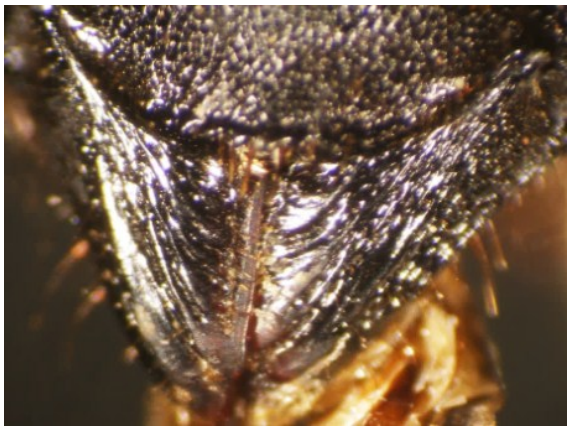

Figure (3). Mandible of *Megachile parietina* (♀).

Mouthparts: elongated, light brown, galea brown color, wider than glossa; end of apical glossa with dense setae erected downward, paraglossa with short setae at edges (Fig. 4).

Figure (4). Mouthparts of *Megachile parientina* (♀).

Antennae: twelve segments, black, antennal socket dark brown, scape elongated, rectangular, narrower at the base, wider at apical; pedicel short, rounded, first flagellomere narrower at the base, wider at apical, other flagellomeres equal in the shape and size, terminal flagellomere rounded.

Thorax: width 5 mm, prothorax larger than mesothaorax and metathorax, black, with densely long black setae especially on meta-

thorax; tegula clear, dark brown.

Wings*:* forewings length 13 mm, dark brown, veins with dark brown color; marginal cell elongated and broadtwo submarginal cell, vein 2rs-m curved outward, vein 2m-cu meets median vein opposite third submarginal cell, basal vein straight, the lower end meeting the longitudinal vein at an acute angle (Fig.6a), jugal lobe of hindwing very short, much less than half length of vannal lobe and not reaching anywhere near as far as vein closing cubital cell (Fig. 5).

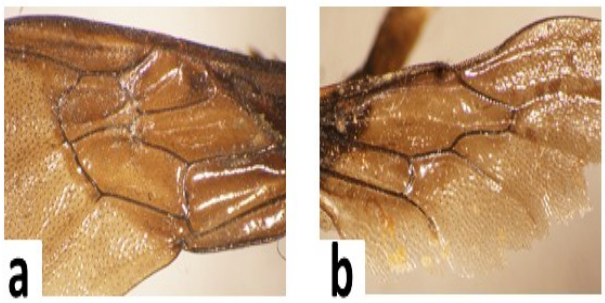

Figure (5). a- Forewing, b- Hindwing of *Megachile parientina* (♀).

Legs: coxa triangular, black and covered by black setae at outside; trochanter rectangular, narrower at the base, wider at apical, black, apical edge dark brown, black setae; femur elongated, wider at base, narrow apically, black with dense and long black setae erected downwards at outside and outer surface, internal surface with a few black setae; tibia narrower at base, wider at apical part, black with dense short black setae erected downwards, dark brown area at the edge of internal tibia, dense long black setae erected downwards at the edges and outer surface, little black setae on the internal surface, tibial spur ciliated from each side, forelegs with one tibial spur, short, dark brown, mid legs with one tibial spur, long, light brown (Fig. 6a), hind legs with two tibial spur, long, light brown (Fig. 6b), tarsus five segments each leg, basitarsus longer than mediotarsus and distitarsus, narrower at the base, wider at the apical, black with dense long black setae erected downwards, mediotarsus three segments equal in the shape and size, clear, dark brown with dark brown robust setae at the apical, distitarsus narrower at the base, wider at the apical, dark brown with little long dark brown setae.

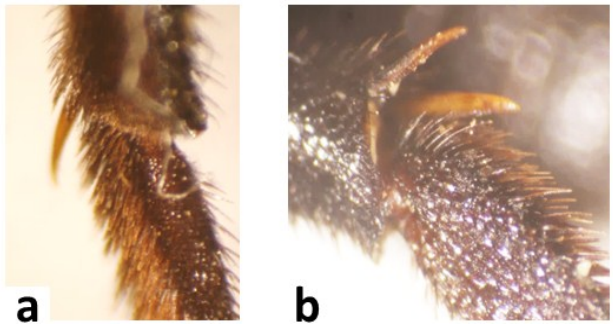

Figure (6). Tibial spur a- midleg, b- hind leg of (♀) *Megachile parientina.*

Pair of long tarsal claws the base dark brown, apical black, arolium absent (Fig. 7).

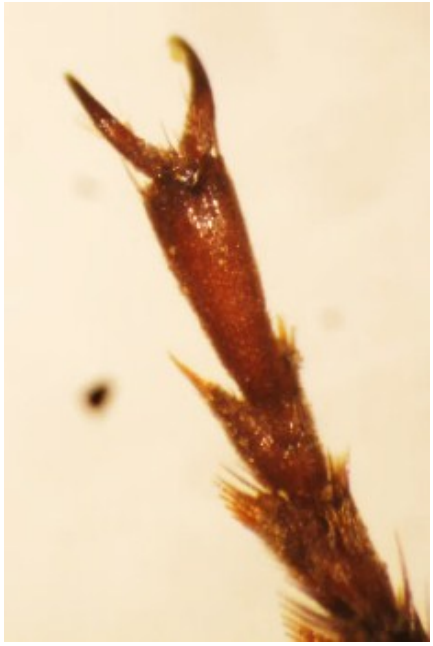

Figure (7). Tarsal claws of (♀) *Megachile parientina.*

Abdomen: width across abdomen 6 mm, six segments, black, dense punctates, tergum I clear curvature at the base, compressed and narrower at the middle, tergum VI triangle shape, narrower than the rest of the other terga, dense long black setae erected downwards (Fig. 8a), sternum black with dense long black setae, dense short black setae at the

edges (Fig. 8b).

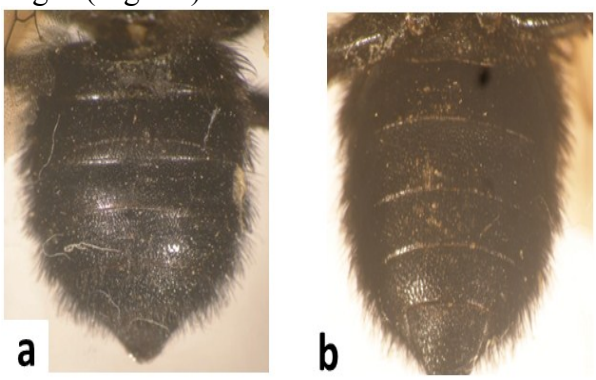

Figure (8). Abdomen of *Megachile parientina* a- Dorsal view, b- Venteral view of (♀) *Megachile parietina.*

***Rhodanthidium sticticum* (Fabricius, 1787).**
Examined material: ♀1 Albaida, 15.5.2018 12 mm body length .

Head: rounded and slightly narrower than the body (Fig. 9a), vertex with band curved in the middle at the apical, orange color with dense long orange setae, dense punctates (Fig. 9b).

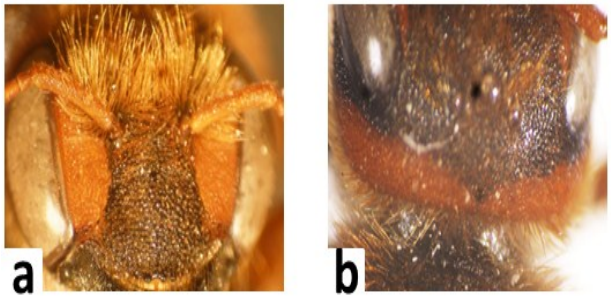

Figure (9). a- The head, b- Vertex of (♀) *Rhodanthidium sticticum.*

Compound eyes: bright black, orange spot between compound eyes and antennae, paraocular carina clear, genal area wide.
Ocelli: triangle shape, light brown, the lateral ocelli slightly higher than the height level of compound eyes, the median ocellus with frontal line.

Clypeus: dark brown, the end of apical ciliated with long orange setae erected downwards, dense punctates.

Mandibules: rectangular, wide, robust, elongated, ends with five sharp teeth, apical tooth long, dark brown with dark brown lope at the connect area with the malar area (Fig. 10).

Figure (10). Mandible of (♀) *Rhodanthidum sticticum.*.

Mouthparts: long, light brown (Fig. 11)

Figure (11). Mouthparts of (♀) *Rhodanthidum sticticum.*

Antenna: twelve segments, scape long, rectangular, orange, pedicel short, rectangular, orange, flagellum ten segments, the first flagellomere longer than the rest of the other flagellomeres, wider at the apical, narrower at the base, the other ninth flagellomeres equal in the shape and size, flagellomeres from first to third orange color, flagellomeres from fourth to tenth dark brown color, the terminal flagellomere of antennae rounded shape (Fig.12).

Figure (12). Antennae of (♀) *Rhodanthidum sticticum.*.

Thorax: width across thorax 4 mm, dark brown, prothorax larger than mesothorax and metathorax, dense long orange setae, dense punctates, tegula clear large, orange (Fig.13).

Figure (13). Thorax of (♀) *Rhodanthidum sticticum.*

Wings: forewings length 11 mm, light brown, the veins dark brown, marginal cell long and broad, apical edge of marginal cell darker brown, the apical of marginal cell not jointed with costa vein, two submarginal cells, vein 1rs-m with the same line vein 1m-cu, vein 2rs-m curved outward, vein 2m-cu meets median vein at the second submarginal cell, basal vein straight, the lower end meeting the longitudinal vein at an acute angle (Fig. 14), jugal lobe of hindwing very short, much less than half length of vannal lobe and not reaching anywhere near as far as vein closing cubital cell.

Figure (14). Forewing of (♀) *Rhodanthidum sticticum.*

Legs: coxa triangle, dark brown with dense long orange setae erected to down at the edges, trochanter narrower at the base, wider at the apical, dark brown with dense orange setae, fumer rectangular, wider dark brown at base, narrower orange at the apical, dense short orange setae erected to down, tibia narrower at the base, wider at the apical, dense short orange setae erected to down, tibial spur ciliated at the inner edge, sharp at the outer edge, forelegs with one tibial spur, short, light brown, midlegs with one tibial spur, long, orange, hind legs with two tibial spur, long, orange (Fig. 15a), tarsus five segments each leg, basitarsus longer than mediotarsus and distitarsus, orange with dense long orange setae erected to down, mediotarsus three segments equal in the shape and size, orange with dense long orange robust setae erected to down at the apical, distitarsus narrower at the base, wider at the apical, orange with little long orange setae erected to down at the apical (Fig. 15b).

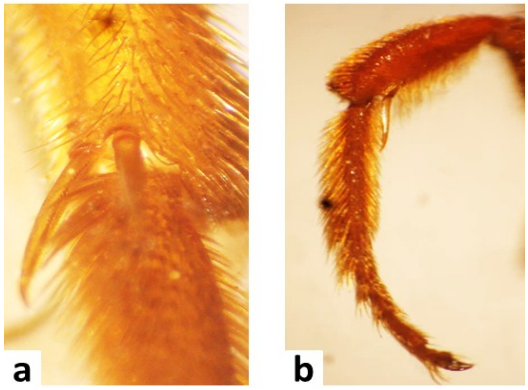

Figure (15). a- Tibial spur of hind legs, b-Midleg of (♀) *Rhodanthidum sticticum.*.

Pair of longed tarsal claws, branched at apical, the lateral longer than internal one, the base orange, apical dark brown, arolium clear, dark brown (Fig.16).

Figure (16). Tarsal claws of. (♀) *Rhodanthidum sticticum*.

Abdomen: width across abdomen 5 mm, six segments, dense punctates, short light orange setae erected to down, contact area of terga I, II clear dark brown, the color of segments black at the middle, orange color from each side, tergum VI triangle shape with two pairs of posteriorly projecting spines (Fig. 17a), sternum dark brown ends with light orange edges, long light orange setae (Fig. 17b).

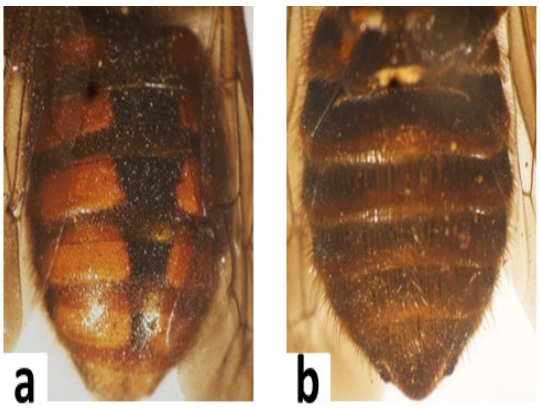

Figure (17). a- Dorsal view, b- Venteral view of (♀) *Rhodanthidum sticticum*..

***Anthidium diadema Latreille,* 1809**

Examined material: ♀ 1 Albaida, 30.v.2018.

13 mm body length.

Head: rounded with clear yellow spots, white setae, dense punctates, vertex curved slightly to the inside, black with two elongated bands, and clear long yellow setae (Fig. 18).

Figure (18). The head of (♀) *Anthidium diadema*.

Compound eyes: large, dark brown.

Ocelli: triangular shape, dark brown, the lateral ocelli less than the height level of compound eyes (Fig. 19).

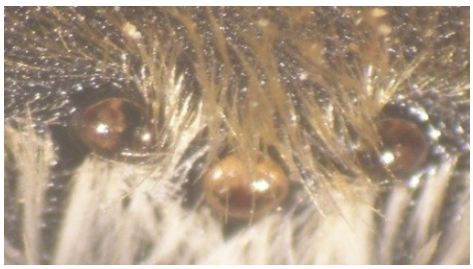

Figure (19). Ocelli of (♀) *Anthidium diadema.*

Clypeus: yellow color, wider than the length.

Mandibules: cylindrical, yellow color, ends with three sharp dark brown teeth, lower tooth long, strong edges (Fig. 20).

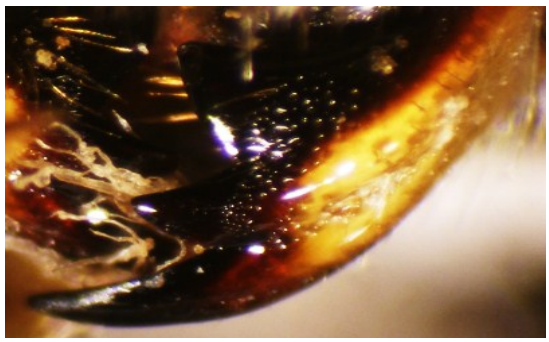

Figure (20). Mandible of (♀) *Anthidium diadema*.

Mouthparts*:* long, light brown.
Antenna: thirteen segments, scape long, narrower at the base, wider at the apical, black with white setae, pedicel short, rounded, dark brown, flagellum eleven segments, dark brown, the first flagellomere narrower at the base, wider at the apical, the second and third flagellomeres wider than the length, flagellomeres from fourth to eleventh equal in the shape and size, the terminal flagellomere of antennae rounded shape (Fig. 21).

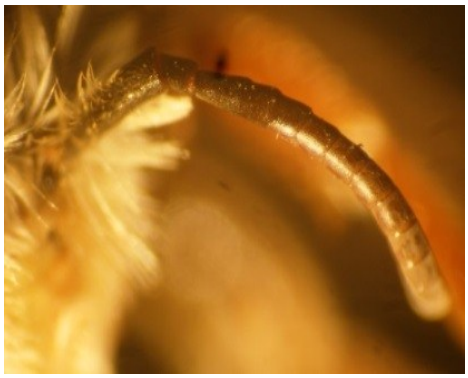

Figure (21). Antennae of (♀) *Anthidium diadema.*

Thorax: width across thorax 5 mm, pronotal lobe cream with a dorsal anterior carina, covered with long white setae, omaulus rounded, scutum with recumbent dense short setae, almost totally black and with reversed J-shaped cream, marking along anterior and lateral edges, axilla rounded, scutellum with cream subapical band, triangular area of propodema large, impunctate shining, mesepisternum and metepisternum with small cream spots, tegula large, reddish-brown, with cream spot anteriorly (Fig. 22).

Figure (22). Thorax of (♀) *Anthidium diadema.*

Wings*:* forewings length 10 mm, transparent brown, the veins dark brown, marginal cell broad with a dark brown line at the apical of margin cell, two submarginal cells, 2smc slightly larger than 1smc, vein 2m-cu meets median vein beyond point where 3rs-m dose, basal vein straight, the lower end meeting the longitudinal vein at an acute angle (Fig. 23), jugal lobe of hindwing very short, much less than half length of vannal lobe and not reaching anywhere near as far as vein closing cubital cell.

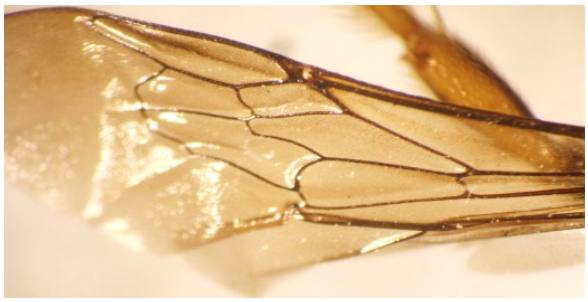

Figure (23). Forewing of (♀) *Anthidium diadema.*

Legs: coxa black, dense punctates, forecoxa and hindcoxa longer than midcoxa, apical edge light brown, dense long white setae erected downwards, midcoxa short, black, long white setae erected downwards, trochanter black, narrower at the base, wider at the apical, dense punctates, dense long white setae erected downwards, fumer elongated, wide, internal surface dark brown with little white setae erected to down, external surface black, apical edge light brown, short black setae, dense punctates, dense long white setae erected downwards at the edges, tibia internal surface wide, dark brown with white setae erected downwards, external surface yellow with white setae, dense punctates, tibial spur ciliated from each side, long, light brown, forelegs and midlegs with one tibial spur (Fig. 24a), hind legs with two tibial spur (Fig. 24b), tarsus five segments each leg, reddish brown with dense long yellow setae erected downwards, basitarsus longer than mediotarsus and distitarsus, mediotarsus three segments equal in the shape and size, distitarsus long, narrower at the base, wider at the apical

reddish brown with short little reddish brown setae erected downwards at the apical.

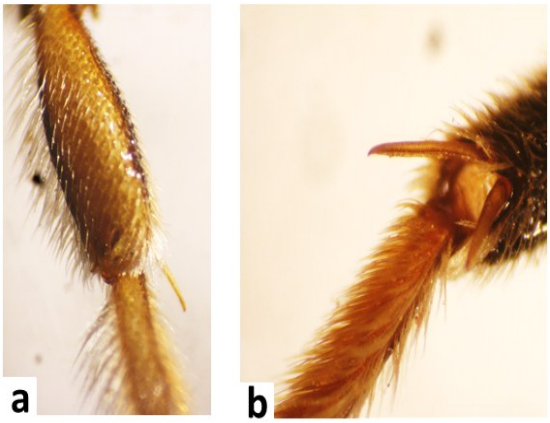

Figure (24). Tibial spur a-midleg, b- hind leg of (♀) *Anthidium diadema.*

Pair of elongated tarsal claws, branched at apical, the lateral longer than the internal one, the base light brown, apical dark brown, arolium absent (Fig. 25).

Figure (25). Tarsal claws of (♀) *Anthidium diadema.*

Abdomen: width across abdomen 5 mm, seven segments with dense punctates.
Tergum I black with a yellow spot on each side.

Tergum II black with a yellow band along the tergum, two dark brown spots with curvature yellow band at middle to down.
Tergum III black with yellow band, two dark brown marks on each side.

Terga IV and V black, yellow band. Tergum VI less wide than other terga with paired, lateral, bright yellow spots. Tergum VII with prominent, hook like projections (Fig. 26a).
Sternum: each sterna with dense long white setae erected downwards (Fig. 26b).

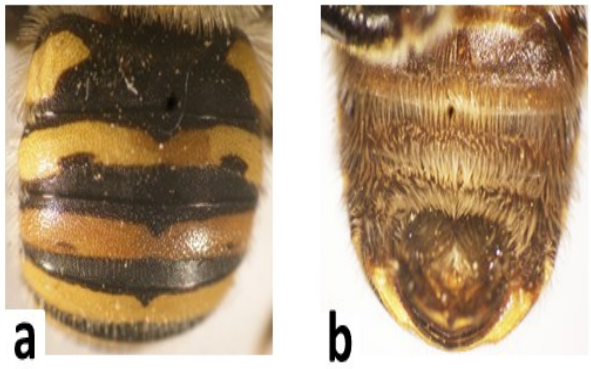

Figure (26). a- Dorsal view, b- Venteral view of (♀) *Anthidium diadema.*

DISCUSSION

The bee fauna of Libya is rich but relatively little known biologically and taxonomically (Almabrouk & Bataw, 2019; Zavattari, 1934). The study of morphological structures of wild bees is conceded as one of the important topics as a results of the importance of bees in the ecosystem.

Undoubtedly, the current study described three species *Megachile (chalicodama) parientina, Rhodanthidium sticticum,* and *Anthidium diadema*. Each of them is a separate species and differs in morphological features. However, we hope to draw more attention and encourage melittologists to investigate and document these morphological structures as well as the floral associations and foraging behavior of all bees that have them in Libya.

CONCLUSION

The current study insists that the Aljabal Alakder region of Libya has an important bee diversity that serves the ecosystem as pollinators of agricultural flowers. The study provides valuable information about Mega-

childae that could help to construct taxonomic keys for the Libyan bee species, and more investigation is needed for the study of wild bees.

REFERENCES

Almabrouk, M., & Bataw, A. A. (2019). Identification and Morphological Description of Xylocopa species (Xylocopidae: Hymenoptera) in North East of Libya. *Al Mukhtar Journal of Science, 34*(4), 288-305 .

Bosch, J., & Blas, M. (1994). Foraging behaviour and pollinating efficiency of Osmia cornuta and Apis mellifera on almond (Hymenoptera, Megachilidae and Apidae). *Applied Entomology and Zoology, 29*(1), 1-9 .

Bosch, J., & Blas, M. (1994). Foraging behaviour and pollinating efficiency of Osmia cornuta and Apis mellifera on almond (Hymenoptera, Megachilidae and Apidae). *Applied Entomology and Zoology, 29*(1), 1-9 .

Gonzalez, V. H., Griswold ،T., Praz, C. J., & Danforth, B. N. (2012). Phylogeny of the bee family Megachilidae (Hymenoptera: Apoidea) based on adult morphology. *Systematic Entomology, 37*(2), 261-286 .

Grace, A. (2010). *Introductory biogeography to bees of the Eastern Mediterranean and Near East*. Bexhill Museum Bexhill .

Guiglia, D. (1942). Gli imenotteri della Libia (Sphecidae, Pompilidae, Scoliidae, Vespidae, Apidae). *Annali del Museo Libico Di Storia Naturale, 20*(3), 228-250 .

Henson, K. A., Campbell, J. W., & Kaplan, D. A .(2019) .Range extension of Megachile lanata (Hymenoptera: Megachilidae), a non-native sunn hemp pollinator, in Florida. *Florida Entomologist, 102*(1), 259-261 .

Khalifa, S. A., Elshafiey, E. H., Shetaia, A. A., El-Wahed, A. A. A., Algethami, A. F., Musharraf, S. G., AlAjmi, M. F., Zhao, C., Masry, S. H., & Abdel-Daim, M. M. (2021). Overview of bee pollination and its economic value for crop production. *Insects, 12*(8), 688 .

Litman, J. R., Danforth, B. N., Eardley, C. D., & Praz, C. J. (2011). Why do leafcutter bees cut leaves? New insights into the early evolution of bees. *Proceedings of the Royal Society B: Biological Sciences, 278*(1724), 3593-3600 .

Michener, C. (2007). The Bees of the World Johns Hopkins University Press. *Baltimore.{Google Scholar}*

Michener, C. D., & Griswold, T. L. (1994). The classification of old world Anthidiini (Hymenoptera, Megachilidae). *The University of Kansas science bulletin, 55*(9), 299 .

Özbek, H., & Zanden, G. V. D. (1992). A preliminary review of the Megachilidae of Turkey Part II. Heriadini (Hymenoptera, Apoidea). *Türkiye Entomoloji Dergisi; Year: 1992 Volume: 16 Number: 3* .

Praz, C. J. (2017). Subgeneric classification and biology of the leafcutter and dauber bees (genus Megachile Latreille) of the western Palearctic (Hymenoptera, Apoidea, Megachilidae). *Journal of Hymenoptera Research, 55*, 1 .

Sakenin, H., Shaaban, A., Nil, B., Majid, N., Hassan, G., & Siavash, T. (2020). A Faunistic Survey On Megachilidae (Hymenoptera: Apoidea) From Northern Iran. *Egypt. J. Plant Prot. Res. Inst, 3*(1), 398 – 408 .

Shebl, M. A., Abdelkader, F. B., Bendifallah, L., Benachour, K., Bataw, A. A., Bufliga, E. M., Osman, M. A., & Kamel, S. M. (2021). The melittology research in Northern Africa and the Middle East: past and present situations. *The Journal of Basic and Applied Zoology, 82*(1), 1-11 .

Stephen, W. P., Bohart, G. E., & Torchio, P. F. (1969). The Biology and External Morphology of Bees with a Synopsis of the Genera of North-western America .

Trunz, V., Packer, L., Vieu, J ،.Arrigo, N., & Praz, C. (2016). Comprehensive phylogeny, biogeography and new classification of the diverse bee tribe Megachilini: Can we use DNA barcodes in phylogenies of large genera? *Molecular Phylogenetics and Evolution, 103*, 245-259 .

Vicens, N & ،.Bosch, J. (2000). Pollinating efficacy of Osmia cornuta and Apis mellifera (Hymenoptera: Megachilidae, Apidae) on 'red Delicious' apple. *Environmental Entomology, 29*(2), 235-240 .

Zakikhani, M., Monfared, A., Mohammadi, H., & Jahromi, A. S. (2021). A survey on Megachilidae (Hymenoptera, Apoidea) species available in Iranian Pollinator Insects Museum of Yasouj University. *Journal of Insect Biodiversity and Systematics, 7*(2), 167–204-167–204 .

Zavattari, E. (1934). Prodormo della Fauna Della Libia, Pavia .

الوصف المورفولوجي لبعض أنواع النحل من عائلة Megachilidae في الجبل الأخضر، ليبيا

مروة يونس المبروك[1]*، علي عبد القادر بطاو[2]*، منصور سالم عطية[2]، عصرانة رمضان محمد[2]، منى محمد الجبالي[2]

[1] قسم علم الحيوان، كلية الآداب والعلوم، الأبيار، جامعة بنغازي – ليبيا

[2] قسم علم الحيوان، كلية العلوم؛ جامعة عمر المختار، ليبيا

تاريخ الاستلام: 08 نوفمبر 2021/ تاريخ القبول: 19 مايو 2022

Doi:https://doi.org/10.54172/mjsc.v37i2.373

المستخلص : يعد النحل من الحشرات ذات التنوع الكبير، التي تنتمي إلى رتبة غشائيات الأجنحة. تمثل عائلة Megachilidae جزءًا كبيرًا من النحل في جميع أنحاء العالم؛ نتيجة لأهميتها كملقحات. هدفت الدراسة إلى وصف الخصائص المورفولوجية لثلاثة أنواع من النحل البري تنتمي إلى *Megachile parientina* (Geoffroy 1785) ، و *Rhodanthidium sticticum* (Fabricius 1787)، و *Anthidium diadema* Latreille 1809، في منطقة الجبل الأخضر بليبيا. جمعت العينات بالشباك اليدوية من مواقع مختلفة في منطقة الدراسة (البيضاء، والواسطية). وصفت الصفات المورفولوجية باستخدام المجهر البصري، وأخذت القياسات بطول الجسم بالكامل (سم)، وطول الأجنحة الأمامية، وعرض الصدر، والبطن، ولون الجسم (الرأس، والبطن، والصدر، والأجنحة) ، ووصفت الدراسة بالتفصيل شكل أجزاء الفم، تعرق الأجنحة، وقرون الاستشعار، وتركيب البطن لجميع الأنواع. أوضحت الدراسة أن التركيبات المورفولوجية تختلف بين الأنواع سواء في اللون، والحجم، والأجنحة. كان طول جسم *M. parientina* 19 ملم، *R. sticticum*، 12 ملم و *A. diadema* كان 13 ملم. يؤكد استنتاجنا أن دراسة الوصف المورفولوجي من الدراسات المهمة التي تساهم في تعريف أنواع النحل في ليبيا.

الكلمات المفتاحية : النحل البري، ميجاكيليدي، الوصف المورفولوجي الجبل الأخضر، ، ليبيا.

*[1]مروة يونس المبروك: marwaalgadi92@gmail.com قسم علم الحيوان، كلية الآداب والعلوم، الأبيار، جامعة بنغازي – ليبيا .

Al-Mukhtar Journal of Sciences 37 (2): 150-161, 2022
ISSN: online 2617-2186 print 2617-2178
Journal Homepage https://omu.edu.ly/journals/index.php/mjsc/index

Identification of Potential Natural Bioactive Compounds from *Glycyrrhiza glabra* as Sars-CoV-2 Main Protease (MPRO) Inhibitors: *In-Silico* Approach

Ashraf Ahmed Ali Abdusalam[1]*, Gazala Mohamed Ben-Hander[2]

[1] *Department of Pharmaceutical Chemistry, Faculty of Health Sciences, Sirte University, Libya*
[2] *Department of Chemistry, Faculty of Sciences, Sirte University, Libya*

Received: 20 March 2022./ Accepted: 04 June 2022
Doi: https://doi.org/10.54172/mjsc.v37i2.679

Abstract: The SARS-CoV-2 virus caused the COVID-19 pandemic declared in early 2020, generating a global health emergency. So far, no approved drugs or vaccines are available. Therefore, there is an urgent need to explore and develop effective new therapeutics against SARS-CoV-2. In addition, the main protease (Mpro) of the SARS-CoV-2 virus is considered essential in the virus replication propagation and considered a drug discovery target. Consequently, plant-derived compounds are an important and valuable source for novel drugs. This study reports molecular docking-based virtual screening (VS) of 20 compounds identified from Glycyrrhiza glabra to search for potent compounds against 3CL proteases (3CLpro). The screening results revealed that the identified compounds Semilicoisoflavone B, Licoflavone B, and Licocoumarin A exhibited low free energy of binding (FEB) values of 10.91, −10.29, and −10.21 kcal/mole for Autodock 4.2 and −9.81, −9.77, and −9.60 kcal/mole, for AutoDockVina, respectively. The obtained results of FEB in this study were better than the coordinated ligand N3, which was -7.4 kcal/mole. The three potential compounds showed different and stable interactions with the essential amino acids, especially the catalytic dyad (Cys145-His41) in the binding pocket of the 3CLpro. Three potential inhibitors were successfully identified from Glycyrrhiza glabra using molecular docking and virtual screening; these compounds obeyed the Lipinski rule of 5 with a little violation and showed low FEB and good interactions with the 3CLpro. These identified compounds may serve as potential leads that help in developing therapeutic agents against the SARS-CoV-2. Further research is recommended (in vitro and in vivo) to verify the above findings.

Keywords: Virtual Screening, Docking, *Glycyrrhiza glabra,* COVID-19, SARS-CoV-2, 3CL protease.

INTRODUCTION

The recent outbreak of severe acute respiratory syndrome (SARS) coronavirus disease-19 (COVID-19) is a novel infectious and highly contagious disease that first appeared in Wuhan, Hubei Province, China, in December, the year 2019 (Phan, 2020; Yang et al., 2020). The virus has spread worldwide, increasing the number of victims and causing significant morbidity and mortality. On March 11, 2020, the World Health Organization (WHO) classified it a pandemic (Asrani et al., 2021; Zehra et al., 2020). SARS-CoV is a novel member of the betacoronavirus genus, which belongs to the Coronaviridae family. It has an enveloped, positive-sense, sin-

***Corresponding author:** Ashraf Ahmed Ali: aalmansory@su.edu.ly , Department of Pharmaceutical Chemistry, Faculty of Health Sciences, Sirte University, Libya.

gle-stranded RNA (Chan et al., 2020; Pal et al., 2020). The viral genomes encode as non-structural proteins (NSPs), which include (3-chymotrypsin-like protease 3CLpro) nsp5, (papain-like protease) nsp3, (helicase) nsp13, and (RNA-dependent RNA polymerase [RdRp]) nsp12, in addition to structural proteins (such as spike glycoprotein and accessory proteins) (Chan et al., 2016; Chan et al., 2020). These two proteases (PLpro and 3CLpro) are involved in the transcription and replication of the virus. However, the 3CLpro mainly has the most important role in virus replication (De Wit et al., 2016).

There is currently no therapeutically licensed inhibitor of the SARS protease, but several are being developed (Stoermer, 2020). In addition, protease inhibitors have been developed for a variety of viruses, including nelfinavir (Gills et al., 2007), amprenavir for HIV (Marcelin et al., 2003), and lopinavir-ritonavir (Sáez-Llorens et al., 2003) for HCV. However, manufacturing those protease inhibitors requires a multistep reaction that is quite costly, and an emergency medicine that is both effective and inexpensive is currently needed. It is well known that several medicinal plants may combat viruses and have active components that produce large quantities of data about their effectiveness. Glycyrrhiza glabra is one of these therapeutic plants, and its active components may have the ability to combat numerous viruses (Pompei et al., 1980). Glycyrrhiza glabra (Gg), often known as 'sweet wood' and 'liquorice', is a member of the Fabaceae family.

It is effective against a variety of RNA viruses, including the influenza A virus, H1N1 virus, H5N1 virus, Rotavirus, Newcastle disease virus, Hepatitis C virus, and severe acute respiratory virus, as well as DNA viruses, including Herpes Simplex virus, Epstein-Barr virus, and Varicella-Zoster virus (Cinatl et al., 2003; Wang et al., 2015). Several potent compounds derived from Gg have been identified as being capable of inhibiting the virus's development. It has been demonstrated in some research studies that Glycerrhizin (Glycyrrhizinate or Glycyrrhizic acid) is effective in inhibiting the binding of viruses to target cells, as well as in controlling viral replication. It has been observed to have considerable antiviral activity (Sharma et al., 2018; Wang et al., 2015).

The application of computational methods in drug discovery has assisted in the acceleration of the discovery and design of new drug candidates while also lowering the overall cost of the process. As a result, virtual screening-based drug discovery has been identified as one of the most effective ways of discovering new drugs.(Zoete et al., 2009). In-silico virtual screening is a searching strategy used to discover novel compounds and chemotypes that can be utilized as alternatives to currently available drugs (Ahmed Ali Abdusalam & Vikneswaran, 2020; Sliwoski et al., 2014). With the help of VS, also known as the step-by-step approach of sequential filters, it is possible to narrow down a large number of compounds to select the most promising lead-like hits that have potential biological activity against a target protein (Jacq et al., 2007; Lavecchia & Di Giovanni, 2013; McInnes, 2007).

In this study, the VS approach was carried out to identify and estimate potential inhibitors against two SARS-CoV-2 3CL proteases obtained from the Allium roseum L plant, followed by molecular docking to discover new inhibitors that may be used in the treatment of coronavirus infections.

MATERIALS AND METHODS

Retrieval and Preparation of Protein Structure*:* The three-dimensional structure of 3CLpro of SARS-CoV-2 in complex with inhibitor N3 was retrieved from the Protein Data Bank (http://www.rcsb.org) (Berman, 2000) (PDB ID: 6LU7), and the structure is shown in Figure 1 (Burley et al., 2017). Autodock Tools (ADT) was used to remove co-factor and unwanted water molecules, add the

polar hydrogen to the protein, compute Gasteiger, and add Kollman charge. Subsequently, the file is saved in the PDBQT format.

Ligand Preparation: The three-dimension structures (3D) of the 20 ligands were obtained from the PubChem site (http://pubchem.ncbi.nlm.nih.gov). The downloaded ligands were in SDF format. BIOVIA Discovery Studio Visualizer 2016 www.accelrys.com was used to convert ligands to PDB, and ligands were converted to PDBQT for VS using raccoon software. Molecular proprieties used for Lipinski's (RO5) (Lipinski, 2004) were evaluated using the online-site Molinspiration https://www.molinspiration.com/cgibin/properties**.**

Virtual Screening: AutodockVina was used to perform an initial virtual screening of 20 bioactive compounds against SARS-CoV-2 3CLpro (PDB ID: 6LU7). The protein file was converted from PDB to PDBQT, and a Config.txt file with all of the information needed for VS with ADT was created; all other options were considered a default.

Moleculaer Docking: Molecular docking is a computational technique for determining the ligand's best shape and orientation when interacting with a receptor (Morris et al., 2009). This research was to take the search one step further by determining the binding affinity of the selected compounds for the target protein. The docking simulation and analysis were carried out using AutoDock 4.2 and AutoDockVina (Trott & Olson, 2010). AutoDock 4.2 was used to find the optimal orientation and interactions between the ligand and bioactive compounds; the grid box parameter was set as 60-60-60 for the x-, y-, and z-axes, respectively, with a spacing of 0.375 Å positioned at the centre of the binding pocket. For each docking experiment, 100 independent runs were performed. For each conformation, the lowest binding energy was chosen.

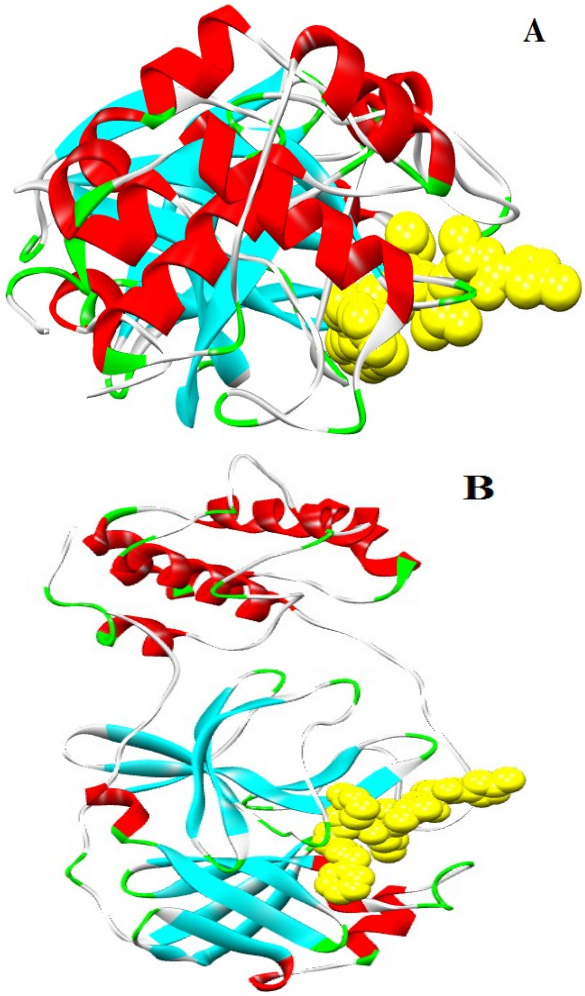

Figure: (1). Diagram representation of the three-dimensional structure 3D of 6LU7 in complex with N3 (yellow color) (A) Orthogonal view (B) Side view.

RESULTS AND DISCUSSION

Validation of The Virtual Screening Protocol: Prior to performing the virtual screening and molecular docking, validation of the docking protocol was evaluated by a re-dock within the acceptable range of the co-crystallized N3 to the target protein's active site (PDB: 6LU7). Here, the N3 pose exhibited the same orientation pattern as the crystallographic pose (RMSD = 0.82 Å, Figure 2, binding affinity −7.2 kcal/mol). Therefore, the results showed that the used protocol was reliable, and the docking software can be trusted and reproduce the expected binding mode of the co-crystallized ligand.

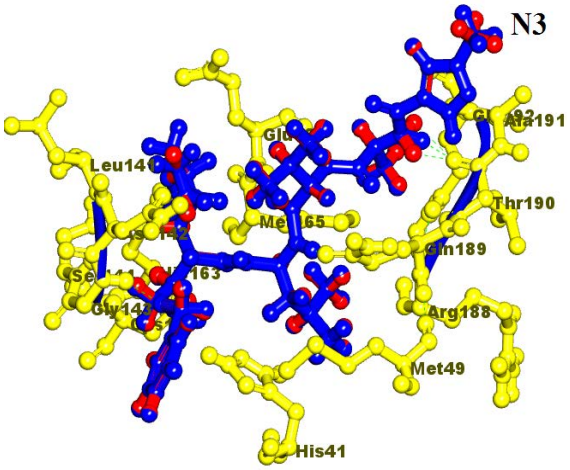

Figure: (2). Superimposition of the docked and crystallographic N3 poses (red and blue), respectively.

Initially, 20 compounds identified from Glycyrrhiza glabra were obtained from the literature (Pastorino et al., 2018). The compounds were virtually screened against the target protein and arranged according to the FEB. The top three compounds that exhibited the lowest energy of binding were chosen. Then, the Lipinski Role of five was used based on the molecular properties of the compounds to assess their similarity with approved drugs. The role of the top potential hits compounds is shown in Table 1. This rule is used to determine the drug-likeness properties should be no more than one violation of the following criteria, ALogP < 5, molecular weight < 500, number of HBD < 5, number of HBA < 10, and rotatable bond < 10. As can be seen from Table 1, the three compounds fall within the acceptable range of the Lipinski rule; the Semilicoisoflavone B compound was fully obeying the rule, while the other two compounds, Licoflavone B and Licocoumarin A, violate only one rule, whereas the coordinated ligand N3 violated more than two rules.

Figure 3 depicts the top three bioactive compounds ranked by AutoDockVina scores. These molecules exhibited the lowest FEB among the other compounds in the protein-ligand complex; subsequently, they were applied in the docking calculation. The docking simulation results showed that all the 20 compounds displayed FEB in the range -9.8- to -3.3 kcal/mol. Therefore, the compounds that showed the lowest FEB were considered the best, Table 2.

Therefore, the top 3 ranked compounds were suggested as the most suitable candidates. Semilicoisoflavone B, Licoflavone B, and Licocoumarin A displayed a minimum FEB of -9.8, -9.7, and -9.6 kcal/mol by AutoDockVina and the energy of -10.91,-10.29, and -10.21 kcal/mol by AutoDock 4.2, respectively, Table 3.

Table: (1). Molecular properties of the three 3CL pro inhibitor candidates.

No	Name	Molecular weight(g/mol)	logp	H-bond donors	H-bond acceptors	Rotatable bonds	Lipinski's rule violation	Drug-likeness alert
1	Semilicoisoflavone B	352.34	3.43	3	6	1	0	Accepted
2	Licoflavone B	390.50	6.3	2	4	5	1	Accepted
3	Licocoumarin A	406.47	5.59	3	5	5	1	Accepted
4	N3	680.35	2.32	5	14	18	2	----------

The clustering analysis is considered the best method to determine if the docking simulation effectively searched the available conformation space. Furthermore, pose clustering is a method for identifying possible poses that are different from energy ranking, and it can help decrease the number of strange poses (Forli et al., 2016; Makeneni et al., 2018; Morris et al., 1998).

Table: (2). Free energy of binding for the 20 compounds against COVID-19 3CLpro.

No	Compound Name	Free energy of binding Kcal/mole
1	Semilicoisoflavone B	-9.8
2	Licoflavone B	-9.7
3	Licocoumarin A	-9.6
4	Shinpterocarpin	-8.8
5	Glabridin	-8.8
6	1-Methoxyficifolinol	-8.6
7	enoxolone	-8.5
8	Licopyranocoumarin	-8.1
9	1-Methoxyficifolinol	-8.0
10	enoxolone	-7.8
11	Glisoflavone	-7.7
12	Isoliquiritigenin	-7.5
13	Liquiritigenin	-7.5
14	Isoangustone	-7.4
15	Liquiritin	-7.3
16	Licoarylcoumarin	-7.3
17	Licochalcone a	-7.2
18	Kanzonol R	-7.2
19	Licoriphenone	-7.1
20	Glycyrrhizic acid	-3.3

Table: (3). FEB Binding energy values of the 3 compounds present in Glycyrrhiza glabra.

No	Compound	AutoDock 4.2 (kcal/ mol)	AutoDock-Vina (kcal/mol)
1	SemilicoisoflavoneB	-10.91	-9.8
2	Licoflavone B	-10.29	-9.7
3	Licocoumarin A	-10.21	-9.6

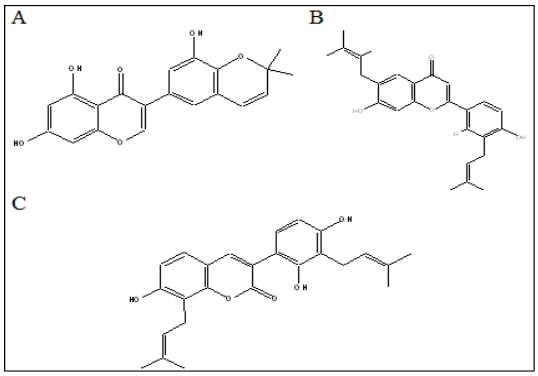

Figure: (1). Structure of the top three 3CL protease inhibitor (A) Semilicoisoflavone B (B) Licoflavone B (C) Licocoumarin A.

The results obtained by AutoDock 4.2 are organized by the FEB and the cluster of solutions that adopt the same pose Table 4 (Smith et al., 2004). The results for compound Semilicoisoflavone B exhibited 58 poses adopted as favourable conformation (this pose is considered the largest cluster out of 100 poses).

Licoflavone B adopted poses 19 times out of 100. Likewise, Licocoumarin A took this pose 46 times. The best docking solution was reported by Autodock (lowest FEB) for each GA run, as well as the cluster rank of the selected docked structure, the docked free energy range of docked structures, and the docked free energy of the selected docked structure Table 4. Only the docking mode that exhibited the lowest FEB was chosen for this cluster. Amino acid residues fully wrapped these molecules at the binding pocket region, as shown in Figure 4.

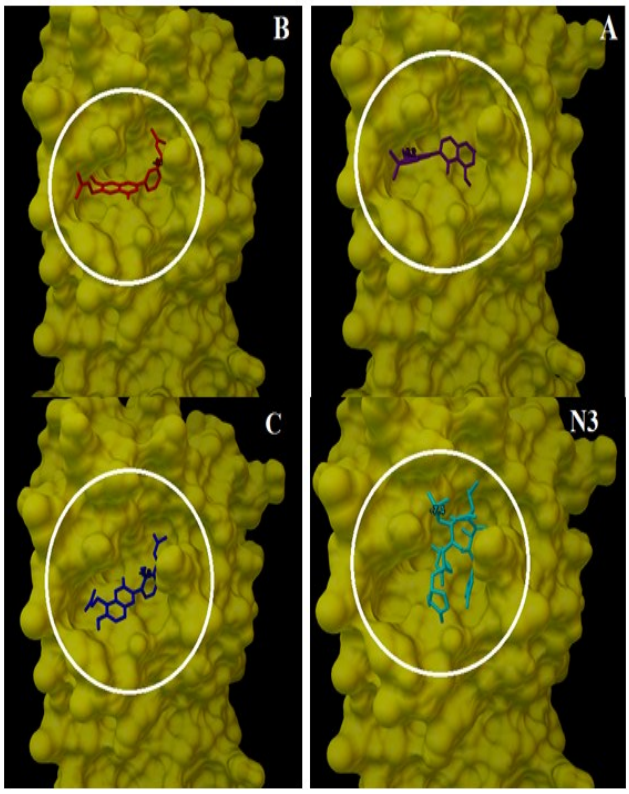

Figure: (4). Enfolding of the three compounds in the binding pocket, (A)Semilicoisoflavone B (B) Licoflavone B and (C) Licocoumarin A.

Table: (4). Docked FEB and relative cluster ranks of the three compounds.

No	compounds	Number of AutoDock clusters a	Cluster rank of selected docked structure	Docked free energy range of docked structures	Docked free energy of selected docked structure
1	Semilicoisoflavone B	58 (100)	4	-10.91 to -8.88	-10.91
2	Licoflavone B	19 (100)	3	-10.29 to -8,21	-10.29
3	Licocoumarin A	46 (100)	2	-10.21to -9.31	-10.21

The docking location of the three compounds was investigated. The interaction analysis results revealed that all compounds occupied the same position in the active pocket with a comparable pattern. Thus, the compounds were covalently bound by the essential amino acid residues of the target protein. The interactions of the docked compounds with the protein were manually examined, and then the location of the compounds in the binding pocket was determined. They showed extensive interactions with the key amino acids residues constructing the binding pocket. The interactions are hydrogen bonds, Van der Waals interaction, Pi-alkyl, Pi-sigma, Pi-cation, Pi-anion, and hydrophobic interaction, as shown in Figure 5.

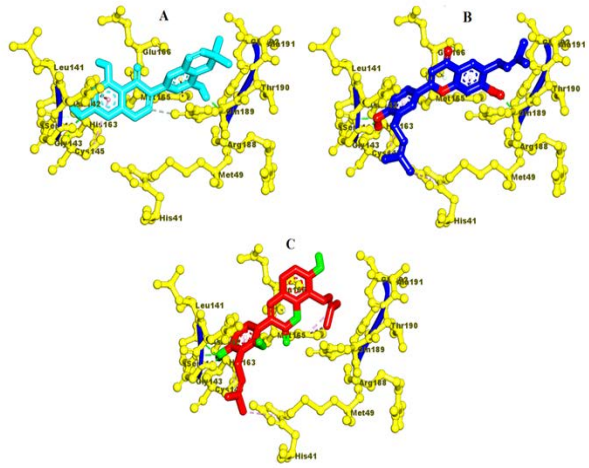

Figure: (5). The 3D structure of the three potential compounds (A) Semilicoisoflavone B (B) Licoflavone B (C) Licocoumarin A

The compound, Semilicoisoflavone B, was found to form five hydrogen bonds, four between amino acids SER144, CYS145, GLY143, LEU141, and oxygen atom O_2, and the fifth H-bond was between ARG188 and the fifth O_2 atom on the compound. The amino acids HIS41, CYS145, and PRO168 showed three Pi-Alkyl bonds between the benzene ring and methyl group, respectively. HIS163 exhibited a Pi-Sulfur bond with a benzene ring on the compounds. Likewise, hydrophobic interactions were displayed with amino acids THR190, PRO168, GLN189, GLU166, ARG188, MET165, ASN142, and HIS41 at the binding pocket. Van der Waals interactions were also noticed between THR190, GLN192, CLU166, and ASN142 and the carbon atoms C-1, C-5, C-11, and the C-14 compound. A carbon-hydrogen bond formed with the amino acid GLN189 and benzene ring (Table 5 and Figure 6).

The Compound Licoflavone B was found to show three hydrogen bonds between amino acids GLY143, ARG188, SER144, and oxygen atom O_2. Amino acid HIS41, CYS145, MET165, and LEU27 formed four Pi-Alkyl bonds with the two benzene rings and two methyl groups. Likewise, a carbon-hydrogen bond formed with amino acid GLU166. In addition, hydrophobic interactions were displayed between amino acids HIS41, CYS145, GLN189, HIS163, LEU144, THR90, AEG188, MET165, and GLU166. The other interaction shown was van der Waals, exhibited between amino acids GLN192, THR190, PRO168, HIS163, LEU141, THR25, ASN142, and carbon atoms C-1, C-2, C-3, C-7, C-13, C-19, C-20, C-23, C-23, and C-25, and different carbon atom on the compound (Table 5 and Figure 6). The compound Licocoumarin A showed three hydrogen bonds, two between amino acids SER144 and oxy-

gen atom O_2, another one with GLY143 and the same oxygen atom. Amino acids HIS41, LEU27, CYS145, LEU167, and MET165 formed six Pi-alkyl bonds, one with a benzene ring and four with methyl groups on the compound. In addition, van der Waals interactions were displayed between amino acids THR29, THR26, ASN142, PRO168, GN192, THR190, GLN189, ARG188, HIS163, LEU141, and carbon atoms C-1, C-2, C-5, C-8, C-15, C-9, C-17, C-19, and C-20 of the compound. The compound formed hydrophobic interactions with amino acids GLN192, THR26, ASN142, LEU27, LEU141, HIS41, HIS163, GLU166, THR190, MET165, GLN189, and ARG188 (Table 5 and Figure 6).

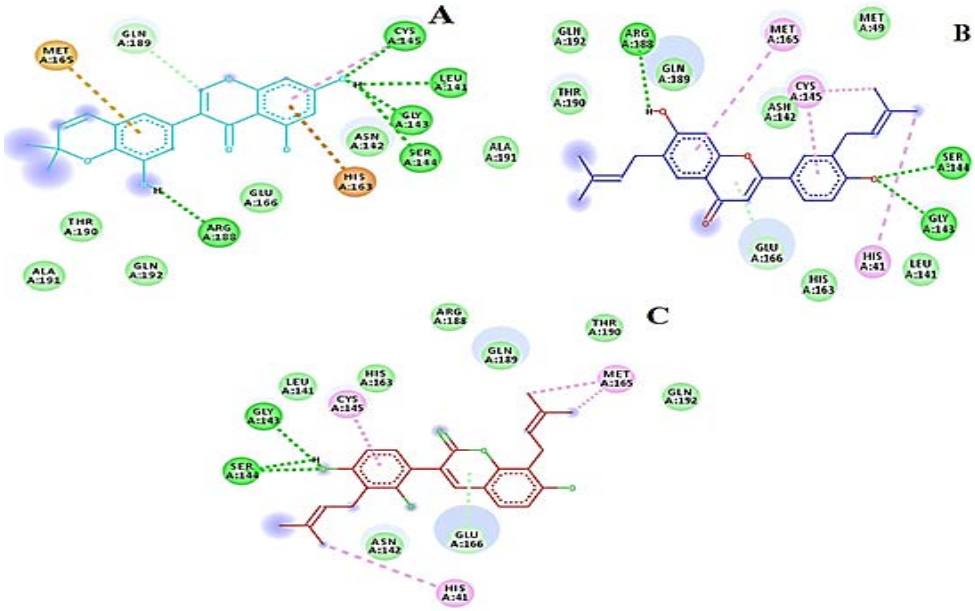

Figure: (6). The 3D structure of the three potential compounds using Discovery studio visualizer (A) Semilicoisoflavone B (B) Licoflavone B (C) Licocoumarin A.

Table: (5). Details of binding interactions of the potential four compounds docked into the active pocket of the COVID-19 3CLprotease.

	Ligands	Residue	Type of interactions
1	Semilicoisoflavone B	CYS145, SER144, GLY143, LEU141, ARG188, THR190, GLN192, CLU166, ASN142, MET165, HIS41, PRO168 GLN189 HIS163 SER144, GLY143,ARG188, GLN192, THR190, PRO168, HIS163, LEU141, THR25, ASN142, HIS41, CYS145, MET165,LEU27 GLU166 CYS145, GLN189, THR90AEG188, MET165, GLU166, LEU144, HIS163, HIS41 SER144, SER144,GLY143 THR29, THR26, ASN142, PRO168, G,N192, THR190, GLN189,ARG188, HIS163, LEU141 HIS41, LEU27, CYS145, LEU167, MET165 LEU27, THR26, ASN142, LEU141, HIS41, HIS163, GLU166, MET165, GLN192, THR190GLN189, ARG188	H-Bond van der Waals Pi-Sulfur Pi-Alkyl Carbon Hydrogen Bond Pi-Cation H-Bond van der Waals Pi-Alkyl Carbon Hydrogen Bond Hydrophobic H-Bond van der Waals Pi-Alkyl Hydrophobic
2	Licoflavone B		
3	Licocoumarin A		

LigPlot (Laskowski & Swindells, 2011) was used to confirm the results of the interactions between the compounds and the target protein; as can be seen in Figure 7, which showed that the compounds occupy the binding pocket and display different interactions such as H-bond, hydrophobic interaction, which indicates the efficiency and effectiveness of these compounds against COVID-19. As mentioned earlier, the hydrogen bond and hydrophobic interactions between the ligands and protein are critical for ligand binding.

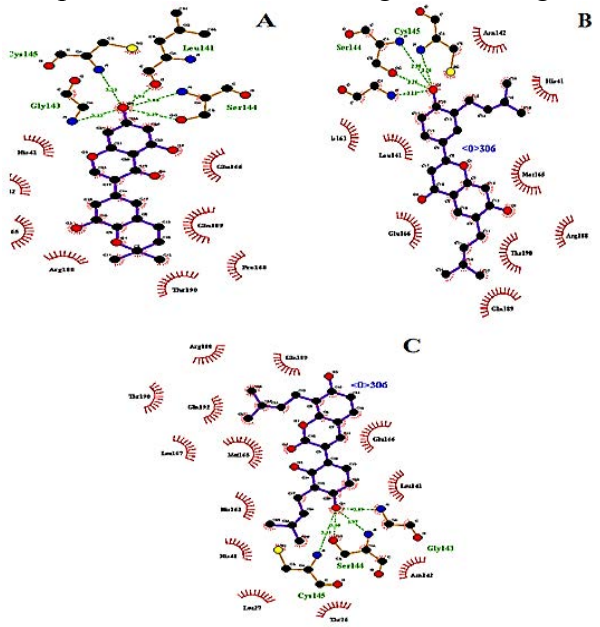

Figure: (7). The 2D structure of the three potential compounds using LigPlot (A) Semilicoisoflavone B (B) Licoflavone B (C) Licocoumarin A.

In this study, in-silico structure-based drug design was employed to apply a logical and inexpensive technique to accelerate the discovery of effective SARS Coronavirus-2 antiviral drugs (Ahmed Ali Abdusalam & Vikneswaran, 2020; Hariyono et al., 2021) The docking results of the three compounds from Glycyrrhiza glabra against the target protein determined minimum FEB, molecular characteristics, binding mode, hydrophobic interactions, and hydrogen-bond between the amino acids residues and compounds in the binding pocket. Therefore, this research involved screening the molecular properties, two docking software (Autodock 4.2 and AutodockVina), hydrogen bonding, and hydrophobic interaction analysis. Even though the use of structural and molecular properties analysis applied in the study was not complicated and easy to use, it helped minimize the costs and the number of docked compounds. In addition, they increased the precision of the virtual screening approach and the consistency of the results of the current study. As long as the catalytic dyad Cys145 and His41 are very important in the covid-19 inhibition, the above finding successfully identified three potential compounds from Glycyrrhiza glabra that displayed good binding interactions and low binding affinity. The three compounds were inhibitors for the catalytic dyad alongside the essential amino acids in the binding pocket. This ability to interact with the essential amino acids in the COVID-19 3CLpro gives additional advantages of inhibiting the virus activity.

CONCLUSION

The current study applied a combination of different molecular modeling techniques, such as two molecular docking approaches, molecular features screening, hydrogen-bond, and hydrophobic interactions analyses, and successfully identified three potential inhibitors for COVID-19 3CLprotease. The three compounds, Semilicoisoflavone B, Licoflavone B, and Licocoumarin A, displayed a high affinity with the 3CLpro binding pocket of COVID-19. The free energy of binding (FEB) values were 10.91, −10.29, and −10.21 kcal/mole for Autodock 4.2 and −9.81, −9.77, and −9.60 kcal/mole for AutoDockVina, respectively. The three compounds obeyed Lipinski's rule of five, with a little violation in one parameter for two compounds compared to the coordinated ligand N3, which violated more than two rules. The obtained results showed that the compounds interacted with the catalytic dyad (Cys145 and His41) in the binding pocket in the COVID-19 main protease, similar to the coordinated ligand N3. To confirm this finding, experimental studies (in vitro and in vivo) are needed to study the interactions between these com-

pounds and COVID-19.

ACKNOWLEDGEMENT

The authors wish to acknowledge the Faculty of Sciences and Faculty of Health Sciences, Sirte University, for supporting this research.

REFERENCES

Abdusalam, A. A. A., & Murugaiyah, V. (2020). Identification of potential inhibitors of 3CL protease of SARS-CoV-2 from ZINC database by molecular docking-based virtual screening. *Frontiers in molecular biosciences, 7*, 419 .

Ahmed Ali Abdusalam, A., & Vikneswaran, M. (2020). Novel Acetylcholinesterase Inhibitors Identified from ZINC Database Using Docking‐Based Virtual Screening for Alzheimer's Disease. *ChemistrySelect, 5*(12), 3593-3599 .

Asrani, P., Afzal Hussain, K. N., AlAjmi, M. F., Amir, S., Sohal ،S. S., & Hassan, M. I. (2021). Guidelines and safety considerations in the laboratory diagnosis of SARS-CoV-2 infection: a prerequisite study for health professionals. *Risk management and healthcare policy, 14*, 379 .

Burley, S. K., Berman, H. M., Kleywegt, G. J., Markley, J. L., Nakamura, H., & Velankar, S. (2017). Protein Data Bank (PDB): the single global macromolecular structure archive. *Protein Crystallography*, 627-641 .

Chan, J., Azhar, E., Hui, D., & Yuen, K. (2016). Coronaviruses: drug discovery and therapeutic options. *Nat Rev Drug Discov, 15*(5), 327-347 .

Chan, J. F.-W., Kok, K.-H., Zhu, Z., Chu, H., To, K. K.-W., Yuan, S., & Yuen, K.-Y. (2020). Genomic characterization of the 2019 novel human-pathogenic coronavirus isolated from a patient with atypical pneumonia after visiting Wuhan. *Emerging microbes & infections, 9*(1), 221-236 .

Cinatl, J., Morgenstern, B., Bauer, G., Chandra, P., Rabenau, H., & Doerr, H. (2003). Glycyrrhizin, an active component of liquorice roots, and replication of SARS-associated coronavirus. *The lancet, 361*(9374), 2045-2046 .

De Wit, E., Van Doremalen, N., Falzarano, D., & Munster, V. J. (2016). SARS and MERS: recent insights into emerging coronaviruses. *Nature Reviews Microbiology, 14*(8), 523-534 .

Forli, S., Huey ،R., Pique, M. E., Sanner, M. F., Goodsell, D. S., & Olson, A. J. (2016). Computational protein–ligand docking and virtual drug screening with the AutoDock suite. *Nature protocols, 11*(5), 905-919 .

Gills, J. J., LoPiccolo, J., Tsurutani, J., Shoemaker ،R. H., Best, C. J., Abu-Asab, M. S., Borojerdi, J., Warfel, N. A., Gardner, E. R., & Danish, M. (2007). Nelfinavir, A lead HIV protease inhibitor, is a broad-spectrum, anticancer agent that induces endoplasmic reticulum stress, autophagy, and apoptosis in vitro and in vivo. *Clinical Cancer Research, 13*(17), 5183-5194 .

Hariyono, P., Patramurti, C., Candrasari, D. S., & Hariono, M. (2021). An integrated virtual screening of compounds from Carica papaya leaves against multiple protein targets of SARS-Coronavirus-2. *Results in chemistry, 3*, 100113 .

Jacq, N., Breton, V., Chen, H.-Y., Ho, L.-Y., Hofmann, M., Kasam, V., Lee, H.-C., Legré, Y., Lin, S. C., & Maaß, A. (2007). Virtual screening on large scale

grids. *Parallel Computing, 33*(4-5), 289-301 .

Laskowski, R. A., & Swindells, M. B. (2011). LigPlot+: multiple ligand–protein interaction diagrams for drug discovery: ACS Publications.

Lavecchia, A., & Di Giovanni, C. (2013). Virtual screening strategies in drug discovery: a critical review. *Current medicinal chemistry, 20*(23), 2839-2860 .

Makeneni, S., Thieker, D. F & ،.Woods, R. J. (2018). Applying pose clustering and MD simulations to eliminate false positives in molecular docking. *Journal of chemical information and modeling, 58*(3), 605-614 .

Marcelin, A.-G., Lamotte, C., Delaugerre, C., Ktorza, N., Ait Mohand, H ،.Cacace, R., Bonmarchand, M., Wirden, M., Simon, A., & Bossi, P. (2003). Genotypic inhibitory quotient as predictor of virological response to ritonavir-amprenavir in human immunodeficiency virus type 1 protease inhibitor-experienced patients. *Antimicrobial agents and chemotherapy, 47*(2), 594-600 .

McInnes, C. (2007). Virtual screening strategies in drug discovery. *Current opinion in chemical biology, 11*(5), 494-502 .

Morris, G. M., Goodsell, D. S., Halliday, R. S., Huey, R., Hart, W. E., Belew, R. K & ،. Olson, A. J. (1998). Automated docking using a Lamarckian genetic algorithm and an empirical binding free energy function. *Journal of computational chemistry, 19*(14), 1639-1662 .

Pal, M., Berhanu, G., Desalegn, C., & Kandi, V. (2020). Severe acute respiratory syndrome coronavirus-2 (SARS-CoV-2): an update. *Cureus, 12*(3 .(

Pastorino, G., Cornara, L., Soares, S., Rodrigues, F., & Oliveira, M. B. P. (2018). Liquorice (Glycyrrhiza glabra): A phytochemical and pharmacological review. *Phytotherapy research* ،(12)32 ، .2339-2323

Phan, T. (2020). Novel coronavirus: From discovery to clinical diagnostics. *Infection, Genetics and Evolution, 79*, 104211 .

Pompei, R., Pani, A., Flore, O., Marcialis, M., & Loddo, B. (1980). Antiviral activity of glycyrrhizic acid .*Experientia, 36*(3), 304-304 .

Sáez-Llorens, X., Violari, A., Deetz, C. O., Rode, R. A., Gomez, P., Handelsman, E., Pelton, S., Ramilo, O., Cahn, P., & Chadwick, E. (2003). Forty-eight-week evaluation of lopinavir/ritonavir, a new protease inhibitor, in human immunodeficiency virus-infected children. *The Pediatric infectious disease journal, 22*(3), 216-223 .

Sharma, V., Katiyar, A., & Agrawal, R. (2018). Glycyrrhiza glabra: chemistry and pharmacological activity. *Sweeteners*, 87 .

Sliwoski, G., Kothiwale, S., Meiler, J., & Lowe, E. W. (2014). Computational methods in drug discovery. *Pharmacological reviews, 66*(1), 334-395 .

Smith, D. M., Daniel, K. G., Wang, Z., Guida, W. C., Chan, T. H., & Dou, Q. P. (2004). Docking studies and model development of tea polyphenol proteasome inhibitors: applications to rational drug design. *Proteins: Structure, Function, and Bioinformatics, 54*(1), 58-70 .

Stoermer, M. (2020). Homology models of coronavirus 3CLpro protease .

Trott, O., & Olson, A. J. (2010). AutoDock Vina: improving the speed and accuracy of docking with a new scoring function, efficient optimization, and multithreading. *Journal of computational chemistry, 31*(2), 455-461 .

Wang, L., Yang, R., Yuan, B., Liu, Y., & Liu, C. (2015). The antiviral and antimicrobial activities of licorice, a widely-used Chinese herb. *Acta pharmaceutica sinica B, 5*(4), 310-315 .

Yang, X., Yu, Y., Xu, J., Shu, H., Liu, H., Wu, Y., Zhang, L., Yu, Z., Fang, M., & Yu, T. (2020). Clinical course and outcomes of critically ill patients with SARS-CoV-2 pneumonia in Wuhan, China: a single-centered, retrospective, observational study. *The Lancet Respiratory Medicine, 8*(5), 475-481 .

Zehra, Z., Luthra, M., Siddiqui, S. M., Shamsi, A., Gaur, N. A., & Islam, A. (2020). Corona virus versus existence of human on the earth: A computational and biophysical approach. *International Journal of Biological Macromolecules, 161*, 271-281 .

Zoete, V., Grosdidier, A., & Michielin, O. (2009). Docking, virtual high throughput screening and in silico fragment‐based drug design. *Journal of cellular and molecular medicine, 13*(2), 238-248.

تحديد المركبات الطبيعية النشطة بيولوجيا من نبات *Glycyrrhiza glabra* كمثبطات للبروتييز الرئيسي لسارس-كوفيد-2 باستخدام النهج *In-silico*

أشرف أحمد علي عبدالسلام*[1]، غزالة محمد بن هندر[2]

[1] قسم العلوم الصيدلانية، كلية العلوم الصحية، جامعة سرت، ليبيا

[2] قسم الكيمياء، كلية العلوم، جامعة سرت، ليبيا

تاريخ الاستلام: 20 مارس 2022 / تاريخ القبول: 04 يونيو 2022

Doi: https://doi.org/10.54172/mjsc.v37i2.679

المستخلص : تسبب فيروس سارس-كورونا-2 في انتشار جائحة كوفيد-19 وتم الاعلان عنها في بداية سنة 2020 مما تسبب في حالة طوارئ صحية عالمية. حتى الآن، لا توجد أدوية أو لقاحات متاحة ومعتمدة، وهناك حاجة ملحة لاستكشاف وتطوير علاجات جديدة فعالة ضد فيروس كورونا المستجد. بالإضافة إلى ذلك، يعتبر البروتياز الرئيسي لفيروس كورونا المستجد ضروريًا في انتشار تكاثر الفيروس ويعتبر هدفًا لاكتشاف الدواء. لذلك، تعتبر المركبات المشتقة من النباتات مصدرًا مهمًا وقيِّمًا للأدوية الجديدة. تشير هذه الدراسة إلى فحص افتراضي قائم على الإرساء الجزيئي لـ 20 مركبًا تم تحديدها من نبات Glycyrrhiza glabra للبحث عن مركبات قوية ضد البروتييز الرئيسي. أظهرت نتائج الفحص أن المركبات المحددة Semilicoisoflavone B و Licoflavone B و Licocoumarin A أظهرت طاقة ترابط منخفضة كانت 10.91 و10.29- و 10.21- كيلو كالوري / مول لـ AutoDock 4.2 و 9.81- و9.77- و9.60- كيلو كالوري / مول، لـ AutoDock Vina على التوالي. كانت النتائج التي تم الحصول عليها من اقل طاقة ترابط في هذه الدراسة أفضل من المركب المرتبط بالبروتين N3 والذي كان طاقته 7.4- كيلو كالوري / مول. أظهرت المركبات الثلاثة المحتملة تفاعلات مختلفة ومستقرة مع الأحماض الأمينية الأساسية، وخاصة الصباغ التحفيزي (سيستين145، هستادين 41) في جيب الربط للبروتييز الرئيسي. في الختام، تم تحديد ثلاثة مثبطات محتملة بنجاح من نبات *Glycyrrhiza glabra* باستخدام الالتحام الجزيئي والفحص الافتراضي؛ امتثلت هذه المركبات لقاعدة لبنسكي 5 مع انتهاك بسيط وأظهرت انخفاض فى طاقة الترابط وتفاعلات جيدة مع البروتييز الرئيسي. قد تكون هذه المركبات المحددة بمثابة مؤشرات محتملة تساعد في تطوير عوامل علاجية ضد فيروس كورونا المستجد. يوصى بإجراء مزيد من البحث (في المختبر وفي الجسم الحي) للتحقق من النتائج المذكورة أعلاه.

الكلمات المفتاحية : فحص افتراضي، إرساء، *Glycyrrhiza glabra*، كوفيد-19، سارس-كوفيد-2، البروتييز الرئيسي.

*[1] أشرف أحمد علي عبدالسلام: aalmansory@su.edu.ly.، قسم العلوم الصيدلانية، كلية العلوم الصحية، جامعة سرت، ليبيا

Al-Mukhtar Journal of Sciences 37 (2): 162-167, 2022
ISSN: online 2617-2186 print 2617-2178
Journal Homepage https://omu.edu.ly/journals/index.php/mjsc/index

Flea Infestations on Domestic Animals in Nafusa Mountain Region, North-West Libya

Waleed Y. M. Aboulqassim [1], Salah Ghana[2*], and Taher Shaibi[2]

[1] *Department of Medical Laboratory Technology, Faculty of Applied Sciences Technology, Al-Awatah, Libya*
[2] *Department of Zoology, Faculty of Science, University of Tripoli, Libya*

Received: 22 March 2022 / Accepted: 01 June 2022
Doi: https://doi.org/10.54172/mjsc.v37i2.645

Abstract: Fleas are ectoparasitic pests on domestic animals and act as vectors of many pathogens to humans. Here, we aim to identify the fleas that parasitize on domestic animals and their seasonality in the Nafusa Mountain region (Gharyan, Zintan, and Nalut). The survey was carried out from summer 2017 to winter 2018/2019. Fleas were collected seasonally from flea-infested animals using a metal comb (11 teeth per cm) and tweezers. One flea species was identified in this survey; *Ctenocephalides felis*, which was collected from goats, sheep, rabbits, donkeys, hens, cats, and dogs. The highest flea prevalence was among goats (66.49 %), followed by sheep (56.17%), whereas in dogs, donkeys, hens, rabbits, and cats, it represented less than 50.00%. The highest flea intensity was among dogs (4.50 ± 3.04 fleas per dog), while the lowest intensity was among hens (0.87 ± 0.59 fleas per hen). The highest mean flea abundance was among cats (8.00), whereas goats, sheep, donkeys, dogs, and hens represented less than 1.50 fleas per host. Summer and autumn represented the highest intensity followed by spring, but no fleas were collected in winter. The finding of the study indicated that *Ct. felis* was common among domestic animals. Consequently, it may become a potential source of pathogen transmission among people and animals.

Keywords: *Ctenocephalides felis*; Siphonaptera; Domestic Animals; Nafusa Mountain; Libya.

INTRODUCTION

Fleas are wingless insects and have medical importance as economic pests in domestic animals around the world (Krämer & Mencke, 2001). They are ectoparasites that cause hypersensitivity and iron deficiency anemia in heavy infestations and responsible vectors of pathogens (plague, rickettsiosis and bartonellosis), and act as intermediate hosts for some endoparasites (Smart, 1956). They can take blood meals from multiple hosts. Consequently, they have the ability to transmit different pathogens to different hosts (Brinkerhoff et al., 2010). The vertebrate hosts provide the main habitat, offering a place for living, feeding, and mating. About 95% of known flea species parasitize on mammals, and the other (5%) parasitize on birds (Krämer & Mencke, 2001). Fleas infest domestic animals such as goats (McCrindle et al., 2011), small ruminants (Kusiluka et al., 1995), cattle (Araujo et al., 1998), and horses (Yeruham et al., 1996).

Some flea species are opportunistic and have a wide range of hosts, while other flea species are highly specific and have a narrow range of hosts (Ford et al., 2017). Domestic animals such as sheep and goats are considered a section of economic resources for people in the Nafusa Mountain region. There are no comprehensive studies in the Nafusa Mountain region

***Corresponding author:** Salah Ghana: s.ghana@uot.edu.ly , Department of Zoology, Faculty of Science, University of Tripoli, Libya.

about fleas that parasitize on domestic animals. The only study in the area was on wild animals (Belgasm et al., 2022). The aim of this study is to identify the fleas that parasitize on domestic animals and their seasonality in the Nafusa Mountain region.

MATERIALS AND METHODS

Study area: The research was conducted in the Nafusa Mountain region, which is located in Libya's northern region (Figure 1). In terms of topography, this region is characterized by a great deal of diversity (mountains, hills, valleys). Seasonal herbs, annuals, and medium-sized plants, such as olive and fig trees, are prominent. The climate is transitional between the desert and the Mediterranean climate. The mean annual rainfall is 49 mm, the mean monthly relative humidity is 15 to 83 %, and the temperature ranges from 4ºC to 43ºC.

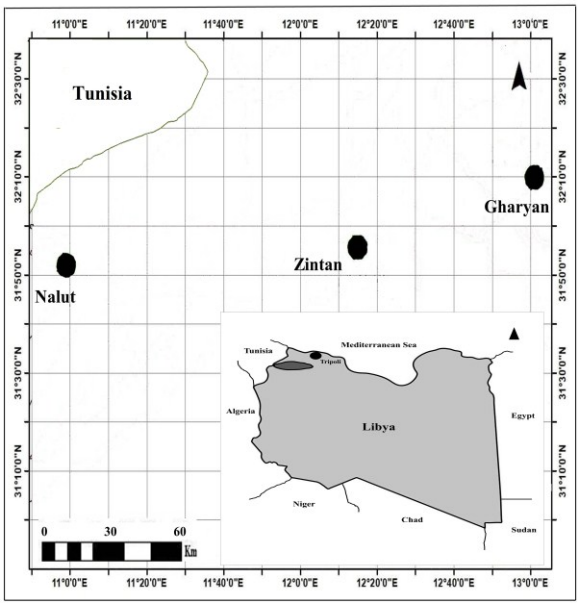

Figure: (1). Map of study area.

Capturing of animals and sampling: Fleas were collected seasonally from summer 2017 to winter 2018/2019 from three locations in Nafusa Mountain region (Gharyan, Zintan and Nalut); from goats (n= 614), sheep (n= 392), rabbits (n= 137), donkeys (n= 37), hens (n= 223), cats (n= 43), dogs (n= 111). Dogs and cats were anesthetized by dissolving 2-5 Calmivet® tablets in milk or placed inside pieces of meat and provided for them. Whereas goats, sheep, hens, rabbits, and donkeys, the fleas were collected from them without anesthetization.

Fleas were collected from all infested hosts by combing the whole body using a metal comb (11 teeth per cm) and tweezers, then transferred to vials containing 70% ethanol by tweezer for preservation. The date of collection, season, number of fleas, host, and collecting place were recorded. The samples were taken to the Laboratory of Entomology in the Zoology Department, Faculty of Science, University of Tripoli, to mount and identify fleas to species level using an identification key (Smit, 1957).

Data analysis: The data were classified according to flea species, host species, seasons of collection, and area. Fleas per host, season, and area were calculated according to International Definitions Indicators, the method of Yin et al. (2011):

$$\text{Flea prevalence (FP)} = \frac{\text{number of hosts infested with fleas}}{\text{total number of surveyed hosts}} \times 100$$

$$\text{Flea intensity (FI)} = \frac{\text{total number of fleas}}{\text{total number of hosts infested with fleas}}$$

$$\text{Mean flea abundance (MFA)} = \frac{\text{total number of fleas}}{\text{total number of surveyed hosts}}$$

The descriptive analysis of main characteristics was performed using means and standard errors (SEs) with flea intensity because it includes the main values of fleas per infested animal. The means of collected fleas per host and season were tested for the normality by the one-sample Kolmogorov-Smirnov test. The means of data were not normally distributed. P-value was ≤ 0.05. The mean of flea intensity was compared by non-parametric tests (Kruskal-Wallis test and Mann-Whitney test) by SPSS (version 23.0.0, 2015).

RESULTS

This survey was carried out from summer 2017 to winter 2018/2019 in the Nafusa mountain region (Gharyan, Zintan and Nalut). A total of 2025 individuals of fleas were collected from 508 infested hosts; goats (246), sheep (141), rabbits (20), donkeys (10), hens (49), cats (6), and dogs (36). Only one flea species was identified, *Ctenocephalides felis*. The highest flea prevalence was among goats (66.79%), followed by sheep (56.17%), whereas among dogs, hens, rabbits, and cats, it represented less than 50.00 % (Figure 2). The Kruskal-Wallis H test revealed no significant difference in the prevalence of

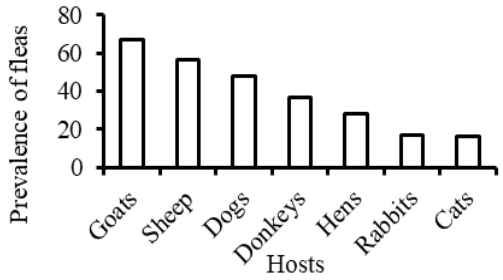

Figure: (2). Prevalence of *Ct. felis* from domestic animals that were collected in the Nafusa Mountain region at the period from summer 2017 to winter 2018/2019

fleas among livestock (H= 11.20, df= 6, P= 0.08). The highest flea intensity was among dogs (4.50 ± 3.04 fleas per dog); the lowest intensity was among hens (0.87 ± 0.59 fleas per hen) (Figure 3).

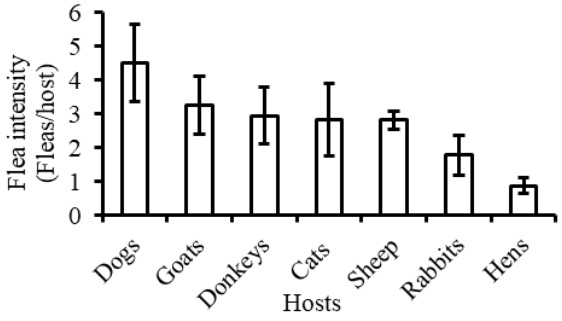

Figure: (3). Intensity of *Ct. felis* per host that were collected from domestic animals from the Nafusa Mountain region at the period from summer 2017 to winter 2018/2019. (Bars represent SE).

There was no significant difference in the intensity of fleas among livestock (Kruskal-Wallis H test, H= 6.00, df= 6, P= 0.42). The highest mean flea abundance was among cats (8.00), whereas goats, sheep, donkeys, dogs, rabbits, and hens showed less than 1.50 (Figure 4). There was no significant difference in flea abundance of fleas among domestic hosts (Kruskal-Wallis H test, H= 3.00, df= 3, P= 0.30).

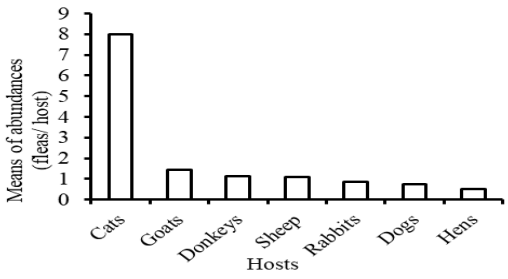

Figure: (4). Mean flea abundance per domestic animals that were surveyed in the Nafusa Mountain region at the period from summer 2017 to winter 2018/2019.

The summer and autumn seasons showed the highest values of flea intensity followed by spring, but no fleas were collected in the winter seasons (Figure 5). There was a significant difference in intensity of *Ct. felis* among seasons in all hosts (Kruskal- wallis H test, H= 18.68, df= 3, P < 0.001). Winter seasons differed significantly from the other seasons (Mann-Whitney U test, P= 0.001). The highest mean flea abundance was in the autumn seasons, followed by the summer seasons, then spring.

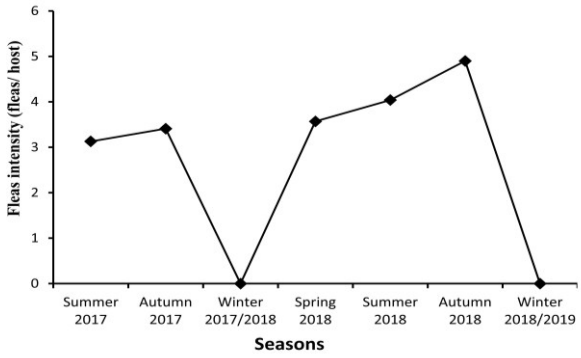

Figure: (5). Intensity of *Ct. felis* per host that were collected in all seasons in the Nafusa Mountain region at the period from summer 2017 to winter 2018/2019.

DISCUSSION

The results of this study indicate that *Ct. felis* infestation was a widespread problem in domestic animals in the Nafusa Mountain region, although Belgasm et al. (2022) reported three species on wild animals in Gharyan; they are *Pulex irritans*, *Xenopsylla cheopis*, and *Leptopsylla segnis*. *P. irritans* was found in Libya infesting dogs, goats, and sheep (Kaal et al., 2006; Elsaid et al., 2013), but we did not record it on domestic hosts. The presence of *Ct. felis* only on domestic animals indicates that there was a transmission of this species among domestic animals in the area. The finding is in agreement with other reports in the El-Khoms area, Libya (Elsaid et al., 2013) and near Tripoli, Libya (Kaal et al., 2006). In this study, dogs were the most infected animals followed by cats. This was found in agreement with the study of Kaal et al. (2006), who reported that *C. felis* is better adapted to dogs and cats. In a similar study in Egypt, *C. felis* was the most prevalent species in dogs (Amin, 1966).

The housing of animals plays an important role in the development cycle of fleas, where the accumulation of droppings (organic materials) in animals' houses provide an appropriate environment for flea proliferation (Kaal et al., 2006). In this study, the highest degree of flea infestation was found in the closed or semi-closed captivities that contain the accumulated droppings, while animals that were grazing in fields and subjected to veterinary care programs were not infested.

In this study, the highest flea infestation was in summer, autumn, and spring, and the decline was in winter. Elsaid et al. (2013) reported that the highest prevalence of fleas was in summer and spring, while the lowest was in winter and autumn in El- Khoms region, Libya. This is probably due to the difference in the environmental conditions (temperature and humidity) because El- Khoms is a coastal region, and the Nafusa Mountain region is about 80 km from the coast.

Although one flea species was recorded in this study, *Ctenocephalides felis* can transmit pathogens including plague, rickettsiosis, and bartonellosis (Dobler & Pfeffer, 2011; Rolain et al., 2003; Wedincamp & Foil, 2002). In addition, *Ct. felis* act as intermediate hosts of rat tapeworm (*Hymenolepis nana*) and dog tapeworm (*Dipylidium caninum*) (Ford et al., 2004; Krämer & Mencke, 2001).

CONCLUSION

The findings of this study revealed that only one species is present on domestic animals. However, the role of this species in transmitting many pathogens cannot be neglected, and further study on this point must be conducted.

ACKNOWLEDGEMENT

We would like to thank friends and colleagues for their assistance in sample collection.

ETHICS

The authors declare that there is no conflict of interest.

REFERENCES

Amin, O. M. (1966). The fleas (Siphonaptera) of Egypt: Distribution and seasonal dynamics of fleas infesting dogs in the Nile valley and delta. *Journal of Medical Entomology,* 3(3-4), 293-298.

Araujo, F., Silva, M., Lopes, A., Ribeiro, O., Pires, P., Carvalho, C., . . . Ramos, J. (1998). Severe cat flea infestation of dairy calves in Brazil. *Veterinary Parasitology,* 80(1), 83-86. doi:10.1016/s0304-4017(98)00181-2

Belgasm, W. Y. M., Shaibi, T., & Ghana, S. (2022). Flea infestation on small wild mammals in Gharyan, Northwest Libya. *Open Veterinary Journal,* 12(1), 17-22. doi:10.5455/ovj.2022.v12.i1.3

Brinkerhoff, R. J., Kabeya, H., Inoue, K., Bai, Y., & Maruyama, S. (2010). Detection of multiple Bartonella species in digestive and reproductive tissues of fleas collected from sympatric mammals. *The ISME Journal,* 4, 955-958. doi:10.1038/ismej.2010.22

Dobler, G., & Pfeffer, M. (2011). Fleas as parasites of the family Canidae. *Parasit Vectors,* 4(139), 6-12.

Elsaid, M. M. A., El-Arifi, E. O., & El-Buni, A. A. (2013). The prevalence of ectoparasites on sheep and goats at El Khoms region, Libya. *Journal of American Science,* 9, 359-363.

Ford, P. L., Fagerlund, R. A., Duszynski, D. W., & Polechla, P. J. (2004). Fleas and Lice of Mammals in New Mexico. *Natural Resources Research Center,* 57, 1-57. doi:0.2737/RMRS-GTR-123

Kaal, J., Baker, K., & Torgerson, P. (2006). Epidemiology of flea infestation of ruminants in Libya. *Veterinary Parasitology,* 141(3), 313-318. doi:10.1016/j.vetpar.2006.05.034

Krämer, F., & Mencke, N. (2001). *Flea biology and control: The biology of the cat flea control and prevention with imidacloprid in small animals*. Berlin Heidelberg: Springer-Verlag.

Kusiluka, L., Kambarage, D., Matthewman, R., Daborn, C., & Harrison, L. (1995). Prevalence of ectoparasites of goats in Tanzania. *Journal of Applied Animal Research,* 7(1), 69-74. doi:10.1080/09712119.1995.9706052

McCrindle, C., Green, E., & Bryson, N. (1999). A primary animal health care approach to treatment and control of flea (*Ctenocephalides felis*) infestation in indigenous goats kept on communal grazing: research communication. *Journal of the South African Veterinary Association,* 70(1), 21-24.

Rolain, J. M., Franc, M., Davoust, B., & Raoult, D. (2003). Molecular detection of *Bartonella quintana*, *B. koehlerae*, *B. henselae*, *B. clarridgeiae*, *Rickettsia felis*, and *Wolbachia pipientis* in cat fleas, France. *Emerging Infectious Diseases,* 9(3), 338- 342. doi:10.3201/eid0903.020278

Smart, J. (1956). *A handbook for the identification of insects of medical importance* (3 ed.). Oxford: The British Museum (Natural History).

Smit, F. G. A. M. (1957). *Handbooks for the identification of British insects, Vol. 1*. London: Royal Entomological Society of London.

Wedincamp, J. J., & Foil, L. D. (2002). Vertical transmission of Rickettsia felis in the cat flea (Ctenocephalides felis Bouché). *Journal of Vector Ecology,* 27 (1), 96-101.

Yeruham, I., Rosen, S., & Braverman, Y. (1996). Ctenocephalides felis flea infestation in horses. *Veterinary Parasitology,* 62(3-4), 341-343. doi:10.1016/0304-4017(95)00889-6

Yin, J. X., Geater, A., Chongsuvivatwong, V., Dong, X. Q., Du, C. H., & Zhong, Y. H. (2011). Predictors for abundance of host flea and floor flea in households of villages with endemic commensal rodent plague, Yunnan Province, China. *PLoS Neglected Tropical Diseases,* 5(3), e997. doi:10.1371/journal.pntd.0000997.

مجلة المختار للعلوم 37 (2): 162-167، 2022

معدلات إصابة الحيوانات المستأنسة بالبراغيث بجبل نفوسة، شمال غرب ليبيا

وليد يوسف محمد بلقاسم[1]، صلاح جقنة[2]، الطاهر الشائبي[2]

[1] قسم تقنية المختبرات الطبية، كلية التقنية للعلوم التطبيقية، العواتة، ليبيا

[2] قسم علم الحيوان، كلية العلوم، جامعة طرابلس، ليبيا

تاريخ الاستلام: 22 مارس 2022 / تاريخ القبول: 01 يونيو 2022

Doi: https://doi.org/10.54172/mjsc.v37i2.645

المستخلص: تعد البراغيث إحدى الطفيليات الخارجية على الحيوانات المستأنسة حول العالم. كما تعمل كنواقل للعديد من مسببات الأمراض للإنسان. هدفت هذه الدراسة لتعريف البراغيث المتطفلة على الحيوانات المستأنسة، وتحديد موسميتها بمنطقة جبل نفوسة. تم إجراء هذا المسح من صيف 2017 إلى شتاء 2019/2018 بمنطقة جبل نفوسة (غريان، الزنتان، نالوت). جمعت البراغيث من الحيوانات المصابة باستخدام مشط حديدي (11 سن لكل سم)، وملاقط. تم تعريف نوع واحد في هذا المسح (*Ctenocephalides felis*)، جُمع من الماعز، والأغنام، والأرانب، والحمير، والدجاج، والقطط، والكلاب. سجلت أعلى نسبة إصابة للعوائل (Prevalence) بين الماعز (66.49%)، ثم الأغنام (56.17%)، بينما بين الكلاب، والحمير، والدجاج، والأرانب، والقطط كانت أقل من 50.00%. و كان أعلى معدل حدة إصابة (Intensity) بين الكلاب (4.50 ± 3.04 برغوث لكل كلب)، وأقلها بين الدجاج (0.87 ± 0.59 برغوث لكل دجاجة). أعلى متوسط للوفرة (Abundance) كان بين القطط (8.00)، بينما كان أقل من 1.50 برغوث/ عائل بين الأغنام، والحمير، والكلاب، والدجاج . فصلا الصيف والخريف مثلا الأعلى من حيث حدة الإصابة، تلاهما فصل الربيع، بينما لم يتم تجميع براغيث في فصل الشتاء. أظهرت نتائج هذه الدراسة أن *Ct. felis* شائع ضمن الحيوانات المستأنسة وقد يكون ناقلا محتملا للممرضات بين الحيوانات، ثم البشر.

الكلمات المفتاحية: *Ctenocephalides felis* ، Siphonaptera، حيوانات مستأنسة، جبل نفوسة ، ليبيا.

[1]* صلاح جقنة اسم القسم ، s.ghana@uot.edu.ly قسم علم الحيوان، كلية العلوم، جامعة طرابلس، ليبيا.

مجلة المختار للعلوم 37 (2): 168-174، 2022
ISSN: online 2617-2186 print 2617-2178
Journal Homepage https://omu.edu.ly/journals/index.php/mjsc/index

اختبار حساسية بكتيريا *Pseudomonas aeruginosa* لمستخلصات طحلب *Asparagopsis taxiformis*

أحمد امراجع عبدالرازق، وسامي محمد صالح*

قسم الأحياء، كلية التربية، جامعة عمر المختار، البيضاء، ليبيا

تاريخ الاستلام: 05 نوفمبر 2021 / تاريخ القبول: 20 يونيو 2022
Doi: https://doi.org/10.54172/mjsc.v37i2.553

المستخلص : تتمتع بكتيريا *Pseudomonas aeruginosa* بمقاومة فريدة للعديد من المضادات الحيوية، مما جعلها في قائمة الأنواع المسببة للعدوى في المستشفيات الليبية. لذلك أجريت الدراسة الحالية بهدف اختبار حساسية ثلاث عزلات من بكتيريا *P.aeruginosa* المعزولة من إصابات مختلفة: التهابات المسالك البولية (Urin)، والتهابات الجروح (Wound)، والإسهال (Diarrhoea) لمستخلصات طحلب *Asparagopsis taxiformis* المائية والايثانولية بتركيزي (50، 100) ملغم/ مل بالإضافة للمضادين النيومايسين، والجنتامايسين، واختبار حساسيتها بطريقة الأقراص. بينت النتائج أن جميع عزلات *P.aeruginosa* حساسة لمستخلصات طحلب *A.taxiformis*، كما لوحظ تفوق المستخلص الايثانولي بتركيز 100ملغم / مل على المضادات الحيوية، والمستخلص المائي، وكانت عزلة المسالك البولية (U) *P.aeruginosa* هي الأكثر حساسية للمستخلصات، بينما كانت عزلة الجروح (W) *P.aeruginosa* هي أكثر العزلات مقاومة للمستخلصات، والمضادات الحيوية، كما بينت النتائج أيضا أن جميع العزلات مقاومة للمضاد الحيوي الجنتامايسين مقارنة بالمضاد الحيوي النيومايسين. خلصت الدراسة إلى إمكانية الاعتماد على *Asparagopsis taxiformis* في التغلب على بكتيريا *Pseudomonas aeruginosa*.

الكلمات المفتاحية : *Pseudomonas aeruginosa*، *Asparagopsis taxiformis*، المضادات الحيوية.

المقدمة

تمثل البكتيريا السالبة *Pseudomonas aeruginosa* العائدة لعائلة Pseudomonadaceae نموذجاً واضحاً للبكتيريا المقاومة للمضادات الحيوية (Cabot et al., 2016)، وترتبط بارتفاع معدلات الوفيات في المستشفيات وخاصةً في غرف العناية المركزة (Alnour et al., 2017)، حيث تسبب عدوى الجهاز التنفسي، ومجرى الدم، والحروق، والجروح، والتهابات المسالك البولية (Al-Obaidi & Al-Dahmoshi, 2020)، وذلك لقدرتها على تكوين هياكل أغشية معقدة تسمى البيوفيلم بالإضافة لامتلاكها جينات متخصصة في مقاومة طيف واسع من المضادات الحيوية، وخاصةً مضادات البيتالاكتام (Sun et al., 2013)، وأجريت العديد من المحاولات في مختلف أنحاء العالم للتغلب على بكتيريا *P.aeruginosa*، والقضاء عليها باستخدام مستخلصات الطحالب البحرية مصدراً علاجياً بديلاً للمضادات الحيوية، حيث كشفت دراسة حديثة إلى إمكانية استخدام العديد من الطحالب البنية في القضاء على هذه البكتيريا (Madkour et al., 2019)، وأشارت دراسة أجريت في الهند إلى حساسية بكتيريا *P.aeruginosa* للمستخلصات الكحولية لنوعين من الطحالب الخضراء (Pushparaj et al., 2014)، وتتميز الطحالب الحمراء Rhodophyta بخصائص دوائية لاحتوائها على مركبات جيدة نشطة بيولوجياً (Cotas et al., 2020)، ومن ضمن أنواعها التي تم تسجيلها حديثاً في شرق

*سامي محمد صالح sami.mohammed@omu.edu.ly ، قسم الاحياء، كلية التربية، جامعة عمر المختار، البيضاء، ليبيا.

السواحل الليبية طحلب *Asparagopsis taxiformis* كأحد أنواع عائلة Bonnemaisoniaceae (Bazairi et al., 2013)، والمسجل كأسوء الأنواع الغازية في منطقة حوض البحر الأبيض المتوسط، له رائحة نفاذة يحتوي على العديد من المركبات الهالوجينية (Zenetos et al., 2010)، يستخدم مكملا غذائيا حيوانيا عالي الكفاءة لتخفيف غاز الميثان أثناء عملية التخمير المعوي في المجترات (Roque et al., 2021).

كما أن له دور في القضاء على العديد من المسببات المرضية، حيث أظهر المستخلص الخام للطحلب تأثيرا قويا ضد داء الليشمانيا نوع *Lishmania infantum* السائد في منطقة حوض البحر الأبيض المتوسط (Vitale et al., 2015)، وأكد (Marino et al., 2016) في إيطاليا أنه يمكن الاعتماد على هذا الطحلب في مجال تربية الأسماك بوصفه مضادا حيويا فعالا ضد البكتيريا، وفي الهند استطاع(Vedhagiri et al., 2009) استخدام طحلب *A.taxiformis* في القضاء على بكتيريا *Leptospira javanica* المسببة لداء البريميات.

أجريت هذه الدراسة في معمل كلية التربية جامعة عمر المختار البيضاء ليبيا، بهدف اختبار حساسية عزلات من بكتيريا *Pseudomonas aeruginosa* لتراكيز مختلفة من مستخلصات طحلب *Asparagopsis taxiformis*.

المواد وطرق البحث

الجمع والإعداد: جمعت عينات طحلب *Asparagopsis taxiformis* من شواطيء منطقة الحمامة شمال مدينة البيضاء/ الجبل الأخضر/ ليبيا، وصنفت في قسم الأحياء/ كلية التربية/ جامعة عمر المختار وفقا (Hayee-Memon & Shameel, 1996)، بعد التنظيف، والتجفيف الطبيعي لمدة أسبوع حفظت لحين الاستعمال.

تحضير المستخلصات: للحصول على المستخلص المائي تمت إذابة 5 جرامات من مسحوق طحلب *Asparagopsis taxiformis* في 100مل من الماء المقطر، ووضعت على حاضنة هزاز لمدة 24ساعة، ثم رشح المحلول بواسطة أوراق ترشيح (0.22 um)، بعدها بخر الراشح بواسطة جهاز المبخر الدوار للحصول على المسحوق الجاف للمستخلص، وحفظ في الثلاجة بدرجة حرارة 4 م° لحين الاستعمال (Alshalmani et al., 2014).

- ولتحضير المستخلص الايثانولي استخدمت الطريقة السابقة نفسها مع استبدال الماء بالايثانول.
- حضر المحلول الأساسي بتركيز 100 ملغم/مل بإذابة 1جم من المسحوق الجاف في 10 مل ماء مقطر.

العزلات البكتيرية: تم الحصول على عزلات معرفة، ومشخصة مسبقاً لإصابات مختلفة من بكتيريا *Pseudomonas aeruginosa*:

- ***P. aeruginosa* (U)** المعزولة من حالات التهابات المسالك البولية، مصدرها مختبر الرازي للتحاليل الطبية، مدينة البيضاء.
- ***P. aeruginosa* (W)** من حالات التهابات الجروح، مصدرها مستشفى الجلاء للحوادث، مدينة بنغازي.
- ***P. aeruginosa* (D)** من حالات الإسهال، مصدرها عيادة التراحم، مدينة البيضاء.

اختبار حساسية البكتيريا: تم إجراء الاختبار بطريقة الأقراصDisk diffusion method، حيث زرعت العزلات الثلاثة على وسط Mueller-Hinton agar، ثم وضعت أقراص مشبعة بمستخلصات طحلب *Asparagopsis taxiformis* بقطر 6 ملم وبمسافات متساوية، وحضنت الأطباق لمدة 24 ساعة بدرجة حرارة 37م (Abdulrraziq & Salih, 2020)، واستخدمت أقراص من المضادين النيومايسين (30µg) والجنتامايسين (10µg) للمقارنة، وتم قياس أقطار مناطق التثبيط الخالية من النمو الميكروبي منقوصا منها أقطار الأقراص للمستخلصات.

تصميم البيانات وتحليلها: تم تصميم تجارب الدراسة المعملية وفق التصميم كامل العشوائية Completely Randomized Design (CRD)، وأجريت عملية التحليل الإحصائي باستخدام برنامج (Minitab17) لتحليل تباين (ANOVA)، وتم إجراء المقارنة بين المتوسطات باستخدام اختبار (Tukey's) عند $P<0.05$.

النتائج

أختبرت حساسية بكتيريا *P.aeruginosa* المعزولة من إصابات مختلفة لمستخلصات طحلب *Asparagopsis taxiformis* المائية، والايثانولية، وبعد قياس أقطار التثبيط، بينت النتائج أن هناك فروقاً معنويةً في مدى حساسية العزلات البكتيرية للمستخلصات، والمضادات الحيوية تبعاً لمصدر الإصابة، ونوع المستخلص، والتركيز المستخدم.

حساسية عزلات *P.aeruginosa* للمستخلصات: أظهرت النتائج من الجدول(1)، والشكل (1) أن بكتيريا *P.aeruginosa* (W) المعزولة من التهابات الجروح أبدت مقاومة للمستخلص المائي، في حين سجلت حساسية ضعيفة للمستخلص الايثانولي بأقطار تثبيط (1.0، 1.5) ملم للتركيزين 50، 100 ملغم / مل على التوالي، وبينت النتائج أيضا أن بكتيريا *P.aeruginosa* (D) المعزولة من حالات الإسهال سجلت حساسية ضعيفة للمستخلص المائي للتركيز 100ملغم / مل بقطر تثبيط (1.0) ملم، بينما كانت ذات حساسية متوسطة للمستخلص الايثانولي بتركيز 50ملغم/ مل بقطر تثبيط (2.4) ملم، في حين سجلت حساسية عالية للتركيز 100 ملغم/ مل بقطر تثبيط (5.2) ملم، كما أظهرت النتائج أن بكتيريا *P.aeruginosa* (U) المعزولة من التهابات المسالك البولية كانت هي الأكثر حساسية لجميع تراكيز المستخلصين المائي والايثانولي بأقطار تثبيط تراوحت من (2.5–6.3) ملم، كان أفضلها للمستخلص الايثانولي بتركيز 100 ملغم / مل.

حساسية عزلات *P.aeruginosa* للمضادات: يتضح أيضاً مدى حساسية بكتيريا *P.aeruginosa* المعزولة من إصابات مختلفة للمضادين النيومايسين، والجنتامايسين، حيث لوحظ أن بكتيريا *P.aeruginosa* (W) المعزولة من التهابات الجروح كانت ذات حساسية ضعيفة تجاه المضادين النيومايسين، والجنتامايسين بقطر تثبيط (2.2، 1.8) ملم على التوالي، بينما كانت بكتيريا *P.aeruginosa* (U) المعزولة من التهابات المسالك البولية أكثر حساسية للمضاد الحيوي النيومايسين بقطر تثبيط (3.9) ملم مقارنة بالمضاد الحيوي الجنتامايسين بقطر تثبيط (2.6) ملم، في حين كانت بكتيريا *P.aeruginosa* (D) المعزولة من حالات الإسهال هي الأكثر حساسية بالمضادين.

جدول(1): حساسية بكتيريا *P.aeruginosa* لمستخلصات طحلب *A.taxiformis* والمضادات الحيوية (المتوسط ± الانحراف المعياري).

العزلة / المستخلص		*P.aeruginosa* (W)	*P.aeruginosa* (D)	*P.aeruginosa* (U)
المائي	50	0.0±0.0 c	0.0±0.0 e	2.5±0.3 b
ملغم/مل	100	0.0±0.0 c	1.0±0.0 d	3.1±0.5 b
الايثانولي	50	1.0±0.0 b	2.4±0.4 c	2.7±0.2 b
ملغم/مل	100	1.5±0.5 b	5.2±0.5 a	6.3±1.0 a
Neomycin	30	2.2±0.2 a	4.5±0.5 ab	3.9±0.5 b
Gentamicin	10	±0.1 ab61	±0.2 b6.3	2.6±0.1 b

• الحروف المختلفة توجد بينها فروق معنوية ضمن العمود نفسه عند مستوى 0.05%.

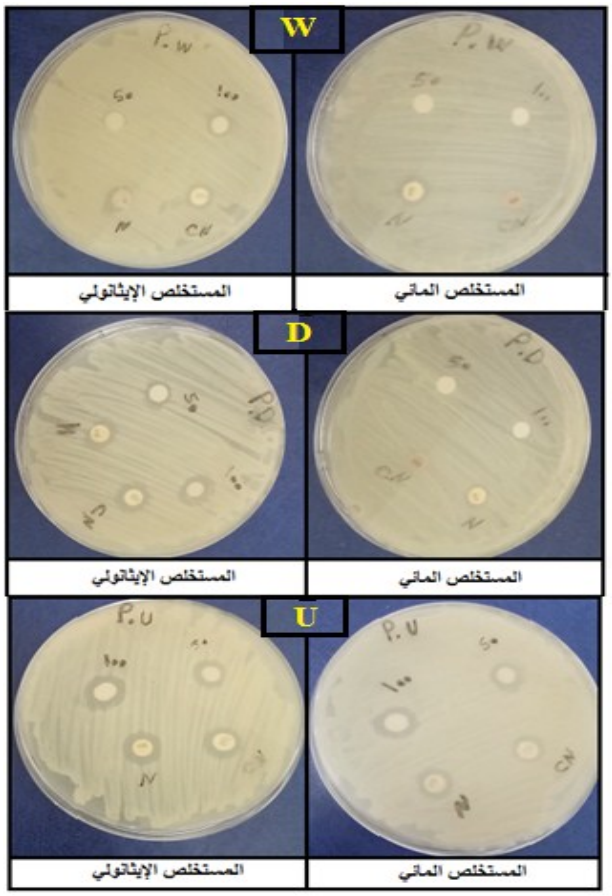

شكل(1): حساسية عزلات *P.aeruginosa* للمستخلصات والمضادات الحيوية.

المناقشة

تعتبر بكتيريا *Pseudomonas aeruginosa* مصدراً للعديد من الالتهابات الحادة والمزمنة، والمقاومة للكثير من المضادات الحيوية (Lavoie et al., 2011)، ولقلة الأبحاث المتداولة حول مدى حساسيتها لمستخلصات الطحالب الحمراء وخاصة الموجودة على السواحل الليبية، اجريت هذه الدراسة التي أظهرت أن بكتيريا *P.aeruginosa* المعزولة من إصابات مختلفة حساسة لمستخلصات طحلب *Asparagopsis taxiformis*، واتفقت هذه النتيجة مع (Bhuyar et al., 2020; Dayuti, 2018) بوجود فاعلية للطحالب الحمراء ضد العديد من مسببات الأمراض البكتيرية، ولوحظ أن جميع عزلات بكتيريا *P.aeruginosa* كانت أكثر حساسية للمستخلص الايثانولي من المستخلص المائي واتفقت هذه النتيجة مع ما ذكره (Manilal et al., 2009) بأن المذيبات الكحولية هي الأفضل في استخلاص المركبات الفعالة، وأشارت النتائج أيضا إلى أن عزلة المسالك البولية (U) *P.aeruginosa* هي الأكثر حساسية للمستخلصات يليها عزلة الإسهال (D) *P.aeruginosa*، وكانت عزلة الجروح (W) *P.aeruginosa* أكثر العزلات مقاومة للمستخلصات، والمضادات الحيوية، كما كانت جميع العزلات حساسة للمضاد الحيوي النيومايسين مقارنة بالمضاد الجنتامايسين، واتفقت هذه النتائج مع (Kılınç et al., 2015) بتفاوت حساسية البكتيريا للمضادات الحيوية ومقاومتها، وأن عزلاتها من الجروح هي الأكثر مقاومة، وتفوق المستخلص الايثانولي بتركيز 100 ملغم / مل على المضادات الحيوية في القضاء على هذه البكتيريا، وقد ترجع الفاعلية التثبيطية لطحلب *Asparagopsis taxiformis* لاحتوائه على halogenated compounds، haloforms، methanes، ketones، acetates، acrylates كمركبات نشطة بيولوجيا (Bansemir et al., 2006).

الخلاصة

نستنتج من هذه الدراسة أنه يمكن الاعتماد على مستخلصات طحلب *Asparagopsis taxiformis* بديلاً للمضادات الحيوية في مقاومة بكتيريا *Pseudomonas aeruginosa* وتوصي الدراسة بإجراء المزيد من الدراسات، والتحقق من فاعلية الطحالب الحمراء في مجال المكافحة الحيوية.

المراجع

Abdulrraziq, A. A., & Salih, S. M. (2020). Biological Effect of Posidonia oceanica Seaweed on Some Pathogenic Microbes. *Al-Mukhtar Journal of Sciences, 35*(4), 339-346 .

Al-Obaidi, R. D., & Al-Dahmoshi, H. (2020). Biofilm and antibiotic resistance profile among Pseudomonas aeruginosa isolated from clinical samples. *Eurasia J Biosci, 14*(1), 1135-1139 .

nutraceutical and therapeutic applications of red seaweeds (Rhodophyta). *Life, 10*(3), 19 .

Dayuti, S. (2018). Antibacterial activity of red algae (Gracilaria verrucosa) extract against Escherichia coli and Salmonella typhimurium. IOP conference series: earth and environmental science ،

Hayee-Memon, A., & Shameel, M. (1996). A taxonomic study of some red algae commonly growing on the coast of Karachi .

Kılınç, Ç ،.Güçkan, R., Çepni, M., Aydın, O., & Çatakoğlu, A. H. (2015). Antibacterial Resistance in Pseudomonas aeruginosa Strains Isolated from Various Clinical Samples. *Respiration, 104*, 31.38 .

Lavoie, E. G., Wangdi, T., & Kazmierczak, B. I. (2011). Innate immune responses to Pseudomonas aeruginosa infection. *Microbes and infection, 13*(14-15), 1133-1145 .

Madkour, F., A El-Shoubaky, G., & A Ebada, M. (2019). Antibacterial activity of some seaweeds from the Red Sea coast of Egypt. *Egyptian Journal of Aquatic Biology and Fisheries, 23*(2), 265-274 .

Manilal, A., Sujith, S., Kiran, G. S., Selvin, J., Shakir, C., Gandhimathi, R., & Lipton, A. P. (2009). Antimicrobial potential and seasonality of red algae collected from the southwest coast of India tested against shrimp, human and phytopathogens. *Annals of Microbiology, 59*(2), 207-219 .

Marino, F., Di Caro, G., Gugliandolo, C., Spano, A., Faggio, C., Genovese, G., Morabito, M., Russo, A., Barreca, D., & Fazio, F. (2016). Preliminary study on the in vitro and in vivo effects of Asparagopsis taxiformis bioactive

Alnour, I., Wagiran, H., Ibrahim, N., Hamzah, S., & Elias, M. (2017). Determination of the elemental concentration of uranium and thorium in the products and by-products of amang tin tailings process. AIP Conference Proceedings ،

Alshalmani, S. K., Zobi, N. H., & Bozakouk, I. H. (2014). Antibacterial activity of Libyan seaweed extracts. *International Journal of Pharmaceutical Sciences and Research, 5*(12 .5425 ،(

Bansemir, A., Blume, M., Schröder, S., & Lindequist, U. (2006). Screening of cultivated seaweeds for antibacterial activity against fish pathogenic bacteria. *Aquaculture, 252*(1), 79-84 .

Bazairi, H., Sghaier, Y. R., Benamer, I., Langar, H., Pergent, G., Bouras, E., Verlaque, M., Soussi, J. B., & Zenetos, A. (2013). Alien marine species of Libya: first inventory and new records in El-Kouf National Park (Cyrenaica) and the neighbouring areas. *Mediterranean marine science*, 451-462 .

Bhuyar, P., Rahim, M., Sundararaju, S., Maniam, G., & Govindan, N. (2020). Antioxidant and antibacterial activity of red seaweed Kappaphycus alvarezii against pathogenic bacteria. *Global Journal of Environmental Science and Management, 6*(1), 47-58 .

Cabot, G., Zamorano ،L., Moyà, B., Juan, C., Navas, A., Blázquez, J., & Oliver, A. (2016). Evolution of Pseudomonas aeruginosa antimicrobial resistance and fitness under low and high mutation rates. *Antimicrobial agents and chemotherapy, 60*(3), 1767-1778 .

Cotas, J., Leandro, A., Pacheco, D., Gonçalves, A. M., & Pereira, L. (2020). A comprehensive review of the

phycoderivates on teleosts. *Frontiers in physiology, 7*, 459 .

Pushparaj, A., Raubbin, R., & Balasankar, T. (2014). An antibacterial activity of the green seaweed Caulerpha sertularioides using five different solvents. *International of Journal PharmTech Research, 6*, 01-05 .

Roque, B. M., Venegas, M., Kinley, R. D., de Nys, R., Duarte, T. L., Yang, X., & Kebreab, E. (2021). Red seaweed (Asparagopsis taxiformis) supplementation reduces enteric methane by over 80 percent in beef steers. *PloS one, 16*(3), e0247820 .

Sun, Z., Jiao, X., Peng, Q., Jiang, F., Huang, Y., Zhang, J., & Yao, F. (2013). Antibiotic resistance in Pseudomonas aeruginosa is associated with decreased fitness. *Cellular Physiology and Biochemistry, 31*(2-3), 347-354 .

Vedhagiri, K., Manilal, A., Valliyammai, T., Shanmughapriya, S., Sujith, S., Selvin, J., & Natarajaseenivasan, K. (2009). Antimicrobial potential of a marine seaweedAsparagopsis taxiformis againstLeptospira javanica isolates of rodent reservoirs. *Annals of Microbiology, 59*(3), 431-437 .

Vitale, F., Genovese, G., Bruno, F., Castelli, G., Piazza, M., Migliazzo, A., Minicante, S. A., Manghisi, A., & Morabito, M. (2015). Effectiveness of red alga Asparagopsis taxiformis extracts against Leishmania infantum. *Open Life Sciences, 10*(1 .(

Zenetos, A., Gofas, S., Verlaque, M., Çinar, M. E., García Raso, J. E., Bianchi, C., Morri, C., Azzurro, E., Bilecenoglu, M., & Froglia, C. (2010). Alien species in the Mediterranean Sea by 2010. A contribution to the application of European Union's Marine Strategy Framework Directive (MSFD). Part I. Spatial distribution .

Sensitivity testing of *Pseudomonas aeruginosa* to *Asparagopsis taxiformis* extracts

Ahmed A. Abdulrraziq and Sami M. Salih*

Department of Biology, Faculty of Education, Omar Al-Mukhtar University, Libya

Received: 05.November 2021./ Accepted: 20 June 2022
Doi: https://doi.org/10.54172/mjsc.v37i2.553

Abstract: *Pseudomonas aeruginosa* has been to possess a unique level of resistance to most antibiotics, therefore made in the list of types to cause infections in Libyan hospitals. This study was conducted to test the sensitivity of three *P.aeruginosa* isolates from different infections: infection tract urinary (U), Wound infection (W), Diarrhoea (D), to aqueous and ethanol extracts of *Asparagopsis taxiformis* at a concentration of (50, 100) mg/ml, compared with Neomycin and Gentamycin. The results showed the sensitivity of all *P.aeruginosa* isolates to *A.taxiformis* extracts, superiority is observed of ethanol extract at a concentration of 100 mg/ml on antibiotics and aqueous extract. *P.aeruginosa* (U) isolates were the most sensitive to extracts, while *P.aeruginosa* (W) isolates were the most resistant to extracts and antibiotics. The results also showed a resistance of all isolates to gentamycin compared to neomycin. Data in this study indicated to possibility use of *Asparagopsis taxiformis* could be a valid alternative for bio-control of *Pseudomonas aeruginosa*.

Keywords: *Pseudomonas aeruginosa*, *Asparagopsis taxiformis*, Antibiotic.

***Corresponding author:** Sami mohammed salih sami.mohammed@omu.edu.ly , Department of Biology, Faculty of Education, Omar Al-Mukhtar University, Libya

مجلة المختار للعلوم 37 (2): 175-184، 2022
ISSN: online 2617-2186 print 2617-2178
Journal Homepage https://omu.edu.ly/journals/index.php/mjsc/index

تأثير الميثوتركسيت على ذاكرة التعرف في إناث الفئران البالغة

وفاء فرج الماطوني*[1]، فاطمة حسين أحمد [1]، هاجر محمد غليو[1]، مصطفى محمد دراه[2]

[1] قسم علم الحيوان، كلية العلوم، جامعة مصراتة، ليبيا
[2] قسم التقنيات الحيوية، كلية العلوم، جامعة مصراتة، ليبيا

تاريخ الاستلام: 11 فبراير 2022/ تاريخ القبول: 12 يونيو 2022
Doi:https://doi.org/10.54172/mjsc.v37i2.617

المستخلص : يُستخدم الميثوتركسيت MTX لعلاج بعض أمراض السرطان، والأمراض الجلدية، والأمراض الروماتيزمية، وقد أثبتت العديد من الدراسات أنه يسبب ضرراً للذاكرة لدى الفئران. وعليه أجريت هذه الدراسة لمعرفة تأثير جرعات مختلفة من الميثوتركسيت على ذاكرة التعرف في الفئران. قسمت 24 أنثى بالغة من الفئران albino mice (تزن ما بين 30-36جم) بالتساوي إلى أربعة مجموعات، كل مجموعة خضعت لأحد المعاملات الآتية: المجموعة الأولى: الضابطة (حقنت بمحلول فسيولوجي)، المجموعة الثانية: المعاملة بجرعة 20 ملجم/كجم من الـ MTX، المجموعة الثالثة: المعاملة بجرعة 40 ملجم/كجم من الـ MTX، المجموعة الرابعة: المعاملة بجرعة 80 ملجم/كجم من الـ MTX. أعطيت جميع الجرعات لمرة واحدة داخل التجويف البروتوني، وبعد الحقن بنصف ساعة مثلا أجري اختبار الذاكرة، والذي يشمل التدريب على الأجسام، واختبار التعرف على الجسم الجديد. أظهرت نتائج هذه الدراسة انخفاض معدل استكشاف الفئران المحقونة بالـ MTX للجسم الجديد مقارنة بالمجموعة الضابطة، وهذا الانخفاض ازداد مع ازدياد الجرعة المحقونة. نستنتج مما سبق أن للميثوتركسيت تأثيراً سلبياً على ذاكرة التعرف لدى الفئران.

الكلمات المفتاحية : اختبار التعرف على الجسم الجديد؛ التجويف البريتوني؛ الميثوتركسيت؛ تدهور معرفي؛ ذاكرة التعرف.

المقدمة

الميثوتركسيت (MTX) Methotrexate هو عامل مضاد للأورام ومثبط للمناعة، استخدم منذ سنة 1948م على نطاق واسع في علاج العديد من الأمراض مثل السرطان، والالتهابات، وأمراض المناعة الذاتية، وبعض الأمراض الجلدية، وكذلك علاج التهاب المفاصل الروماتويدي(Akman, 2021).

يعتبر الميثوتركسيت (4 أمينو 10 ميثيل حمض الفوليك (4-amino-10-methylfolic acid)) مادة مناظرة ومضادة لحمض الفوليك (Bedoui et al., 2019). يعمل MTX على منع عمل أنزيم ثنائي هيدرو حمض الفوليك (Dihydrofolate reductase)، مسبباً تثبيطاً في عملية تخليق البيورين، والبريميدين (Purine and Pyrimidine)، مما يوقف صنع الـ DNA، وتضاعفه، وبالتالي توقف الخلايا التي تتكاثر بسرعة مثل: الخلايا السرطانية (Akman, 2021; Bedoui et al., 2019).

هناك العديد من الآثار الجانبية لاستخدام الميثوتركسيت علاجا، فبعضها طفيف نادر لا يهدد حياة الشخص كالغثيان، والصداع، وتساقط الشعر، والشعور بالضعف العام. إلا أن هناك بعض الآثار السمية لهذا العقار قد تهدد الحياة وتشمل:

*وفاء فرج الماطوني: elmatonw@sci.misuratau.edu.ly, قسم علم الحيوان، كلية العلوم، جامعة مصراتة، ليبيا

انخفاض أعداد خلايا الدم البيضاء، وأمراض الكبد، والكلى الناتجة عن سمية MTX (Bedoui et al., 2019). كما أن استخدام MTX قد يسبب حدوث خلل طويل الأمد في الانتباه، وتدهور وظائف الدماغ، وأيضا له تأثير سلبي على الذاكرة (John et al., 2021; Madhyastha et al., 2002; Naewla et al., 2019).

وتعرف ذاكرة التعرف (Recognition Memory) بأنها القدرة على التعرف على الأحداث، أو الأشياء، أو الأشخاص الذين تمت مواجهتهم مسبقًا (Broadbent et al., 2010). أصبحت مهمة التعرف على الأجسام الجديدة Novel Object Recognition مهمة قياسية لتقييم ذاكرة التعرف لدى القوارض، حيث تستغل هذه المهمة ميل القوارض الطبيعي لاستكشاف أجسام جديدة، إذ يمكن الوصول إلى استنتاجات حول الذاكرة من خلال قياس المدة الزمنية التي تستغرقها القوارض في استكشاف هذه الأجسام (Cohen & Stackman Jr, 2015).

بينت دراسات عديدة التأثير الضار للميثوتركسيت على ذاكرة القوارض (John et al., 2021). عند حقن جِرَاء الفئران بالـ MTX (1 أو 2ملجم / كجم) داخل التجويف البريتوني في الأيام 14 و 15 و 16 بعد الولادة، لوحظ تدهور ذاكرة الفئران (اختبار التعرف على الأجسام الجديدة) بعد مرور تسعة عشر يومًا من المعاملة، هذا التدهور شمل الذاكرة على فترات قصيرة (ساعة واحدة) وطويلة (24 ساعة) (Bisen-Hersh et al., 2013).

تسبب حقن جرعتين من الـ MTX (75 ملجم/ كجم/ اليوم في اليومين السابع، والرابع عشر من التجربة) في الوريد الذيلي للجرذان البالغة في تدهور ذاكرة التعرف لدى هذه الجرذان، وحدوث انخفاض في تركيز مجموعة من البروتينات التي تلعب دورا مهما في وظيفة التذكر لدى الجرذان (Sritawan et al., 2021)، كما حدث انخفاض في عدد الخلايا العصبية غير الناضجة في منطقة الحصين Hippocampus (Sritawan et al., 2020).

أشار (Seigers et al., 2008) إلى أن حقن الـ MTX (250 ملجم /كجم) في وريد الجرذان أدى إلى انخفاض وظيفة الحُصين، مما جعل الجرذان تفشل في تمييز الجسم الجديد من الجسم القديم، أي حدث ضعف في ذاكرة التعرف على الأجسام الجديدة لدى هذه الجرذان.

أدى حقن أربع جرعات من الـ MTX (0.5 ملجم / كجم) في فترة أسبوعين داخل التجويف البريتوني لذكور الجردان إلى عجز في ذاكرة التعرف، استمر هذا العجز لمدة ثلاثة أشهر على الأقل بعد الحقن (Vijayanathan et al., 2011).

تسبب حقن جرعة واحدة من الـ MTX (75 ملجم / كجم) في وريد الجردان البالغة، إلى عجز في الذاكرة، وانخفاض كبير في تكاثر الخلايا العصبية غير الناضجة، وهذه النتائج اتضحت عند إجراء اختبار التعرف على الأجسام الجديدة (Naewla et al., 2019).

ونظرا للاستخدام الواسع لعقار الـ MTX في علاج السرطان (Aldosouky et al., 2011)، وعلاج التهاب المفاصل الروماتويدي في ليبيا بجرعات منخفضة مختلفة، وحيث أن معظم المصابين كانوا من النساء (Etaher et al., 2021) فإن هذه الدراسة تهدف إلى قياس التأثير السمي لثلاث جرعات مختلفة (منخفضة، ومتوسطة، وعالية) من الميثوتركسيت على ذاكرة التعرف على أجسام جديدة لدى إناث الفئران البالغة.

المواد وطرق البحث

الكيمياويات المستخدمة: سائل الميثوتركسيت (Methotrexate ® 50 mg/2ml, Mylan, France) ومحلول فسيولوجي(0.9%) Normal saline .

الحيوانات المختبرية Experimental Animals : استخدم في هذه الدراسة 24 أنثى بالغة من الفئران البيضاء mice Female albino أوزانها ما بين (30–36 جرام)، والتي تحصل عليها من بيت الحيوان التابع لكلية الصيدلة

مصراتة. تم إيواء هذه الفئران في أقفاص بلاستيكية (طول 60 سم ×عرض 30 سم ×ارتفاع 32 سم)، حيث هُيئت لها الظروف المختبرية المطلوبة والمناسبة لها من ضوء (12ساعة ظلام: 12ساعة إضاءة)، ودرجة حرارة (22 ± 2 0م)، وعليقة خاصة بتغذيتها (ذرة، وشعير، وقمح)، وكان الماء والغذاء متاحا لها طول فترة التجربة. تم التعامل مع الحيوانات وفق أخلاقيات البحث العلمي.

تصميم التجربة Experimental Design: قُسمت حيوانات التجربة إلى أربع مجموعات عشوائيا، بواقع ستة فئران لكل مجموعة، عُزلت الإناث عن الذكور لمدة شهر سمح لها خلال ذلك بالأقلمة مع الظروف البيئية (بيت الحيوان بكلية العلوم مصراتة). استغرقت دراسة الذاكرة مدة أسبوع، حيث سُمح للفئران بالتأقلم مع الصندوق الخاص باختبار الذاكرة، في اليوم الأول (كل مجموعة فئران على حدة)، واليوم الثاني، والرابع (كل فأر على حدة)، أما في اليوم الخامس عُوملت حيوانات التجربة وفق التالي (Elens et al., 2019; Ermens et al., 1989; Naewla et al., 2019):

•المجموعة الأولى (المجموعة الضابطة Control Group):حُقنت بمحلول فسيولوجي (0.9%) بحجم مماثل لحجم جرعة الـ MTX .

•المجموعة الثانية :حُقنت بـ 20 ملجم/ كجم من الـMTX.

•المجموعة الثالثة : حُقنت بـ40 ملجم/كجم من الـMTX.

•المجموعة الرابعة :حُقنت بـ 80 ملجم/كجم من الـMTX.

أعطيت جرعة الـ MTX عن طريق الحقن في التجويف البريتوني. بعد الحقن بساعة أجري التدريب على الأجسام، ثم بعد أربع وعشرين ساعة من انتهاء التدريب أجري اختبار التعرف على الجسم الجديد لقياس ذاكرة التعرف لدى الفئران .

اختبار الذاكرة Memory test : أجري اختبار التعرف على الأجسام الجديدةObject recognition memory لقياس تأثير MTX على ذاكرة التعرف لدى الفئران، طُبِق هذا الاختبار في غرفة ذات إضاءة خافتة وهادئة. واستخدم في هذا الاختبار صندوق خشبي أسود مستطيل (طوله 30سم، عرضه25سم، ارتفاعه 25سم)، مفتوح من الأعلى. أما الأجسام فهي عبارة عن ثلاث عبوات زجاجية ذات ألوان مختلفة أبيض شفاف (الجسمA)، بني (الجسم B) ، وأخضر (الجسمC)، اختيرت هذه الأجسام بناء على تجارب سابقة أجريت في المعمل. أجري اختبار الذاكرة على 3 مراحل: فترة تأقلم Habituation period (قبل يوم الحقن بأربعة أيام)، ويوم التدريبTraining، ويوم الاختبارTesting.

أولا فترة التأقلم: تأقلمت الفئران على الصندوق الفارغ على مرحلتين: المرحلة الأولى أُجريت بوضع كل مجموعة من الفئران على حدة لمدة 10 دقائق في يوم واحد، أما في المرحلة الثانية وُضع كل فأر في صندوق الاختبار الفارغ لمدة 5 دقائق لمدة يومين، يُساعد تأقلم الفئران التعرف على الصندوق واستكشافه.

ثانيا التدريب Training: أُجري يوم التدريب بعد حقن الميثوتركسيت بساعة، حيث وُضع الجسمان A، وB في الصندوق، وعلى مسافة 10 سم من الجدار وسُمح لكل فأر باستكشاف الجسمين لمدة 5 دقائق مع مراعاة تسجيل الملاحظات.

ثالثا أُجري الاختبار Test: بعد انتهاء التدريب بأربع وعشرين ساعة، وذلك باستبدال الجسم B بآخر جديدC ، وسُمح لكل فأر باستكشاف الجسمين لمدة 5 دقائق .

سُجل زمن استكشاف كل فأر لكل جسم (بالثواني) يدوياً باستخدام ساعة إيقاف. ثم حُسب معدل استكشاف الفأر لكل جسم (%) بالنسبة للزمن الكلي لاستكشاف الجسمين. استخدم كحول الإيثانول (70%) لمسح الصندوق، والأجسام الزجاجية بين كل فأر وآخر (Lyons et al., 2011; Reger et al., 2009). انظر الشكل 1 يوضح خط سير التجربة.

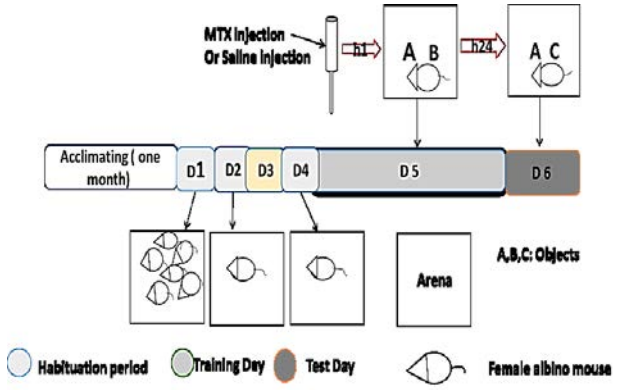

شكل (1). خط سير التجربة.

التحليل الإحصائي Statistical Analysis : استخدم البرنامج الإحصائيSPSS لإجراء التحاليل الإحصائية الخاصة بالدراسة, أعدت الأشكال البيانية ببرنامجGraphpad prism. وعُبر عن النتائج بالمتوسط ± الخطأ المعياري. استخدم تحليل اختبار التباين الأحادي One Way ANOVA لمقارنة نتائج الزمن الكلي للاستكشاف، وكذلك لإيجاد الفروقات في نتائج اختبار الذاكرة بين المجموعات الأربعة. وأجري اختبار T لعينتين مرتبطتين T paired test للمقارنة بين الفرق في معدل استكشاف الجسمين داخل المجموعة الواحدة. واستخدم اختبار الأقل فرق معنوي Least Significant Difference (LSD) لمعرفة أي الفروقات ذات دلالة إحصائية. حدد مستوى المعنوية عن$P\leq0.05$.

النتائج

تأثيرMTX على زمن الاستكشاف الكلي في يوم التدريب: بينت النتائج أن زمن الاستكشاف الكلي للجسمين A و B في يوم التدريب للمجموعة MTX(40mg/kg) أعلى من المجموعات الأخرى، ثم تليها المجموعة MTX(20mg/kg)، أما المجموعة MTX(80mg/kg) فتأتي في المرتبة الثالثة، في حين كانت فئران المجموعة الضابطة أقل المجموعات استكشافا للجسمين. إلا أنه عند إجراء اختبار التباين الأحادي تبين عدم وجود دلالة معنوية لهذه الفروقات (p=0.062) (شكل2).

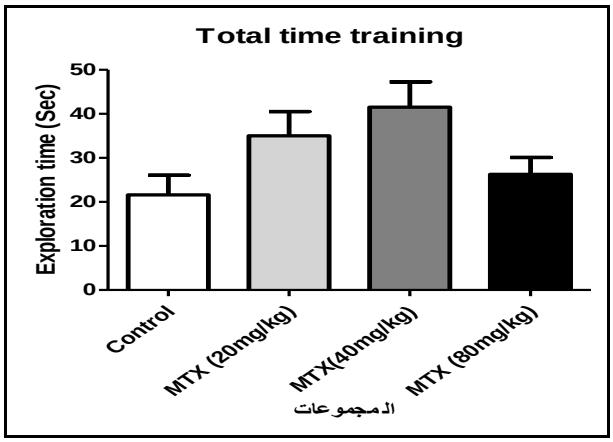

شكل(2). تأثير MTX على زمن الاستكشاف الكلي يوم التدريب.

تأثير MTX على زمن الاستكشاف الكلي في يوم الاختبار: أظهرت النتائج أن زمن الاستكشاف الكلي للجسمين A و C في يوم الاختبار للمجموعة MTX(40mg/kg) أعلى من المجموعات الأخرى، ثم تليها المجموعة MTX(20 mg/kg) كانت المجموعة الضابطة Control group في المرتبة الثالثة، في حين كانت فئران المجموعة MTX(80mg/kg) أقل المجموعات استكشافا للجسمين. بين اختبار التباين الأحادي عدم وجود دلالة معنوية لهذه الفروقات (p=0.078) (شكل3).

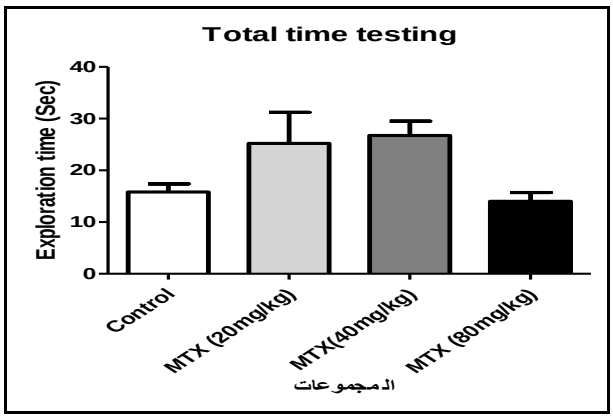

شكل (3). تأثير MTX على زمن الاستكشاف الكلي يوم الاختبار.

تأثير MTX على معدل استكشاف الجسمينA و B يوم التدريب : أوضحت النتائج أن معدل استكشاف الفئران للجسم A بالمجموعتين الضابطة، و MTX(80mg/kg) أعلى من معدل استكشافها للجسمB، والعكس صحيح بالنسبة للمجموعتين(MTX(20mg/kg ، و MTX(40mg/kg)

أي أن معدل استكشاف الجسم B أعلى من الجسم A داخل كلا المجموعتين. وعند إجراء اختبار T تبين عدم وجود فرق معنوي بين معدل استكشاف الفئران للجسمين A و B داخل كل مجموعة. أما عند مقارنة زمن استكشاف الفئران للجسمين في المجموعات المختلفة لوحظ أن زمن استكشاف الجسم A في المجموعتين الضابطة Control ، و MTX (80mg/kg) أعلى من المجموعتين MTX(20mg/kg)، و MTX (40mg/kg)، بينما العكس صحيح بالنسبة لمعدل الاستكشاف للجسم B أي أنه كان أعلى في المجموعتين MTX (20mg/kg), MTX (40mg/kg)عنه في المجموعتين الضابطة، و MTX (80 mg/kg) وعند إجراء اختبار التباين الأحاديOne way ANOVA تبين عدم وجود دلالة معنوية لهذه الفروقات (p=0.441) (شكل4).

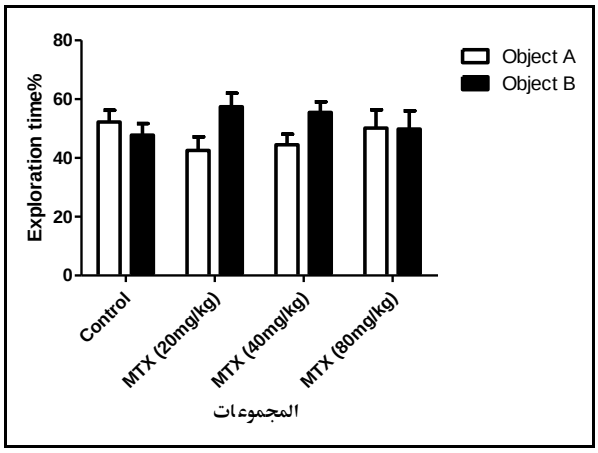

شكل (4). تأثير MTX على معدل الاستكشاف للجسمين A,B يوم التدريب

تأثير MTX على معدل استكشاف الجسمين A,C يوم الاختبار: أوضحت النتائج أن معدل استكشاف فئران المجموعة الضابطة، والمجموعة MTX(20mg/kg) للجسم C أعلى من معدل استكشافها للجسم A، في حين أن معدل استكشاف الفئران للجسم A أعلى من معدل استكشافها للجسم C داخل المجموعتين MTX (40mg/kg) ، و MTX (80mg/kg)عند إجراء اختبار T تبين وجود فرق معنوي داخل مجموعة الضابطة فقط أما باقي المجموعات لا يوجد. أما بالنسبة لمعدل استكشاف الفئران للجسمين A, C في المجموعات المختلفة فإن استكشاف الفئران للجسم A في المجموعات الثلاثة للميثوتركسيت أعلى من المجموعة الضابطة، بينما العكس صحيح لمعدل استكشافها للجسم C ، حيث كان أعلى في المجموعة الضابطة من باقي المجموعات. أي معدل استكشاف الفئران الجسم C في مجموعات MTX انخفض مقارنة بالمجموعة الضابطة، وهذا الانخفاض ازداد بزيادة الجرعة، والعكس بالنسبة للجسم A ، بين اختبار التباين الأحادي One Way ANOVAوجود فروق معنوية بينها(p=0.0001)، أظهر اختبار LSD وجود الفرق المعنوي بين معدل استكشاف الجسمين A,C في المجموعة الضابطة فقط ، وأيضا هناك فرق معنوي بين معدل استكشاف فئران المجموعة الضابطة للجسم A، و معدل استكشاف فئران باقي المجموعات للجسمA، و هناك فرق معنوي بين معدل استكشاف فئران المجموعة الضابطة للجسم C، و معدل استكشاف فئران باقي المجموعات للجسم(شكل 5).

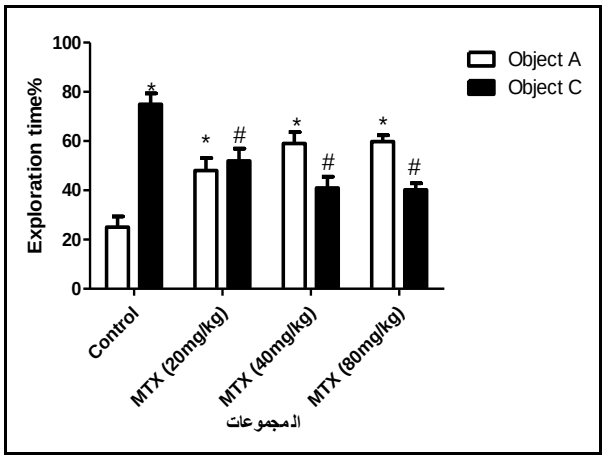

* فرق معنوي مع الجسم A في المجموعة الضابطة

فرق معنوي مع الجسم C في المجموعة الضابطة

شكل (5). تأثير MTX على معدل الاستكشاف للجسمين A,C يوم الاختبار.

المناقشة

في هذه الدراسة لم تُظهر نتائج اختبار التعرف على الجسم الجديد NOR الذي أجري بعد حقن MTX أي فروق معنوية في زمن الاستكشاف الكلي بين مجاميع الدراسة في يومي التدريب والاختبار، مما يشير إلى أن الـ MTX لم يتداخل مع

النشاط الحركي لحيوانات التجربة. وعليه فإن أي تغيرات تطرأ على معدل استكشاف الفئران للأجسام سيكون راجعاً إلى وجود تأثير للـ MTX على ذاكرة الفئران.

بينت نتائج استكشاف الفئران للجسمين A,B في يوم التدريب عدم وجود فروق معنوية بينهما في داخل كل مجموعة وبين المجموعات المختلفة، أي أن فئران كل مجموعة لم تفضل أيا من الجسمين على الآخر عند استكشافها لهما. في حين أن هناك فروق معنوية لمعدل استكشاف فئران المجموعة الضابطة بين الجسمين A,C في يوم الاختبار، أي أن معدل استكشاف الفئران للجسم C أعلى من معدل استكشافها للجسم A. والعكس صحيح في مجاميع الفئران المحقونة بجرعات المختلفة MTX حيث كان معدل استكشافها للجسم A أعلى من معدل استكشافها للجسمC ، أي أنها لم تتعرف على الجسم Cعلى أنه جسم جديد، مما يوضح أن جرعات MTX الثلاثة أدت إلى عجز ذاكرة التعرف لدى الفئران، وضعفها.

تعد هذه النتائج مماثلة لدراسة (Naewla et al., 2019) التي استنتجت أن حقن الـ MTX (75ملجم/كجم) في الوريد الذيلي للفئران أدى إلى إحداث عجز في ذاكرة التعرف (اختبار التعرف على الأجسام الجديدة)، ويعود هذا التدهور إلى انخفاض تكاثر خلايا الحصين Hippocampal Neurogenesis، والتي يعتقد أن تكاثرها يشارك في سلوك التعلم والذاكرة، حيث أشار (Kempermann, 2002) أن التغيرات في معدل تكوين الخلايا العصبية له تأثير على سلوك التعلم .

اتفقت نتائج الدراسة الحالية مع دراسة (Elens et al., 2019) حيث تسبب حقن جراء الفئران بجرعة 20 ملجم/كجم (في التجويف البريتوني) في تدهور ذاكرة التعرف لدى هذه الفئران عند البلوغ. في حين اختلفت نتائج الدراسة الحالية مع دراسة (Li et al., 2010) الذين بينوا أن حقن الجرذان البالغة بجرعة 250 ملجم/كجم من MTX في التجويف البريتوني لم تسبب عجزا في ذاكرة التعرف لدى الجردان في حين أدت إلى تدهور الذاكرة المكانية لديها، قد يعود السبب في ذلك لاختلاف البروتكول المتبع عند إجراء اختبار NOR في الدراستين.

عند مقارنة معدل استكشاف الفئران للجسمين A,C بين المجموعات المختلفة، تبين أن معدل استكشاف الجسم C في مجموعات MTX انخفض مقارنة بالمجموعة الضابطة وهذا الانخفاض يزداد بزيادة الجرعة. اتفقت هذه النتائج مع نتيجة (Seigers et al., 2008) حيث أشار أن حقن MTX بجرعة (250ملجم/كجم) في الوريد الذيلي للفئران سبب في إحداث عجز في ذاكرة التعرف (اختبار التعرف على الأجسام الجديدة)، مما أدى إلى انخفاض تكاثر خلايا الحصين، ويعتمد هذا الانخفاض على الجرعة (كلما زادت الجرعة قل تكاثر الخلايا الحصينية) .

الميثوتركسيت MTX قادر على اجتياز حاجز الدم في الدماغ Blood-Brain Barrier (Dukic et al., 2000; Lyons et al., 2011) بالتالي فإنه إذا حقن هذا العقار بالتجويف البريتوني، يكون قادرا على الوصول إلى أنسجة الدماغ وخلاياه مسببا العديد من التغييرات التي قد تؤدي إلى تدهور ذاكرة التعرف لدى الفئران. حيث يسبب المثوتركسيت انخفاضاً في عوامل النمو بالدماغ (Sritawan et al., 2021)، وانخفاض مستوى الفوليت Folate في السائل المخي الشوكي، وكذلك في المصل (Elens et al., 2019; Li et al., 2010).

الميثوتركسيت MTX يقوم أيضا بتثبيط عملية انقسام الخلايا غير الناضجة بالحصين في الدماغ (Sritawan et al., 2020)، كما أنه يقلل من كثافة المادة البيضاء في الجسم الثفني Corpus callosum في حين أنه لا يسبب موت خلايا الحصين البالغة (Aukema et al., 2009; Seigers et al., 2009).

بالرغم من وجود دراسة تثبت أن الأدوية المعالجة للسرطان تُصغر من حجم المادة الرمادية في الدماغ (Inagaki et al., 2007)، فإن هناك دراسات-أجريت عن طريق التصوير

المقطعي Computed tomography والتصوير بالرنين المغناطيسيMagnetic resonance imaging تشير إلى عدم وجود دليل على تأثر المادة الرمادية بالتأثير السلبي للـ MTXعلى الذاكرة (Wilks et al., 2002).

الاستنتاج

تكشف هذه الدراسة أن العلاج الكيميائي لـ MTX يسبب إعاقات معرفية (اضطراب في عمليات التعلم، وذاكرة التعرف على الأجسام الجديدة) وذلك بحسب الجرعات المختلفة (المنخفضة ، المتوسطة، والمرتفعة). وتؤكد الدراسة الحاجة إلى إجراء العديد من البحوث لمعرفة التأثير السمي للميثوتركسيت، والحصول على تفسيرات علمية وافية.

الشكر والتقدير

يتقدم الباحثون بالشكر الجزيل لكلية الصيدلة بجامعة مصراتة، ومشرف بيت الحيوان بقسم علم الحيوان/ كلية العلوم، السيد الزروق الزقل.

المراجع

Akman, A. U. (2021). Methotrexate Induced Hepatotoxicity and Antioxidants. *Sabuncuoglu Serefeddin Health Sciences, 3*(1), 22-35 .

Aldosouky, E., Elfagieh, M., & Jebriel, A. (2011). Pediatric Burkitt's lymphoma (diagnosis and treatment evaluation) in NCI ،Pediatric Oncology Unit: Misurata/Libya initial experience. *Journal of Clinical Oncology, 29*(15_suppl), e20000-e20000 .

Aukema, E. J., Caan, M. W., Oudhuis, N., Majoie, C. B., Vos, F. M., Reneman, L., Last, B. F., Grootenhuis, M. A., & Schouten-van Meeteren, A. Y. (2009). White matter fractional anisotropy correlates with speed of processing and motor speed in young childhood cancer survivors. *International Journal of Radiation Oncology* Biology* Physics, 74*(3), 837-843 .

Bedoui, Y., Guillot, X., Sélambarom, J., Guiraud, P., Giry, C., Jaffar-Bandjee, M. C., Ralandison, S., & Gasque, P. (2019). Methotrexate an old drug with new tricks. *International journal of molecular sciences, 20*(20), 5023 .

Bisen-Hersh, E. B., Hineline, P. N., & Walker, E. A. (2013 .(Effects of early chemotherapeutic treatment on learning in adolescent mice: implications for cognitive impairment and remediation in childhood cancer survivors. *Clinical Cancer Research, 19*(11), 3008-3018 .

Broadbent, N. J., Gaskin, S., Squire, L. R & ،. Clark, R. E. (2010). Object recognition memory and the rodent hippocampus. *Learning & memory, 17*(1), 5-11 .

Cohen, S. J., & Stackman Jr, R. W. (2015). Assessing rodent hippocampal involvement in the novel object recognition task. A review. *Behavioural brain research, 285*, 105-117 .

Dukic, S., Heurtaux, T., Kaltenbach, M., Hoizey, G., Lallemand, A., & Vistelle, R. (2000). Influence of schedule of administration on methotrexate penetration in brain tumours. *European Journal of Cancer, 36*(12), 1578-1584 .

Elens, I., Dekeyster, E., Moons, L., & D'Hooge, R. (2019). Methotrexate affects cerebrospinal fluid folate and tau levels and induces late cognitive deficits in mice. *Neuroscience, 404*, 62-70 .

Ermens, A. A., Schoester, M., Spijkers, L. J., Lindemans ،J., & Abels, J. (1989). Toxicity of methotrexate in rats preexposed to nitrous oxide. *Cancer research, 49*(22), 6337-6341 .

journal of physiology and pharmacology, 80(11), 1076-1084 .

Naewla, S., Sirichoat, A., Pannangrong, W., Chaisawang, P., Wigmore, P., & Welbat, J. U. (2019). Hesperidin alleviates methotrexate-induced memory deficits via hippocampal neurogenesis in adult rats. *Nutrients, 11*(4), 936 .

Reger, M. L., Hovda, D. A., & Giza, C. C. (2009). Ontogeny of rat recognition memory measured by the novel object recognition task. *Developmental Psychobiology: The Journal of the International Society for Developmental Psychobiology, 51*(8), 672-678 .

Seigers, R., Schagen, S. B., Beerling, W., Boogerd, W., Van Tellingen, O., Van Dam, F. S., Koolhaas, J. M., & Buwalda, B. (2008). Long-lasting suppression of hippocampal cell proliferation and impaired cognitive performance by methotrexate in the rat. *Behavioural brain research, 186*(2), 168-175 .

Seigers, R., Schagen, S. B., Coppens, C. M., van der Most, P. J., van Dam, F. S., Koolhaas, J. M & ،.Buwalda, B. (2009). Methotrexate decreases hippocampal cell proliferation and induces memory deficits in rats. *Behavioural brain research, 201*(2), 279-284 .

Sritawan, N., Prajit, R., Chaisawang, P., Sirichoat, A., Pannangrong, W., Wigmore, P., & Welbat, J. U. (2020). Metformin alleviates memory and hippocampal neurogenesis decline induced by methotrexate chemotherapy in a rat model. *Biomedicine & Pharmacotherapy, 131*, 110651 .

Sritawan, N., Suwannakot, K., Naewla, S., Chaisawang, P., Aranarochana ،A., Sirichoat, A., Pannangrong, W., Etaher, N. A., Saeed, N. M., Elmejrab, M. M., Sherif, R. F., & Sherif, F. M. (2021). Prescribing Patterns of Methotrexate in Libyan Patients with Rheumatoid Arthritis. *City, 29*, 24 .

Inagaki, M., Yoshikawa, E., Matsuoka, Y., Sugawara, Y., Nakano, T., Akechi, T., Wada, N., Imoto, S., Murakami, K., & Uchitomi, Y. (2007). Smaller regional volumes of brain gray and white matter demonstrated in breast cancer survivors exposed to adjuvant chemotherapy. *Cancer, 109*(1), 146-156 .

John, J., Kinra, M., Mudgal, J., Viswanatha, G., & Nandakumar, K. (2021). Animal models of chemotherapy-induced cognitive decline in preclinical drug development .*Psychopharmacology, 238*(11), 3025-3053 .

Kempermann, G. (2002). Why new neurons? Possible functions for adult hippocampal neurogenesis. *Journal of neuroscience, 22*(3), 635-638 .

Li, Y., Vijayanathan, V., Gulinello, M. E., & Cole, P. D. (2010). Systemic methotrexate induces spatial memory deficits and depletes cerebrospinal fluid folate in rats. *Pharmacology Biochemistry and Behavior, 94*(3), 454-463 .

Lyons, L., ElBeltagy, M., Umka, J., Markwick, R., Startin, C., Bennett, G., & Wigmore, P. (2011). Fluoxetine reverses the memory impairment and reduction in proliferation and survival of hippocampal cells caused by methotrexate chemotherapy. *Psychopharmacology, 215*(1), 105-115 .

Madhyastha, S., Somayaji, S., Rao, M., Nalini, K., & Bairy, K. L. (2002). Hippocampal brain amines in methotrexate-induced learning and memory deficit. *Canadian*

Wigmore, P., & Welbat, J. U. (2021). Effect of metformin treatment on memory and hippocampal neurogenesis decline correlated with oxidative stress induced by methotrexate in rats. *Biomedicine & Pharmacotherapy, 144*, 112 .280

Vijayanathan, V., Gulinello, M., Ali, N., & Cole, P. D. (2011). Persistent cognitive deficits, induced by intrathecal methotrexate, are associated with elevated CSF concentrations of excitotoxic glutamate analogs and can be reversed by an NMDA antagonist. *Behavioural brain research, 225*(2), 491-497 .

Wilks, M. J., Tie, M. L., & Pozza, C. H. (2002). CT and MRI appearances of methotrexate leucoencephalopathy. *Australasian radiology, 46*(1), 80-83 .

Effect of Methotrexate on Recognition Memory in Adult Female Mice

Wafa F. El Matoni [1]*, Fatima H. Ahmed[1], Hajer M. Ghliwo[1], Mustafa M. Drah[2]

[1]*Zoology Department, Faculty of Science , Misurata University, Libya*
[2] *Biothocnology Department, Faculty of Science, Misurata University, Libya*

Received: 11 February 2022/ Accepted: 12 June 2022
Doi: https://doi.org/10.54172/mjsc.v37i2.617

Abstract: Methotrexate MTX is used to treat some types of cancers, skin diseases, and rheumatic diseases. Many studies have suggested that it may lead to memory damage in mice. Accordingly, this study was conducted to investigate the effect of different doses of methotrexate on recognition memory in mice. Twenty-four adult female albino mice (weighing between 30-36 g) were divided equally into four groups and subjected to one of the following treatments: the control group (injected with normal saline), the second group treated with a dose of 20 mg/kg of MTX, the third group treated with a dose of 40 mg/kg of MTX, the fourth group treated with a dose of 80 mg/kg of MTX. All doses were given once intraperitoneally. A memory test was performed half an hour after injection, comprising object training and a new object recognition test. The results of this study showed that the MTX-injected mice had a lower rate of exploration of the novel object compared to the control group, and MTX has a dose-dependent negative effect on cognitive behavior. These findings suggest that methotrexate has a negative effect on the recognition memory of mice.

Keywords: Novel recognition task; Intraperitoneally; Methotrexate; Cognitive impairment; Recognition memory.

***Corresponding author:** Wafa F. El Matoni: *elmatonw@sci.misuratau.edu.ly* : Zoology Department, Faculty of Science , Misurata University, Libya